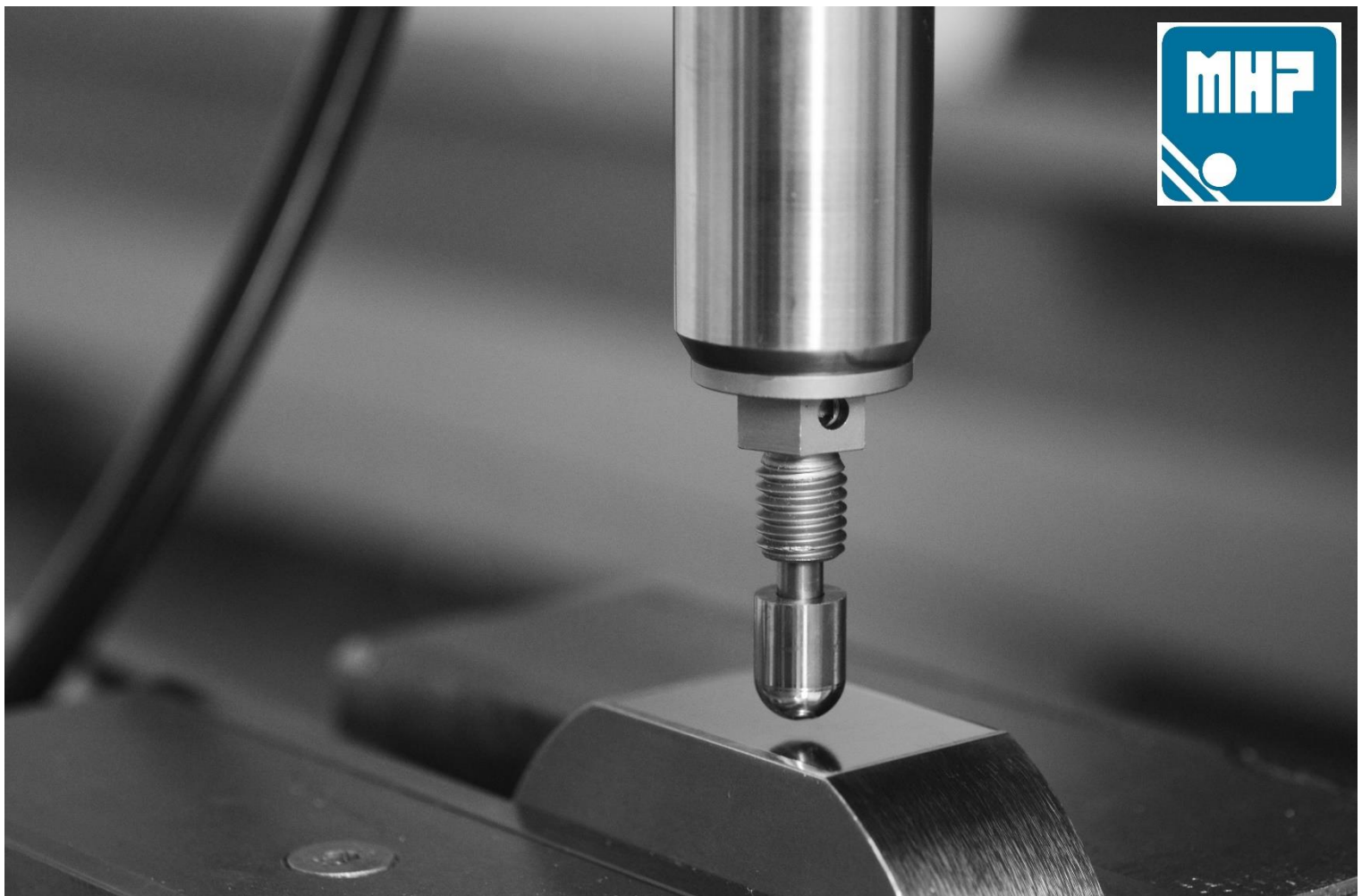


Symposium **Mechanical** **Surface Treatment 2019**

8th Workshop Machine Hammer Peening

Karlsruhe
22 and 23 October 2019



Symposium Mechanical Surface Treatment 2019
8th Workshop Machine Hammer Peening

22 and 23 October 2019, Karlsruhe

DOI: 10.5445/IR/1000099108

Contact

Prof. Dr.-Ing. habil. Volker Schulze

Director of Manufacturing and Materials Technology

wbk Institute of Production Science

Phone: +49 721 608-42440

Volker.Schulze@kit.edu

Publisher

wbk Institute of Production Science

Karlsruhe Institute of Technology

www.wbk.kit.edu

Authors

Prof. Dr.-Ing. habil. Volker Schulze

Dr.-Ing. Michael Gerstenmeyer

Patrick Neuenfeldt, M.Sc.

Preface

Dear colleagues,
ladies and gentlemen,

on behalf of the entire wbk Institute of Production Science, I would like to welcome you to this year's eighth edition of the Machine Hammer Peening workshop in Karlsruhe. Launched in 2012 as the "Fachforum Festklopfen" in Darmstadt, the workshop, which alternates annually between the universities of Darmstadt, Vienna, Karlsruhe and Aachen, is enjoying increasing popularity.

At the same time this workshop is the 63rd meeting of the Working Group Mechanical Surface Treatments of the Deutsche Gesellschaft für Materialkunde (DGM). The group meets twice a year at German industrial and academic sites and discusses new aspects of all mechanical surface treatments starting with the technologies via the resulting surface states up to the improvements in the performance of the treated components in application.

Therefore the actual meeting is a kind of an experiment to bring together complementary but mutually interested groups from manufacturing technology and materials technology. This will enhance discussions which can be driven from both disciplines or viewpoints which have aims in common.

We are convinced that the technologies of mechanical surface treatments and especially the still new variants in the field of machine hammer peening have enormous potential in the field of finishing highly loaded machine components and tools and will continue to gain in importance in the future. The interaction of the DGM-group Mechanical Surface treatments running since a long time and the workshop Machine Hammer peening participants joins two really active groups and hopefully will glue.

With this in mind, I wish you an exciting and interesting workshop with many stimulating discussions.

Karlsruhe, 22 October 2019



Prof. Dr.-Ing. habil. Volker Schulze

Machine Hammer Peening (MHP)

Facing recent challenges

In the course of current and future technological and social trends, new fields of application are opening up for the MHP. In addition to shortening throughput in production, the MHP promises an improvement in the service life of dynamically highly stressed components and an increase in tool life. This results in an increase in productivity while simultaneously reducing costs. In addition, the MHP will gain in importance in the future in the field of finishing of additively manufactured components.

WMHP – An innovative exchange platform

The workshop focuses on the personal exchange and discussion between speakers, participants and scientists about research results, technology developments and successful applications. In addition, the workshop offers the opportunity to identify previously untapped potential of the MHP and to make it tangible for future research due to the bundling of competencies of different specialist areas.

To master machine hammer peening

By bringing together different technical expertise, the technologically complex interactions in machine hammer peening can be researched and discussed at the highest level. This enables sound scientific research under industrial boundary conditions.

DGM Technical Committee – Mechanical Surface Treatments

Mechanical surface treatments as shot peening and deep rolling are important procedures to work hardening of surface areas and to induce compressive residual stresses. Mostly the aim is the improvement of fatigue properties, wear resistance or corrosion resistance of components of mechanical engineering, automotive and aviation. Alternative processes as ultrasonic, laser or cavitation peening including modifications using prestressing or thermal treatments are also included in the committees work. The committee meets every half year at an industrial member or at university institutes.

Aims of the DGM Technical Committee

- Covering industrial and scientific topics in the area of mechanical surface treatments with the focus on the improvement of component properties and the further development of the processes
- Working on a science-based knowledge of correlations of process parameters of mechanical surface treatments, component states and component properties
- Initiating of research and development projects: Joint projects of universities, research institutes and industry
- Exchange of experiences between teams working in the field of mechanical surface treatments, and networking

Workshop History

Darmstadt, 11 October 2012

- Foundation event “Fachforum Festklopfen” (FFF)
- 15 participants

Vienna, 16 October 2013

- Continuation as Workshop Machine Hammer Peening (WMHP)
- First draft of terminology for MHP
- Development of a Wikipedia entry for MHP
- 23 participants

Aachen, 28 November 2014

- 3rd Workshop Machine Hammer Peening
- Revised terminology
- 30 participants

Karlsruhe, 24 November 2015

- 4th Workshop Machine Hammer Peening
- VDI guideline for MHP for a uniform nomenclature
- 36 participants

Darmstadt, 03 November 2016

- 5th Workshop Machine Hammer Peening
- Wikipedia entry for MHP online available
- Joint CIRP paper
- 43 participants

Vienna, 22 November 2017

- 6th Workshop Machine Hammer Peening
- 43 participants

Aachen, 12 and 13 November 2018

- 7th Workshop Machine Hammer Peening
- 29 participants

Lecture programme

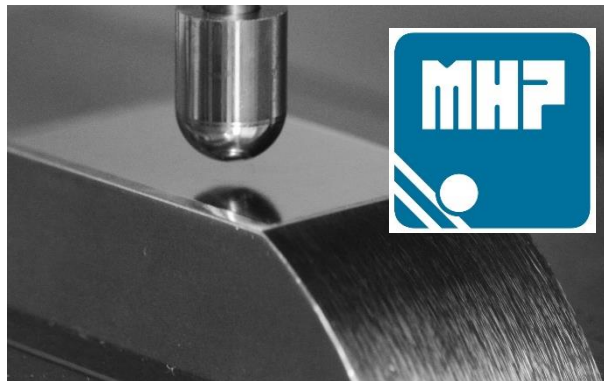
Reception	1
Prozesssicherheit bei der mechanischen Oberflächenbearbeitung	7
FE Simulation of the HFMI Treatment – Previous and Upcoming Results	20
Influence of mechanical surface treatments on propagation and opening behavior of physically short cracks in Inconel 718	35
Controlled Pneumatic Needle Peening – New Peening Technology for Aerospace Applications	49
Experimental analysis of the surface integrity of stainless steel modified by robot based machine hammer peening	65
Analyses of technical and true overlap in hammer peening operations	76
Influence of the process parameters on the penetration behaviour of ceramic particles in Composite Peening	85
Residual stress relaxation in HFMI-treated fillet welds after single overload peaks	100
Interne Verfestigungsdomänen durch mechanische Oberflächenbehandlung während der additiven Fertigung	109
Influence of MHP on the material structure of CrNi steels	122
Influence of the hammer head geometry when machining higher strength materials by MHP	135
Optimization of the stream finishing process for mechanical surface treatment by numerical and experimental process analysis	138

Reception

Prof. Dr.-Ing. habil. Volker Schulze

wbk Institute of Production Science

Karlsruhe Institute of Technology








wbk INSTITUTE OF PRODUCTION SCIENCE

Karlsruhe, October 22th 2019


KIT – The Research University in the Helmholtz Association







www.wbk.kit.edu

KARLSRUHE INSTITUTE OF TECHNOLOGY (KIT)




The Research University in the Helmholtz Association



 ESTABLISHED 1. October 2009	 COURSES OF STUDIES 43	 STUDENTS 25.495
 STAFF 9.297	 PROFESSORS 367	 TURNOVER 902 Mio. €

Reference(s): Manuel Balzer (KIT)

2 22.10.2019 Prof. Dr.-Ing. J. Fleischer, Prof. Dr.-Ing. G. Lanza, Prof. Dr.-Ing. habil. V. Schulze



LOCATIONS



Institute of Production Science

	Ehrenhof Karlsruhe Germany <i>Manufacturing and materials technology</i>		Campus Nord Eggenstein- Leopoldshafen Germany <i>Machines, equipment and process automation</i>		Shanghai China <i>AMTC - Advanced Manufacturing Technology Center</i>
	Fasanengarten Karlsruhe Germany <i>Production systems Machines, equipment and process automation</i>		Material Research Center for Energy Systems Karlsruhe Germany <i>Manufacturing and materials technology</i>		Suzhou China <i>GAMI - Global Advanced Manufacturing Institute</i>









3 22.10.2019 Prof. Dr.-Ing. J. Fleischer, Prof. Dr.-Ing. G. Lanza, Prof. Dr.-Ing. habil. V. Schulze



RESEARCH PORTFOLIO



Institute of Production Science

 Manufacturing and Materials Technology	 Machines, Equipment and Process Automation	 Production Systems	
			Micro Production 
			Lightweight Manufacturing 
			Electric Mobility 
			Additive Manufacturing 
			Industry 4.0 



Prof. Dr.-Ing. Jürgen Fleischer  Prof. Dr.-Ing. Gisela Lanza  Prof. Dr.-Ing. habil. Volker Schulze 

4 22.10.2019 Prof. Dr.-Ing. J. Fleischer, Prof. Dr.-Ing. G. Lanza, Prof. Dr.-Ing. habil. V. Schulze



MANUFACTURING AND MATERIALS TECHNOLOGY



PRECISION MACHINING

- Turning, drilling, milling
- Stream Finishing
- Combined processes for process chain consolidation
- μ laser ablation und μ milling
- Simulation of manufacturing processes (chip formation, cooling strategies, particle flow)
- Surface Engineering: Load-adapted adjustment of surface layer conditions through optimized process control

GEAR ENGINEERING

- Soft- und hard machining for skiving
- Whirling and special processes for thread production and polygonal manufacturing
- Special kinematics for precision gearing
- Control of the process chain during broaching
- Optimized cooling lubricant strategy
- Kinematics simulation for die design and for analyzing local parameters

ADDITIVE MANUFACTURING

- Analysis and optimization of additive manufacturing processes
- Laser Beam Melting (LBM)
- Lithography-based Ceramic Manufacturing (LCM)
- Development of metal powders for high-performance components
- Chipping and mechanical surface treatment of additive manufactured parts
- Multi-material processing
- Digital process chain analysis



5

22.10.2019

Prof. Dr.-Ing. J. Fleischer, Prof. Dr.-Ing. G. Lanza, Prof. Dr.-Ing. habil. V. Schulze



MACHINES, EQUIPMENT AND PROCESS AUTOMATION



MACHINE TOOLS AND MECHATRONICS

- Intelligent mechatronic components for production machines
- Condition Monitoring and predictive maintenance
- Simulation and optimization of machines and components

LIGHTWEIGHT MANUFACTURING

- Development of innovative, hybrid manufacturing processes
- Joining technologies for hybrid parts
- Intelligent tools for fibre composite manufacturing
- Intelligent, sensor based gripping technologies
- Flexible, robot based manufacturing processes for lightweight construction applications

ELECTRIC MOBILITY

- Gripping, handling and mounting systems for battery cell, -module, electric motor and fuel cells
- Process and Prototype development, simulation and evaluation of immature manufacturing processes
- Process control and optimization for energy storage and electric motor production



6

22.10.2019

Prof. Dr.-Ing. J. Fleischer, Prof. Dr.-Ing. G. Lanza, Prof. Dr.-Ing. habil. V. Schulze



PRODUCTION SYSTEMS



GLOBAL PRODUCTION STRATEGIES

- Strategic planning of production networks
- Site-specific production using Industry 4.0
- Information and quality management in supply chain networks
- Order-based production and logistics planning in networks

PRODUCTION SYSTEM PLANNING

- Adaptive production systems
- Industry 4.0 methods
- Digitalization strategies
- Machine learning and data mining
- Agile factory planning
- Robust, intelligent production control
- Cost evaluation and simulative validation
- Technology planning

QUALITY ASSURANCE

- In-line measurement technology for immature processes
- Soft sensors for intelligent data analysis
- Function-oriented measurements
- Autonomous measurement technology
- Measurement uncertainty evaluation
- Process control based on quality data



7

22.10.2019

Prof. Dr.-Ing. J. Fleischer, Prof. Dr.-Ing. G. Lanza, Prof. Dr.-Ing. habil. V. Schulze



GAMI



Global Advanced Manufacturing Institute



The Global Advanced Manufacturing Institute (GAMI) tries to deepen the understanding of global production structures according to the three KIT pillars research, innovation and teaching and to develop new, robust and controlled production networks for industrial enterprises for the local framework conditions.

FOUNDED	LOCATION	ENGINEERS	ADMINISTRATION	STUDENTS
2008	Suzhou	20	4	5

Global Advanced Manufacturing Institute

Applied Research

Industry Consulting for German Firms

Continuing Education / Training / Coaching

8

22.10.2019

Prof. Dr.-Ing. J. Fleischer, Prof. Dr.-Ing. G. Lanza, Prof. Dr.-Ing. habil. V. Schulze



AMTC



Advanced Manufacturing Technology Center



Founded as a cooperation of the Chinese-German University College (CDHK) with the wbk (KIT) and the College of Mechanical Engineering (Tongji University), the AMTC offers practical education and training for engineers working in China in production engineering, contract research and development for manufacturing companies in China as well as basic research in the field of automated manufacturing.

FOUNDED	LOCATION	ENGINEERS	ADMINISTRATION	STUDENTS
2012	Shanghai	3	4	20

Advanced Manufacturing Technology Center

Education

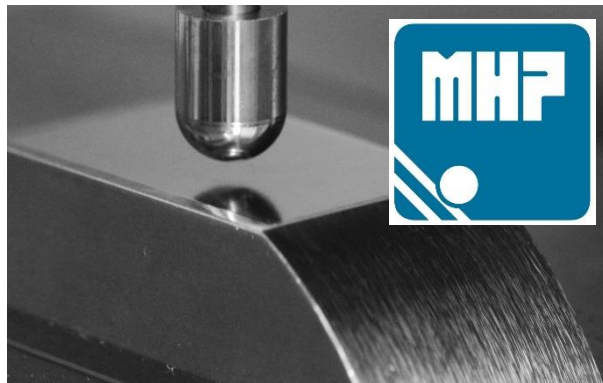
Research

Technological Exchange

Prozesssicherheit bei der mechanischen Oberflächenbearbeitung

Dr.-Ing. Oliver Maiß
Alfred Ostertag

Ecoroll AG Werkzeugtechnik








Prozesssicherheit bei der mechanischen Oberflächenbearbeitung
Systeme der Prozessüberwachung beim Walzen und Hämmern

Dr.-Ing. Oliver Maiß, Alfred Ostertag
 Karlsruhe, 22.10.2019

www.ecoroll.de



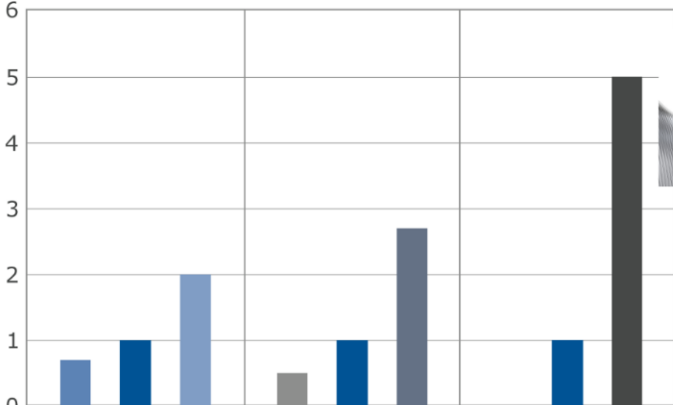
Lebensdauersteigerung durch Festwalzen

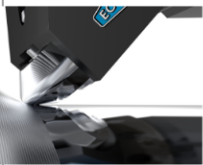
Material

Geometry

Surface treatment

Effect on lifetime





	Material			Geometry			Surface treatment	
Rm [N/mm ²]	750	900	1000	900	900	900	900	900
p / d	0,2	0,2	0,2	0,15	0,2	0,2	0,2	0,2
s / d	0,45	0,45	0,45	0,45	0,45	0,6	0,45	0,45
Process	turn.	turn.	turn.	turn.	turn.	turn.	turn.	roll.

08.10.2019
DGM Fachausschuss, Karlsruhe - O. Maiß, A. Ostertag
www.ecoroll.de
OM/0020
1


Effekte des Glatt- und Festwalzens



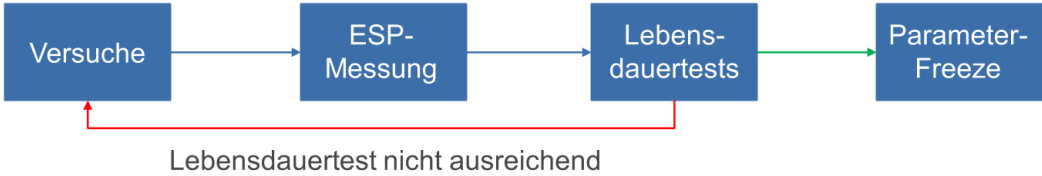
Eigen-spannungen sind Spannungen im inneren eines Bauteils, die auch vorliegen, wenn keine äußeren Kräfte, Momente oder Temperaturgradienten anliegen.

08.10.2019 DGM Fachausschuss, Karlsruhe - O. Maiß, A. Ostertag www.ecoroll.de OM/0031 2

Motivation




Prozess zur Festlegung von „richtigen“ Prozesseinstellgrößen:



```
graph LR; A[Versuche] --> B[ESP-Messung]; B --> C[Lebens-dauertests]; C --> D[Parameter-Freeze]; C -- "Lebensdauertest nicht ausreichend" --> A;
```


Wie kann die Eigen-spannung in der QS erfasst werden?

08.10.2019 DGM Fachausschuss, Karlsruhe - O. Maiß, A. Ostertag www.ecoroll.de 3

Agenda 

- 1 **Digitale Walzkraftmessung für mechanische Walzwerkzeuge**
- 2 **Prozessüberwachung beim Walzen mit hydrostatischen Walzwerkzeugen**
- 3 **Überwachung der Schlagenergie beim MHP**

08.10.2019 DGM Fachausschuss, Karlsruhe - O. Maiß, A. Ostertag www.ecoroll.de 4

Agenda 

- 1 **Digitale Walzkraftmessung für mechanische Walzwerkzeuge**
- 2 **Prozessüberwachung beim Walzen mit hydrostatischen Walzwerkzeugen**
- 3 **Überwachung der Schlagenergie beim MHP**

08.10.2019 DGM Fachausschuss, Karlsruhe - O. Maiß, A. Ostertag www.ecoroll.de 5



Bestimmung der Walzkraft im Prozess



Originalbetriebsanleitung
Betriebsanleitung Nr. 171001/2
Einrollen-Glatzwalzwerkzeug EG5-40M



Das ECOROLL Einrollen Glatzwalzwerkzeug EG5-40M entspricht dem Stand der Technik und den anerkannten sicherheitstechnischen Regeln. Dennoch können bei seiner Verwendung Gefahren für Leib und Leben des Benutzers oder Dritter bzw. Beeinträchtigungen des Werkzeugs und anderer Sachwerte entstehen.
 Werkzeug nur in technisch einwandfreiem Zustand sowie bestimmungsgemäß, sicherheits- und gefahrlos unter Beachtung der Betriebsanleitung benutzen! Insbesondere Störungen, die die Sicherheit beeinträchtigen können, umgehend beseitigen!
 Werkzeuge nur mit Original ECOROLL Teilen oder von ECOROLL zugelassenen Teilen verwenden! Bei Mischung kann es zum Erlöschen der Herstellergarantie kommen.

ECOROLL AG Werkzeugtechnik
 Postfach 31 42 Hans-Heinrich-Warke-
 D-29231 Celle
 D-39227 Celle
 Tel. +49 5141 9865-0
 Fax +49 5141 881440
 Web www.ecoroll.de
 E-Mail mail@ecoroll.de

ECOROLL Corporation Tool Technology
 502 Teche Center Drive Suite C
 Millford, OH 45150
 USA
 Tel. +1 513 248 4700
 Fax +1 513 248 4265
 Web www.ecoroll.com
 Email mail@ecoroll.com



Fehlert Verweisspalle konnte nicht gefunden werden, zeigt die mitteilbaren Maße für die Glatzwalkkraft, die aus Tabelle 1 in Abhängigkeit vom Werkstückdurchmesser und der Werkstofffestigkeit entnommen wurden. Die Federcharakteristik wurde für ein spezifisches EG5-40M-Werkzeug gemessen, für andere Werkzeuge können die Werte bis zu ±20% abweichen.



Fig. 6 Federcharakteristik (Beispiel)
 Falls erforderlich, können zur Optimierung des Walzergebnisses folgende Parameter verändert werden:

Rautiefe verringern	Rautiefe erhöhen
<ul style="list-style-type: none"> • Vorspannung erhöhen • Vorschub verringern • Zweiten Durchgang mit gleicher Einstellung walzen 	<ul style="list-style-type: none"> • Vorspannung reduzieren • Vorschub erhöhen • Drehzahl erhöhen

Tabelle 2 Optimierung des Walzergebnisses
 Die Maßnahmen zur Erhöhung der Rautiefe bis zum zulässigen Maß sind:
 • Erhöhung der Vorspannung
 • Erhöhung des Vorschubs
 • Erhöhung der Drehzahl
 • Erhöhung der Walzgeschwindigkeit
 • Erhöhung der Walztemperatur
 • Erhöhung der Restrautiefe als auch Zerteilspannung

Federkennlinie in Betriebsanleitung

Betriebsanleitung Nr. 171001/2
EG5-40M

© ECOROLL AG/ECOROLL Corp.
Technische Änderungen vorbehalten


Druckdatum: 28.04.2019
Erstellt am: 01.03.2002
Seite 10/22

Betriebsanleitung Nr. 171001/2
EG5-40M

© ECOROLL AG/ECOROLL Corp.
Technische Änderungen vorbehalten

Druckdatum: 28.04.2019
Erstellt am: 01.03.2002
Seite 10/22

08.10.2019 DGM Fachausschuss, Karlsruhe - O. Maiß, A. Ostertag
www.ecoroll.de
7



Prozessfehler bei mechanischen Walzwerkzeugen

- Zustellfehler beim Walzen
- Veränderung der Federkonstanten durch Kollision
- Geometrieabweichung bei Vorbearbeitung
- Zerspanwerkzeug fehlerhaft eingemessen

08.10.2019 DGM Fachausschuss, Karlsruhe - O. Maiß, A. Ostertag

www.ecoroll.de

8

Digitale Messuhr





Einfache Datenanalyse per eigener App

KSS-beständiges Gehäuse

Direkte Kraftanzeige

Kabellose Datenübertragen

Prozessüberwachung und -dokumentation



EMO
Hannover
16-21-9-2019

08.10.2019 DGM Fachausschuss, Karlsruhe - O. Maiß, A. Ostertag www.ecoroll.de 9

Agenda



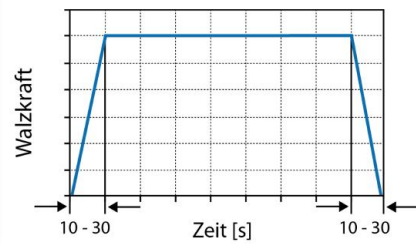
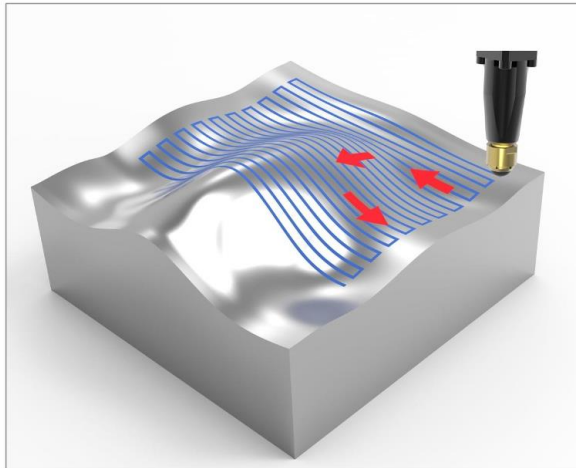
- 1 **Digitale Walzkraftmessung für mechanische Walzwerkzeuge**
- 2 **Prozessüberwachung beim Walzen mit hydrostatischen Walzwerkzeugen**
- 3 **Überwachung der Schlagenergie beim MHP**

08.10.2019 DGM Fachausschuss, Karlsruhe - O. Maiß, A. Ostertag www.ecoroll.de 10

Verfahren - 3D-Walzen von Freiformflächen



Das Nachführsystem der HG-Werkzeuge ermöglicht das Glatt- und Festwalzen von Freiformflächen

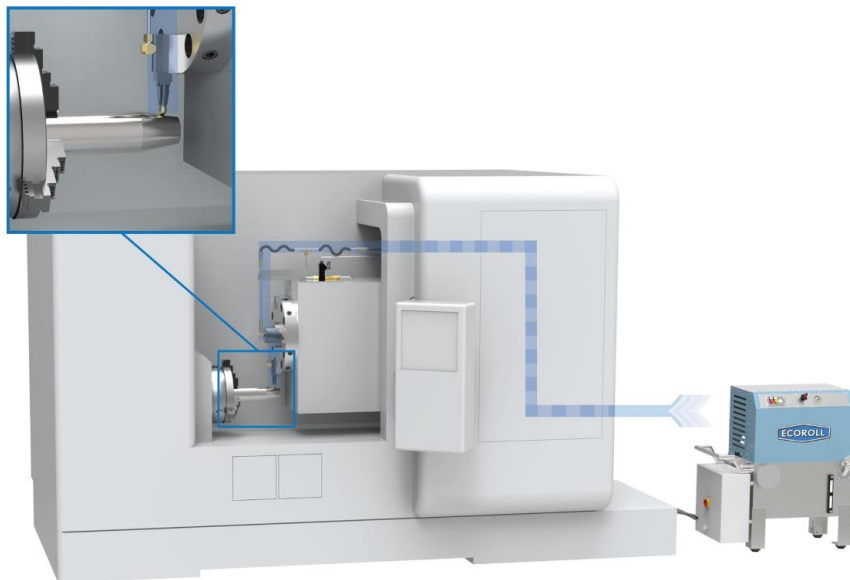


08.10.2019 DGM Fachausschuss, Karlsruhe - O. Maiß, A. Ostertag

www.ecoroll.de

11

Hydrostatisch gelagerte Werkzeuge




08.10.2019 DGM Fachausschuss, Karlsruhe - O. Maiß, A. Ostertag

www.ecoroll.de

12

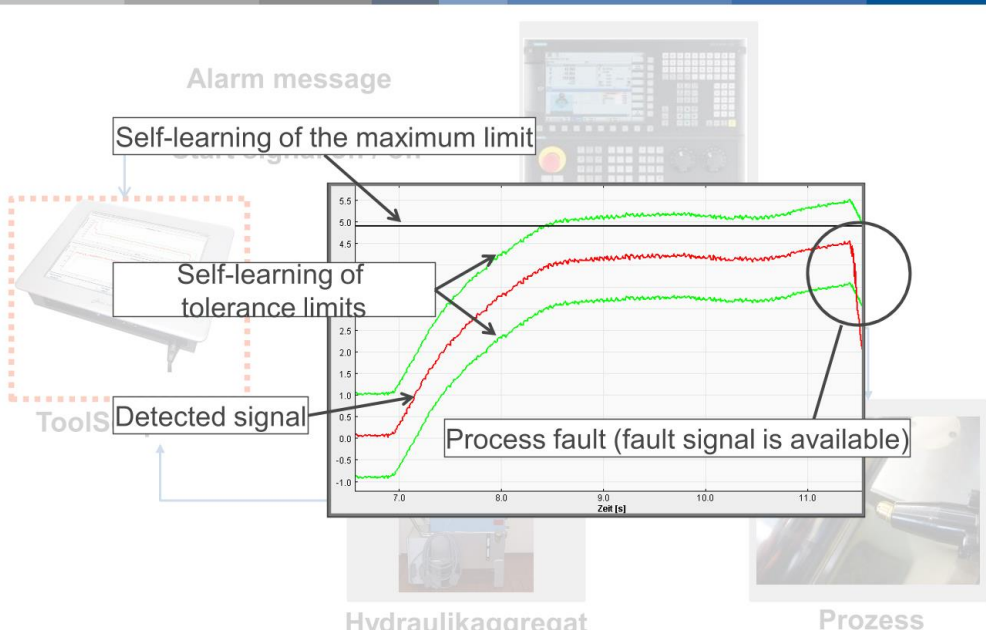

Prozessfehler beim Walzen mit hydrostatischen Werkzeugen



- Drossel verstopft
- Druckeinstellung durch Bediener fehlerhaft
- Aggregat ist defekt

08.10.2019 DGM Fachausschuss, Karlsruhe - O. Maiß, A. Ostertag www.ecoroll.de 13

Prozessüberwachung mit ToolScope



Alarm message

Self-learning of the maximum limit

Self-learning of tolerance limits

ToolScope


Detected signal

Process fault (fault signal is available)

Hydraulikaggregat

Prozess

08.10.2019 DGM Fachausschuss, Karlsruhe - O. Maiß, A. Ostertag www.ecoroll.de 14



Agenda

3

Überwachung der Schlagenergie beim MHP


2

Prozessüberwachung beim Walzen mit hydrostatischen Walzwerkzeugen

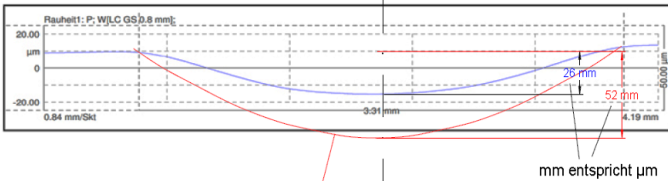
1

Digitale Walzkraftmessung für mechanische Walzwerkzeuge

08.10.2019 DGM Fachausschuss, Karlsruhe - O. Maiß, A. Ostertag
www.ecoroll.de
15



Analyse des Schlagvorganges



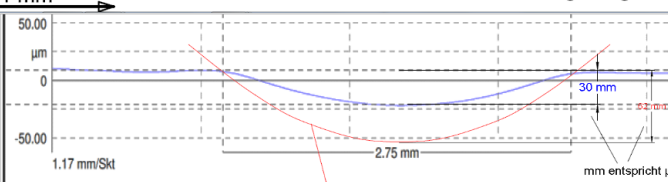
Rauheit: P: WJLC GS 0.8 mm_t

mm entspricht µm

Werkzeugradius R 25

Maßstab
 50 µm
 1 mm

Einzeleinschlag Nr.1
 R25 42CrMo4V
 Einschlagenergie 2000 mJ



mm entspricht µm

Werkzeugradius R16

Maßstab
 50 µm
 1 mm

Einzeleinschlag Nr.3
 R16 42CrMo4V
 Einschlagenergie 2000 mJ

08.10.2019 DGM Fachausschuss, Karlsruhe - O. Maiß, A. Ostertag
www.ecoroll.de
16

Hämmerwerkzeuge ECOpeen (Konzept)



Schlagsystem:
Mechanisch-pneumatisch,
Bekannt aus marktgängigen
Bohrhämmern
Rückstoßfrei!



Rückhub



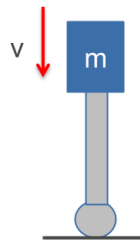
Schlag

08.10.2019 DGM Fachausschuss, Karlsruhe - O. Maiß, A. Ostertag

www.ecoroll.de

17

Schlagenergie - Schlagkraft



Kinetische Energie (Schlagenergie)

$$E_{kin} = \frac{1}{2} m v^2$$



Umformenergie

$$E_U = \frac{1}{2} F s$$

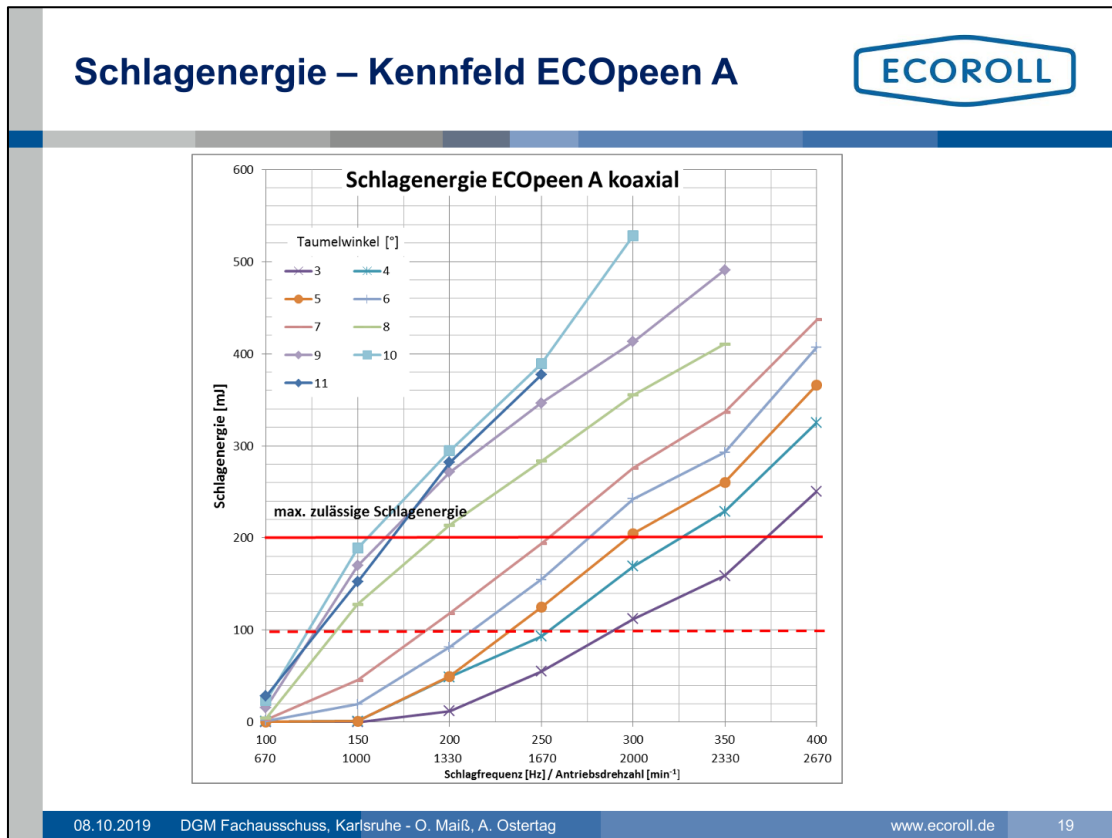
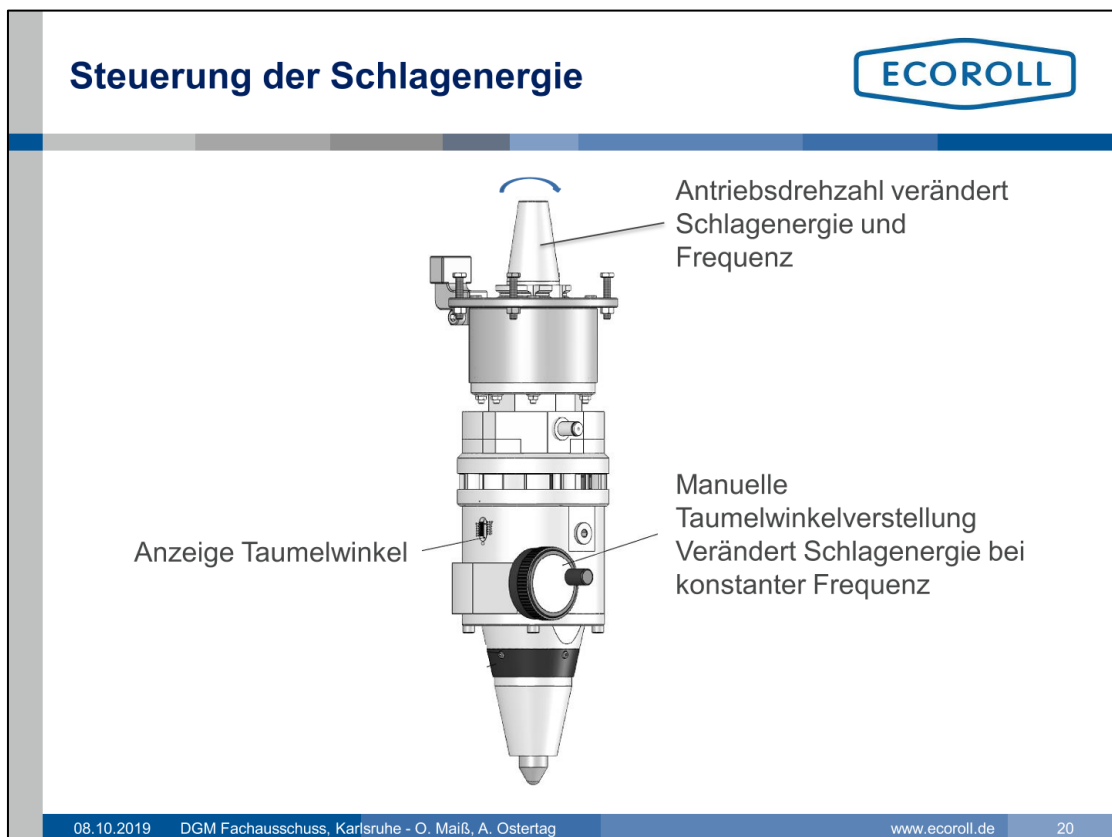
Schlagkraft

$$F = \frac{2E_U}{s}$$

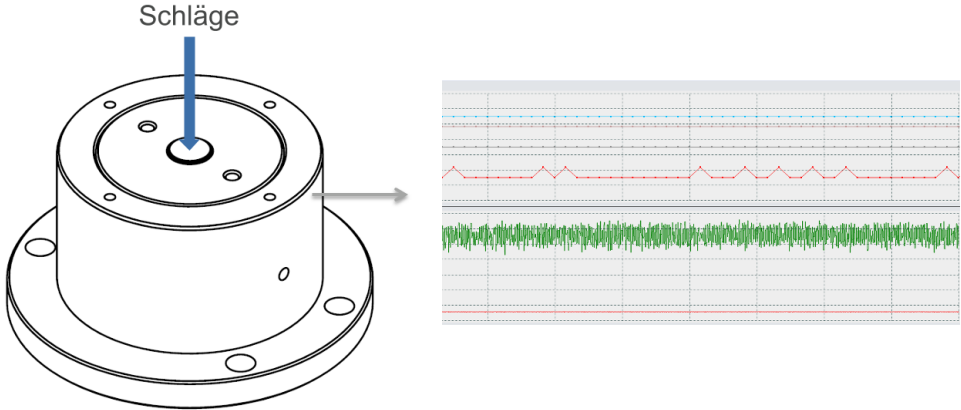

Schlussfolgerung:

- Schlagkraft ist abhängig von Schlagenergie und Verformungsweg.
- Ist als Leistungsangabe von Hämmerwerkzeugen ungeeignet.

www.ecoroll.de


08.10.2019 DGM Fachausschuss, Karlsruhe - O. Maiß, A. Ostertag
www.ecoroll.de
19

08.10.2019 DGM Fachausschuss, Karlsruhe - O. Maiß, A. Ostertag
www.ecoroll.de
20

Messung der Schlagenergie



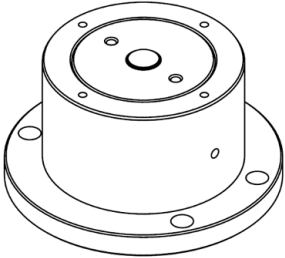

The diagram shows a cylindrical hammer peening machine with a sensor mounted on top. A blue arrow labeled 'Schläge' (blows) points to the center of the machine's top surface. An arrow points from the sensor to a graph showing a red signal with periodic peaks and a green signal with high-frequency noise.

Schläge

Schlagenergiesensor

08.10.2019 DGM Fachausschuss, Karlsruhe - O. Maß, A. Ostertag www.ecoroll.de 21

Verifizierung der Schlagenergie



- Einbau des Schlagenergiesensors in den Arbeitsraum der Maschine.
- Zyklisches Anfahren des Sensors für Kontrollmessungen.
- Bei Abweichung Korrektur der Taumelwinkel-Einstellung oder Antriebsdrehzahl.

08.10.2019 DGM Fachausschuss, Karlsruhe - O. Maß, A. Ostertag www.ecoroll.de 22

Vielen Dank für Ihre Aufmerksamkeit



ECOROLL AG Werkzeugtechnik
Hans-Heinrich-Warnke-Str. 8
29227 Celle
www.ecoroll.de

Dr.-Ing. Oliver Maiß
Leiter Konstruktion
Tel.: 05141 / 9865-51
Mail: oliver.maiss@ecoroll.de

Alfred Ostertag
Berater
Tel.: 05141 / 9865-51
Mail: alfred.ostertag@ecoroll.de

www.ecoroll.de

FE Simulation of the HFMI Treatment – Previous and Upcoming Results

Stefanos Gkatzogiannis

Steel & Lightweight Structures

Karlsruhe Institute of Technology





FE Simulation of the HFMI Treatment - Previous and Upcoming Results

Stefanos Gkatzogiannis, Peter Knoedel, Thomas Ummenhofer

Karlsruhe Institute of Technology
Steel & Lightweight Structures
Research Center for Steel, Timber & Masonry
Germany



Agenda



- 1 What is HFMI? – Application in Practice
- 2 Simulation of HFMI – Necessity and Main Aspects
- 3 Simulation of HFMI – Modelling of the Pin Motion
- 4 Simulation of HFMI – Calibration based on Drop Tests
- 5 Summary and Future Results

Problem Statement

The HFMI post-weld treatment process

Stefanos Gkatzogiannis, 8th Workshop Machine Hammer Peening – 22 and 23 October, Karlsruhe Institute of Technology, Germany

3

The HFMI Post Weld Treatment

The High Frequency Mechanical Impact or HFMI [Marquis, 2016] treatment is a post-weld mechanical treatment method applied for the increase of fatigue life of welded structures.

An appropriate device carrying a pin of hardened steel runs along the weld toe, deforms it by hammering and introduces compressive residual stresses at the surface layer, which counterbalance the welding tensile ones. Therewith, a significant increase of the weldment's fatigue life is achieved.

There are two manufacturers of HFMI devices in Germany: HIFIT and PITEC.



HIFIT



PITEC

Stefanos Gkatzogiannis, 8th Workshop Machine Hammer Peening – 22 and 23 October, Karlsruhe Institute of Technology, Germany



HIFIT treatment of a fillet weld

4

The HFMI Post Weld Treatment

The High Frequency Mechanical Impact (HFMI) treatment is a post-weld mechanical process that significantly increases the fatigue life of welded joints.

An appropriate device carrying a hammering tool, deforms it by hammering at the surface layer, which causes a beneficial residual stress state. Therewith, a significant increase in fatigue resistance is achieved.

There are two manufacturers of HFMI devices: HIFIT and PITEC.





HIFIT

Stefanos Gkatzogiannis, 8th Workshop Machine Hammer Peening – 22 and 23 October, Karlsruhe Institute of Technology, Germany

Triple effect:

- Introduction of compressive residual stresses
- Reducing the notch effect
- Local hardening of the surface

treatment of a fillet weld



5

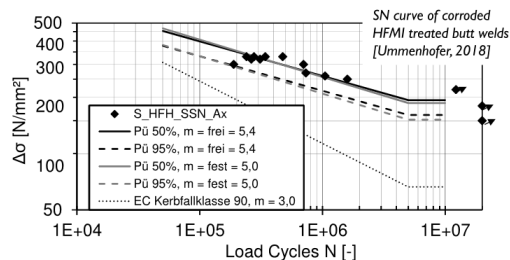
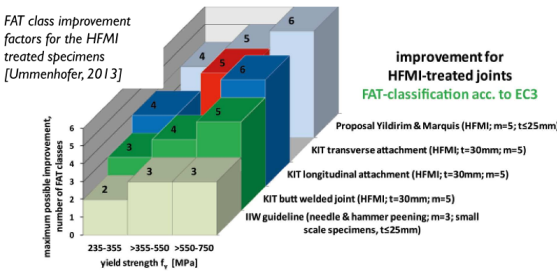
The HFMI Post Weld Treatment – Experimental Validation

The method has been thoroughly investigated experimentally and is proven to increase the fatigue resistance in the high cycle regime of welded joints by even more than 100%.

A thorough review of experimental work up to 2013 is given in [Yildirim, 2013].

The KIT Steel and Lightweight Structures Institute has as well carried numerous experimental investigations on HFMI efficiency. Some of them are:

- The REFRESH project [Ummerhofer, 2009]
- The DAST Richtlinie project [Kuhlman, 2018]
- The HFH-Korrosion project [Ummerhofer, 2018]

improvement for HFMI-treated joints FAT-classification acc. to EC3

Proposal Yildirim & Marquis (HFMI; m=5; ts25mm)

KIT transverse attachment (HFMI; t=30mm; m=5)


KIT longitudinal attachment (HFMI; t=30mm; m=5)

KIT butt welded joint (HFMI; t=30mm; m=5)

IIW guideline (needle & hammer peening; m=3; small scale specimens, ts25mm)

FAT class improvement factors for the HFMI treated specimens [Ummerhofer, 2013]

Stefanos Gkatzogiannis, 8th Workshop Machine Hammer Peening – 22 and 23 October, Karlsruhe Institute of Technology, Germany

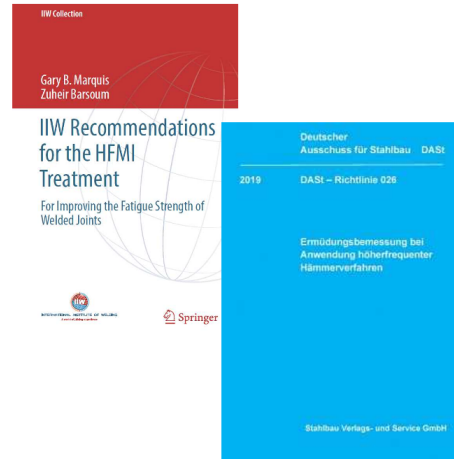


6

The HFMI Post Weld Treatment in Civil Engineering

- The method is applicable in both mechanical and structural civil engineering fields. Its application is regulated according to:
 - IIW recommendations [Marquis, 2016]
 - A new DAST guideline is now active for application as well in structural engineering [DAST, 2019]

 - Possible Fields of application in Structural Engineering:
 - Steel and composite bridges
 - Welded Details of Towers and Jacket Structures like in Offshore Wind Energy Turbines
 - Cranes
- and eventually every fatigue loaded structural welded detail.



Stefanos Gkatzogiannis, 8th Workshop Machine Hammer Peening – 22 and 23 October, Karlsruhe Institute of Technology, Germany

7

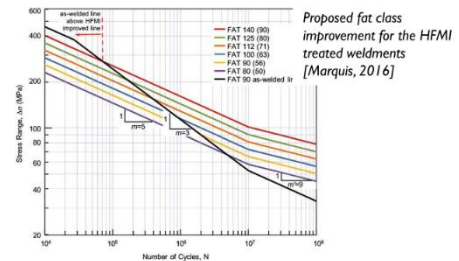
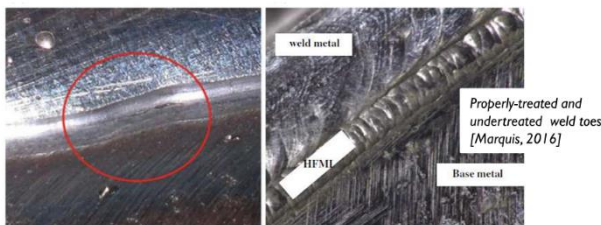
The HFMI Post Weld Treatment – Practical Aspects

- The two guidelines cover mostly practical aspects:
 - Application of the HFMI treatment including angle and working speed
 - Quality control based on groove geometry and surface quality
 - Fatigue design of HFMI treated weldments based on FAT classes and the approaches of nominal and hot-spot stress taking into consideration size effects etc.

Table 2 Sample treatment procedure parameters for two HFMI tools

Parameter	HFMI tool	
	High frequency impact treatment (HFIT) [22]	Ultrasonic impact treatment (UIT) [21, 23]
Power source	Pneumatic	Ultrasonic magnetostrictive
Number of indenters	1	1-4
Angle of the axis of the indenters with respect to the plate surface, ϕ (see Fig. 6)	60°-80°	30°-60° [21] 40°-80° [23]
Angle of the axis of the indenters with respect to the direction of travel, ψ (see Fig. 6)	70°-90°	90° (all pins should contact the weld toe)
Working speed	3-5 mm/s	5-10 mm/s [21] 5-25 mm/s [23]
Other		The self-weight of the tool is sufficient [21, 23] Minimum of 5 passes [23]

Application parameters according to [Marquis, 2016]



Stefanos Gkatzogiannis, 8th Workshop Machine Hammer Peening – 22 and 23 October, Karlsruhe Institute of Technology, Germany

8

Simulation of HFMI

Stefanos Gkatzogiannis, 8th Workshop Machine Hammer Peening – 22 and 23 October, Karlsruhe Institute of Technology, Germany

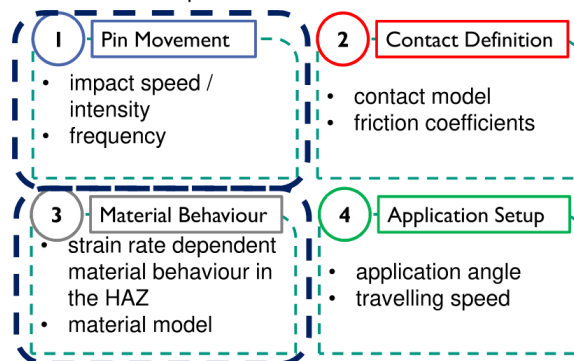
9

Simulation of the HFMI Treatment

- The validation of a simulation model that predicts the introduced residual stresses can enable a less conservative design and offer a better overview of the method through sensitivity analyses
- Coupling with fracture mechanics is possible, in order to predict with even better accuracy the fatigue life of a component
- Several simulation models have been proposed in the past neglecting though in most cases significant aspects of the problem
- Same physical problem with the indentation of a semi-infinite plate with a spherical indenter under significant initial velocity (non static case)

HFMI simulation is a multi-parameter analysis

Main aspects of the FE simulation of HFMI



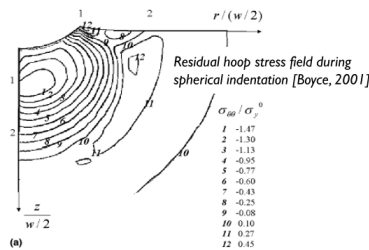
Stefanos Gkatzogiannis, 8th Workshop Machine Hammer Peening – 22 and 23 October, Karlsruhe Institute of Technology, Germany

10

HFMI Simulation – Material Behavior

Reversed plasticity

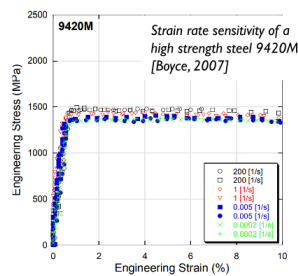
During spherical indentation, underneath the treatment surface, compressive stresses are introduced which are counterbalanced by outer tensile ones. During continuous treatment along a line, reversal of the plastic strains' and residual stresses' sign takes place.



Stefanos Gkatzogiannis, 8th Workshop Machine Hammer Peening – 22 and 23 October, Karlsruhe Institute of Technology, Germany

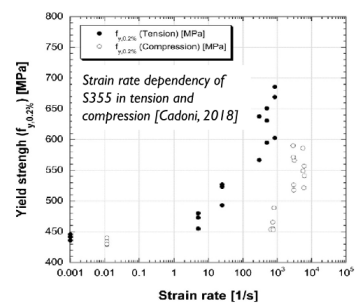
Strain rate dependency

During HFMI strain rates of up to 400 s⁻¹ are referred. Previous analyses have proven that yield stress is predominant for the introduced residual stresses. Its strain rate dependency under the present strain rate has to be considered.



Compression / Tension

Previous investigations [Cadoni, 2018] have shown that the strain rate sensitivity of structural steel significantly deviates in tension and compression.



HFMI simulation – Specimens of Parent Material

Specimens of parent material

- Specimens of parent material S355 simulated and measured in a previous study [Foehebach, 2016] were simulated as a first step for the validation of the method

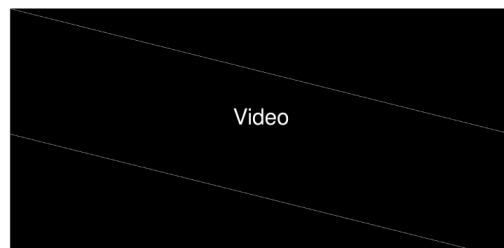
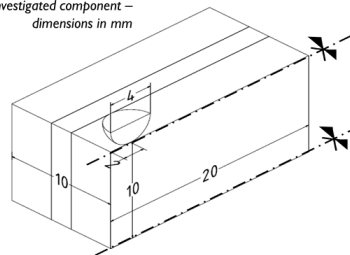
Highlights of the Simulation

- Simulation is carried out with LS Dyna [LS-Dyna, 2016]
- Coulomb-friction is applied: coefficients in previous studies and from textbook knowledge deviate from each other significantly, 0.30 to 0.15 is currently applied
- Bilinear material model, with kinematic, isotropic and mixed hardening is applied
- Strain-rate dependency is taken into consideration with the Cowper-Symonds model
- Rigid body properties (mass, inertia) attributed to the HFMI Pin

The Cowper Symonds material model

$$\dot{\epsilon}_{pl} = D \cdot \left(\frac{\sigma_y'}{\sigma_y} - 1 \right)^q$$

investigated component – dimensions in mm



Stefanos Gkatzogiannis, 8th Workshop Machine Hammer Peening – 22 and 23 October, Karlsruhe Institute of Technology, Germany

Simulation of HFMI

Modelling the Pin Motion

Stefanos Gkatzogiannis, 8th Workshop Machine Hammer Peening – 22 and 23 October, Karlsruhe Institute of Technology, Germany

13

HFMI Simulation – Modelling the Pin Motion

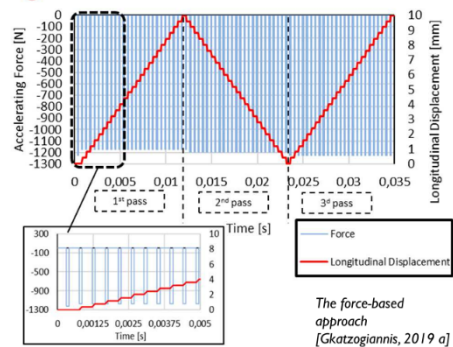
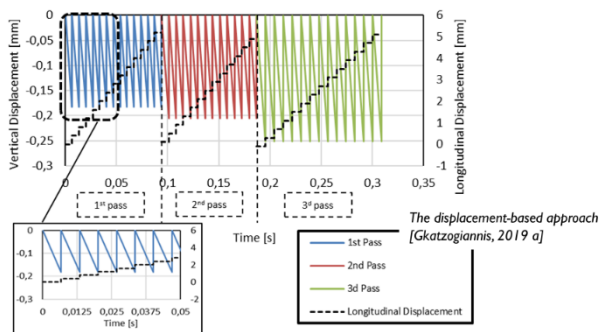
Two methods can be applied for modelling the pin vertical motion, a displacement- and a force-based

Displacement-based

- + more straightforward to simulate
- + measurement of the trace
- unrealistic strain rate evolution – erroneous coupling with strain rate dependent material

Force-based

- + calibration of the model through trial and error is needed
- + realistic strain rate evolution
- measurement of contact force or impact velocity



Stefanos Gkatzogiannis, 8th Workshop Machine Hammer Peening – 22 and 23 October, Karlsruhe Institute of Technology, Germany

14

Drop Tests

Calibration of Material Behavior Through Drop Tests

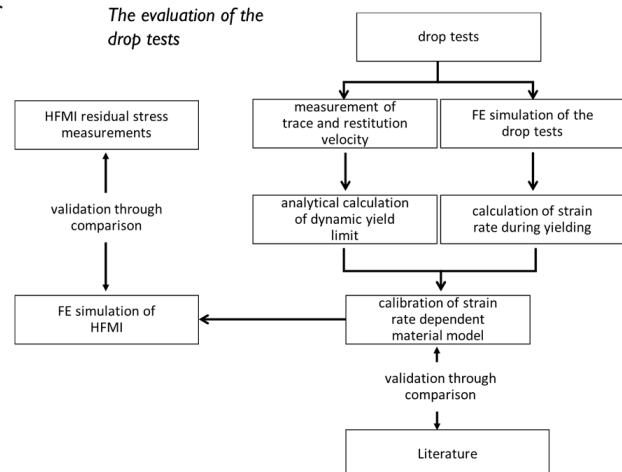
Stefanos Gkatzogiannis, 8th Workshop Machine Hammer Peening – 22 and 23 October, Karlsruhe Institute of Technology, Germany

15

Drop Tests

- A series of drop tests was carried out in order to reproduce a single HFMI impact in the laboratory under known impact velocity and force (mass)
- Goal was the evaluation of the dynamic yield stress under the present deformation mode
- FE analyses would provide the strain rate for each impact
- Analytical calculations based on measurements of the trace or the rebound velocity would be applied for the calculation of the dynamic yield stress
- 1st step validation through comparison with high strain rate tensile tests [HFH-Simulation], literature – 2nd step validation through application of the calibrated material model in a HFMI Simulation and comparison with RS

The evaluation of the drop tests



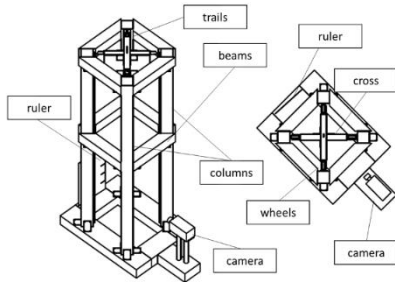
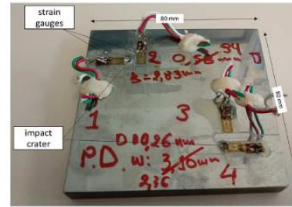
Stefanos Gkatzogiannis, 8th Workshop Machine Hammer Peening – 22 and 23 October, Karlsruhe Institute of Technology, Germany

16

Drop Tests

Test setup for the drop tests

- A wooden bearing structure carries 4 rails – an impact assembly runs across the rails, the pin on its bottom hits the target
- Satisfactory accuracy:
 - impact velocities in the range of the measured for HIFIT and PITEC achieved (2 m/s – 5 m/s),
 - maximum rotation of $\pm 1^\circ$
 - adequate tolerance, no breaking down of the free fall
 - rebound velocity measured with video camera 120 fps, accuracy of ± 0.001 m/s



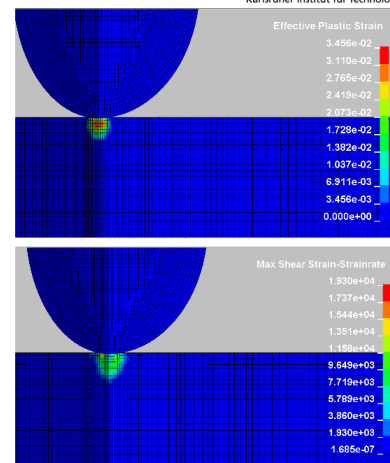
Stefanos Gkatzogiannis, 8th Workshop Machine Hammer Peening – 22 and 23 October, Karlsruhe Institute of Technology, Germany

17

Drop Tests

Results

- Determination of the strain rate with FE simulation of the experiment:
 - strain rate independent elastic-plastic behavior
 - strain rates too high especially at initiation of contact (singularities)
 - split Hopkinson bar impact velocities of 9, 18 and 27 m/s lead to strain rates of 900 to 7000 s^{-1} [Cadoni, 2018]
- Analytical calculation of the dynamic yield stress based on trace measurement analogous to cylindrical indentation [Lim, 1998]: not possible for present impact velocities and a spherical indenter
- Analytical calculation of the dynamic yield stress based on rebound velocity [Tabor, 1948 - Johnson, 1985]:
 - measurement of rebound velocity was successful
 - satisfactory results for S355 - unsatisfactory results for S690, S960
- Factors of the method producing errors are:
 - the assumption of strain rate independent material behavior in the FE simulation of the experiment
 - the formula for calculating yield strength based on rebound velocity far too empirical

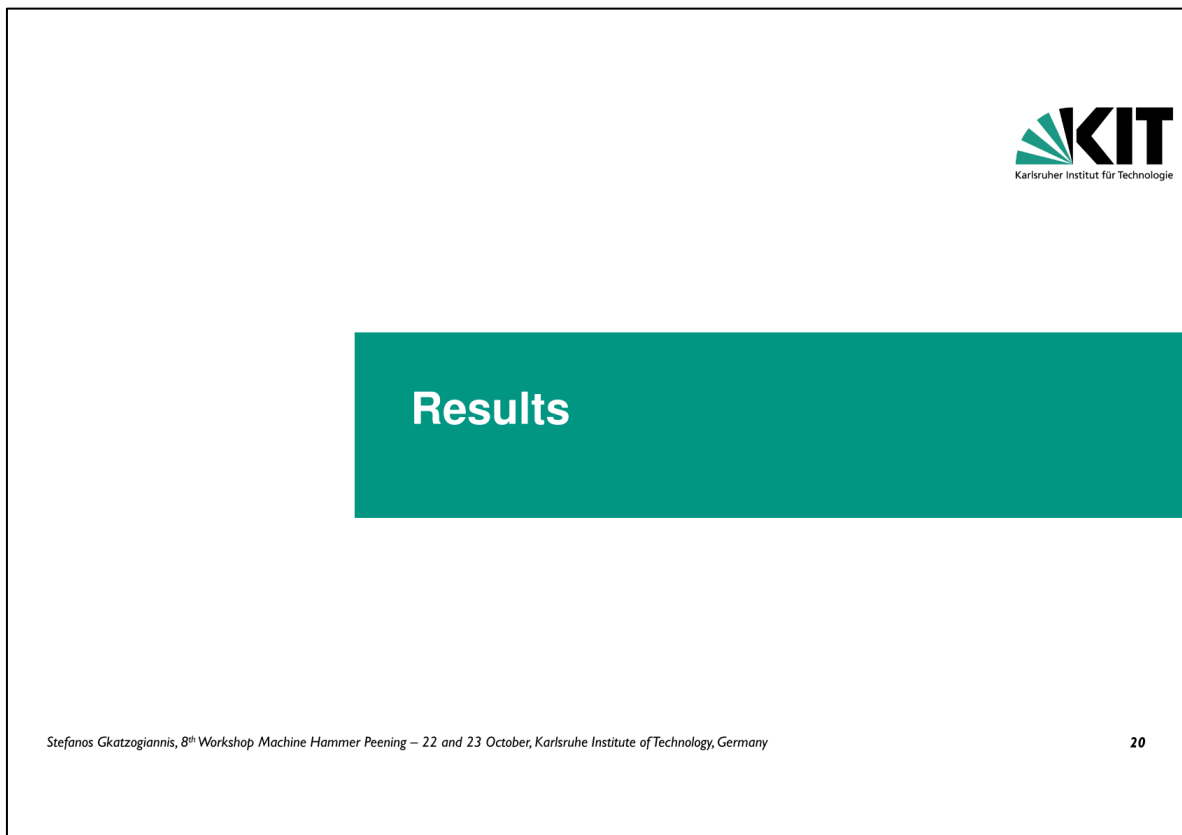
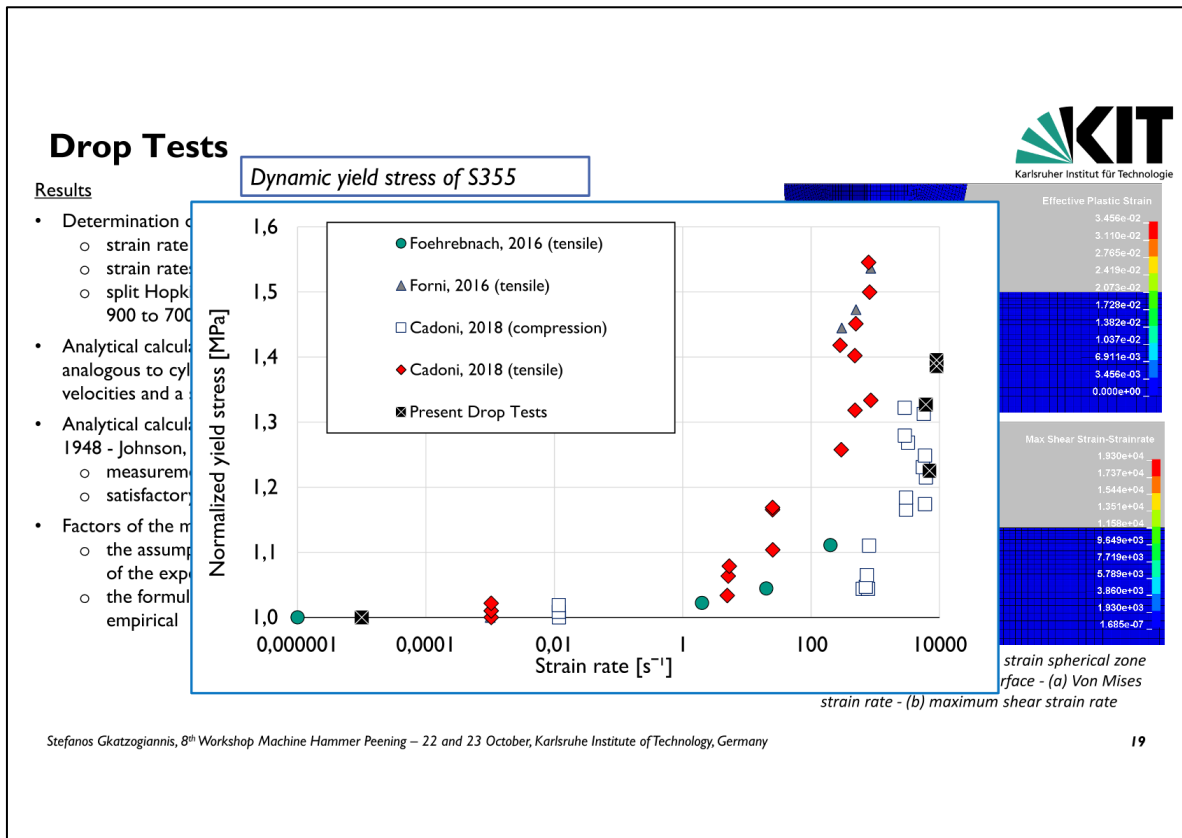


Introduction of the plastic strain spherical zone underneath the impact surface - (a) Von Mises strain rate - (b) maximum shear strain rate

Stefanos Gkatzogiannis, 8th Workshop Machine Hammer Peening – 22 and 23 October, Karlsruhe Institute of Technology, Germany

18

#



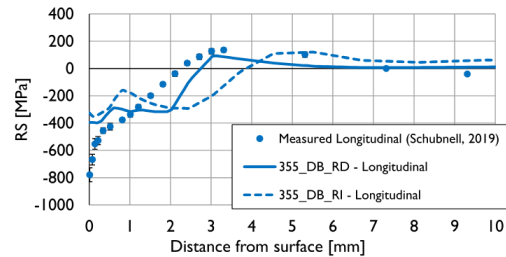
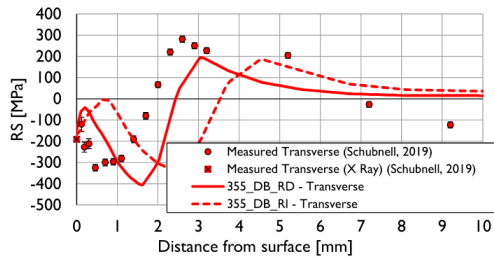
HFMI Simulation - Results

Results referenced as [Schubnell, 2019] are the same ones from [Foehrenbach, 2016]

Results with the displacement-based (DB) method

- Two models were simulated, a strain rate independent (RI) and a dependent (RD)
- Simulated RS results follow qualitatively the pattern of the measured transverse RS – nevertheless, the peak lies significantly deeper in the simulation
- In the case of the longitudinal RS, the model does not predict the RS profile not even qualitatively, especially near the surface

- The introduction of the strain rate dependency seems to improve the agreement between measurements and simulation, nevertheless its use with a displacement base approach is questionable and has no potential for further improvement (measurement restrictions)



Stefanos Gkatzogiannis, 8th Workshop Machine Hammer Peening – 22 and 23 October, Karlsruhe Institute of Technology, Germany

21

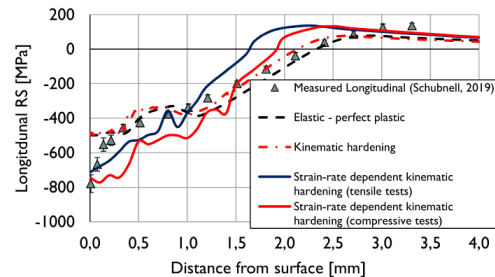
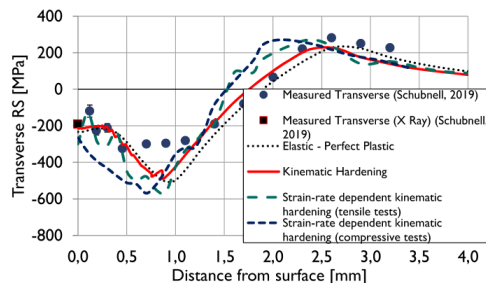
HFMI Simulation - Results

Results referenced as [Schubnell, 2019] are the same ones from [Foehrenbach, 2016]

Results with the force-based (FB) method

- Four different models were simulated
- Simulated RS results follow qualitatively and quantitatively the pattern of the measured RS, both for the transverse and the longitudinal case
- In the case of the transverse RS, all models provide similar agreement with the measured stresses

- Against initial expectations the compressive strain rate dependent model is less accurate – input data is to be accounted for [Gkatzogiannis, 2019 a]
- In the case of the longitudinal RS, the strain rate independent models seem to underestimate the RS near the surface
- The overall evaluation of the results strain rate dependency is predominant for S355



Stefanos Gkatzogiannis, 8th Workshop Machine Hammer Peening – 22 and 23 October, Karlsruhe Institute of Technology, Germany

22

Summary and Upcoming Results

Stefanos Gkatzogiannis, 8th Workshop Machine Hammer Peening – 22 and 23 October, Karlsruhe Institute of Technology, Germany

23

HFMI Simulation – Summary of Previous Results and Open Questions

Two main aspects of the HFMI Simulation were investigated by modelling specimens of parent material:

- Modelling the movement of the HFMI Pin:
 - Two different approaches for simulating the predominant vertical motion of the pin were applied: a displacement- and a force-based
 - Introduction of strain rate dependency into the simulation improves significantly the agreement between simulated and measured RS, however introduction to the displacement-based simulation is questionable
 - Force-based approach provides better agreement with the measured profiles and allows for the consideration of a strain rate dependent behaviour
- Calibration of Material behaviour based on the Dropt Tests:
 - Cowper Symonds strain rate dependent material model was calibrated based on the results of the drop tests
 - Compressive results by [Cadoni, 2018] were taken into consideration as well to increase the sample
 - Simulation of HFMI using the calibrated, strain rate dependent material model, presents much better agreement with the measured RS than the strain rate independent plasticity models

Open Questions

- Real scale welded components – numerical capacity problems arise [Gkatzogiannis, 2019 b]
- Influence of WRS – coupling with welding simulation [Gkatzogiannis, 2019 b]
- Coupling with fracture mechanics investigations

Stefanos Gkatzogiannis, 8th Workshop Machine Hammer Peening – 22 and 23 October, Karlsruhe Institute of Technology, Germany

24

HFMI Simulation – Upcoming Results



KIT
Karlsruher Institut für Technologie

- Dissertation [Gkatzogiannis, 2019 b]
- Ongoing research project ends in December, 2019:

Schubnell J., Gkatzogiannis S., Farajian M., Knoedel P., Ummerhofer T.: IGF-Vorhaben Nr. 19227 N – Rechnergestütztes Bewertungstool zum Nachweis der Lebensdauerverlängerung von mit dem Hochfrequenz-Hämmerverfahren (HFMI) behandelten Schweißverbindungen aus hochfesten Stählen

Research partners:



Fraunhofer
IWM



KIT
Karlsruher Institut für Technologie
VERSUCHSANSTALT
FÜR STAHL, HOLZ & STEINE

Funded by:



DVS



Bundesministerium
für Wirtschaft
und Energie



AF

Industrial partners:



BILFINGER



ACCTH



VOLVO
Construction Equipment



KREBS+KIEFER



RAMBOLL IMS



get it right®



HiFIT
High Frequency Impact Treatment



aerodyn®



SCHACHTBAU
NORDHAUSEN



BOMBARDIER



ipu



MAURER SÖHNE
forces in motion



Ingenieurbüro für
Bautechnik



tkb. Technologiekontor Bremerhaven




SENVION



PIT EC voestalpine
EINEN SCHRITT VORAUS.

25

HFMI Simulation – Upcoming Results




KIT
Karlsruher Institut für Technologie


- Dissertation [Gkatzogiannis, 2019 b]
- Ongoing research project ends in December, 2019:

Schubnell J., Gkatzogiannis S., Farajian M., Knoedel P., Ummerhofer T.: IGF-Vorhaben Nr. 19227 N – Rechnergestütztes Bewertungstool zum Nachweis der Lebensdauerverlängerung von mit dem Hochfrequenz-Hämmerverfahren (HFMI) behandelten Schweißverbindungen aus hochfesten Stählen

Research partners:




Fraunhofer
IWM




KIT
VERSUCHSANSTALT
FÜR STAHL, HOLZ & STEINE

Funded by:

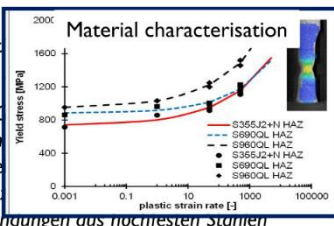


DVS

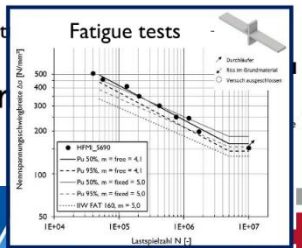


AF

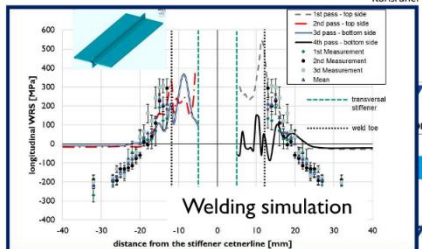
Material characterisation



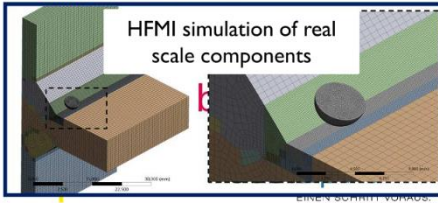
Fatigue tests



Welding simulation



HFMI simulation of real scale components



26

Thank you very much for your attention!



References

[Boyce, 2001]	Boyce B. L., Chen X., Hutchinson J. W., Ritchie R. O.; The Residual Stress State due to a Spherical Hard-Body Impact, <i>Mechanics of Materials</i> 33, pp. 441-454, 2001.
[Boyce, 2007]	Boyce B. L., Crenshaw T. B., Dilmore M. F.; The Strain-Rate Sensitivity of High-Strength High-Toughness Steels, SANDIA REPORT, SAND2007-0036, Unlimited Release, January 2007.
[Cadoni, 2018]	Cadoni E., Forni D., Gielela R., Kruszka L.; Tensile and Compressive Behaviour of S355 Mild Steel in a Wide Range of Strain Rates; <i>The European Physical Journal Special Topics</i> 227, pp. 29-43, 2018.
[DAST, 2019]	DAST – Richtlinie 026; Ermüdungsverbesserung bei Anwendung höherfrequenter Hämmerverfahren, 2019.
[Foehrenbach, 2016]	Foehrenbach J., Hardenacke V., Farajian M.; High Frequency Mechanical Impact Treatment (HFMI) for the Fatigue Improvement: Numerical and Experimental Investigations to describe the Condition in the Surface Layer, <i>Welding in the World</i> 60 (4), pp. 749–755, 2016.
[Forni, 2016]	Forni D., Chiaia B., Cadoni E.; Strain Rate Behaviour in Tension of S355 Steel: Base for Progressive Collapse Analysis, <i>Engineering Structures</i> 119, pp. 167-173, 2016.
[Gkatzogiannis, 2019]	Gkatzogiannis S., Knoedel P., Ummenhofer T.; Calibration of HFMI Simulation based on Drop Tests, <i>EUROMAT 19</i> , 1-6 September, Stockholm, 2019.
[Gkatzogiannis, 2019 b]	Gkatzogiannis S.; Finite Element Simulation of Residual Stresses from Welding and High Frequency Hammer Peening, Doctoral Dissertation, Karlsruhe Institute of Technology, Steel- and Lightweight Structures, to be submitted in 2019.
[Kuhlman, 2018]	Kuhlman U., Breunig S., Ummenhofer T., Weidner P.; Entwicklung einer DAST-Richtlinie für höherfrequente Hämmerverfahren - Zusammenfassung der durchgeführten Untersuchungen und Vorschlag eines DAST-Richtlinien-Entwurfs, <i>Stahlbau</i> 87 (10), pp. 967-983, 2018.
[LS Dyna, 2016]	LS-DYNA, Theory Manual, Livermore Software Technology Corporation (LSTC), Livermore California 2016.
[Marquis, 2016]	Marquis G. B., Barsoum Z.; IIW Recommendations for the HFMI Treatment – For Improving the Fatigue Strength of Welded Joints, 1st Edition, Springer Singapore (IIW Collection), Singapore 2016.
[Ummenhofer, 2009]	Ummenhofer T.; REFRESH: Lebensdauererlängerung bestehender und neuer geschweißter Stahlkonstruktionen, Abschlussbericht D 761, KIT Stahl- und Leichtbau, Versuchsanstalt für Stahl, Holz und Steine, Karlsruhe, 2009.
[Ummenhofer, 2013]	Ummenhofer T., Weidner P.; Improvement Factors for the Design of Welded Joints subjected to High Frequency Mechanical Impact Treatment, <i>Steel Construction</i> 6 (3), pp. 191-199, 2013.
[Ummenhofer, 2018]	Ummenhofer T., Engelhardt I., Knoedel P., Gkatzogiannis S., Weinert J., Loeschner D.; Erhöhung der Ermüdungsfestigkeit von Offshore-Windenergieanlagen durch Schweißnahtnachbehandlung unter Berücksichtigung des Korrosionseinflusses, Schlussbericht, DVS 09069 – IGF 18457 N, KIT Stahl- und Leichtbau, Versuchsanstalt für Stahl, Holz und Steine, Karlsruhe und Hochschule für angewandte Wissenschaften München, Labor für Stahl- und Leichtmetallbau, Germany, 2018.
[Yildirim, 2013]	Yildirim H. C., Marquis G. B.; Overview of Fatigue Data for High Frequency Mechanical Impact Treated Welded Joints, <i>Weld World</i> 56 (7-8), pp. 82-96, 2013.

Stefanos Gkatzogiannis, 8th Workshop Machine Hammer Peening – 22 and 23 October, Karlsruhe Institute of Technology, Germany

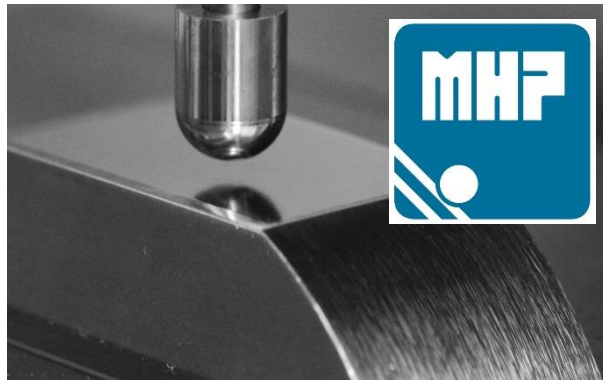
27

Influence of mechanical surface treatments on propagation and opening behavior of physically short cracks in Inconel 718

Alexander Klumpp

IAM-WK – Institute for Applied Materials

Karlsruhe Institute of Technology

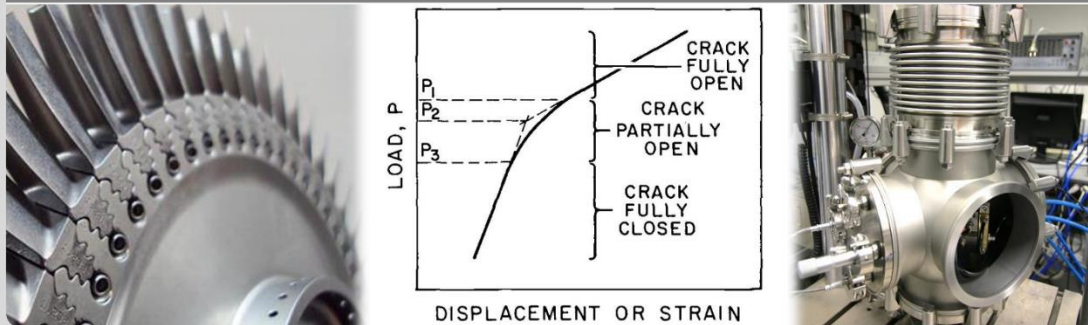


Influence of mechanical surface treatments on propagation and opening behavior of physically short cracks in Inconel 718

Einfluss mechanischer Oberflächenbehandlungen auf das Ausbreitungs- und Öffnungsverhalten physikalisch kurzer Risse in Inconel 718

Symposium Mechanische Oberflächenbehandlung, 22.10.2019
 Alexander Klumpp

Institut für Angewandte Materialien - Werkstoffkunde



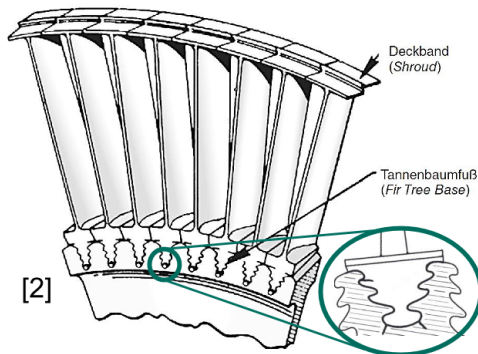
KIT – Die Forschungsuniversität in der Helmholtz-Gemeinschaft



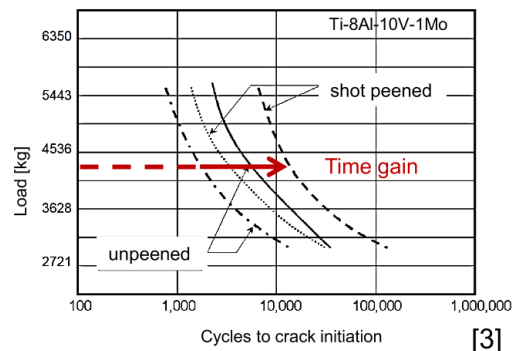
www.kit.edu

Motivation: Turbine disc material Inconel 718

- Fir tree base („Tannenbaumfuß“) for vibration damping
 - Complex highly-stressed
 - Shot peening: SAE / AMS; Intensity: 0,18 ~ 0,25 mmA [1]
- Low cycle fatigue design



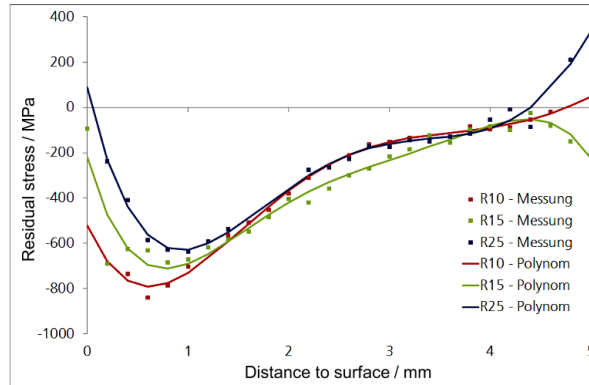
[1] Polanetzki, H. (MTU AG): DGM workshop material
 [2] Bräunling, W.: Flugzeugtriebwerke, Springer 2015



- Scope: Characterization of near-surface short crack growth
 - Focus: Physically short cracks (0,2 mm a <math>< 1</math> mm); K-concept

[3] Curtiss-Wright Corp., Online-Brochure

Motivation: Recent developments in machine hammer peening (MHP)



ECOROLL AG /
Fraunhofer IWM

- Studies regarding residual stress evolution in Inconel 718:
 - Mechanical MHP system type „EcoPeen“
 - Several millimeters of residual stress penetration depth are feasible
 - Investigation of crack behavior after shot peening and other mechanical surface treatments

3

22.10.2019

Alexander Klumpp: Influence of mechanical surface treatments on propagation and opening behavior of physically short cracks in Inconel 718



Outline



- Basics of fracture mechanics
- Material and mechanical surface treatments
- Experimental setup for characterization of short crack propagation and opening
- Results and discussion
- Conclusion

4

22.10.2019

Alexander Klumpp: Influence of mechanical surface treatments on propagation and opening behavior of physically short cracks in Inconel 718





K-concept and „intrinsic“ approach

- Stress intensity $K_I / K / K_{nom}$ for characterization of mechanical crack load in mode I

$$K_{nom} = \sigma \sqrt{\pi a} Y \text{ (static load)}$$

$$\Delta K_{nom} = \Delta \sigma \sqrt{\pi a} Y = K_{max} - K_{min}$$

$$R_{nom} = \frac{K_{min}}{K_{max}} \text{ (cyclic fatigue load)}$$

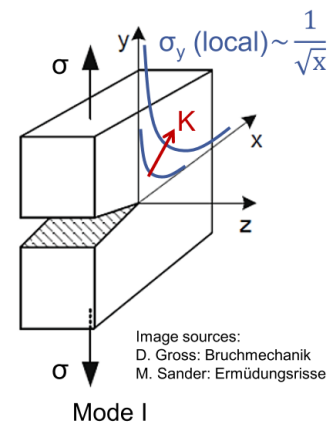
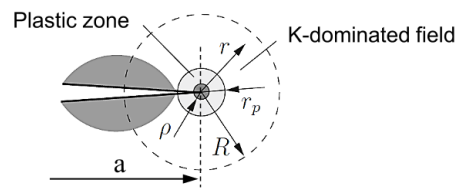


Image sources:
 D. Gross: Bruchmechanik
 M. Sander: Ermüdungsrisse

- Cyclic fatigue crack growth governed by the material's „intrinsic“ resistance (Ritchie, 1988)
 → Against formation of new surfaces

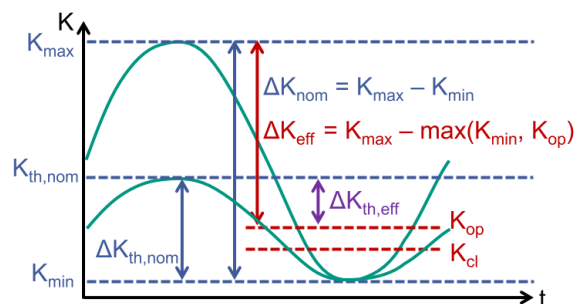
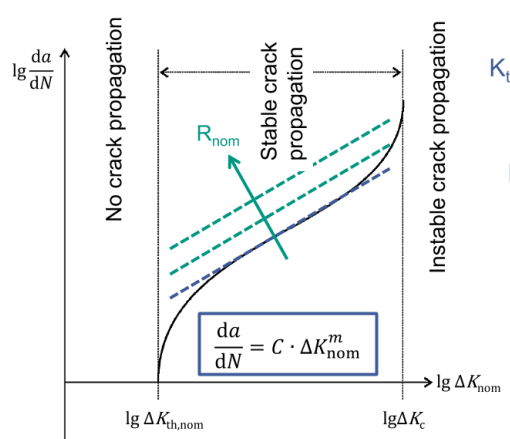
Literature: Ritchie, R. O. (1988). Mechanisms of fatigue crack propagation in metals, ceramics and composites: role of crack tip shielding. *Materials Science and Engineering: A*, 103(1), 15-28.



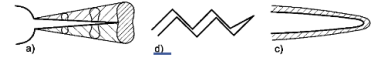
Closure-based („extrinsic“) concept



- Paris diagram (1961) for long crack propagation



- Crack closure effect** (Elber, 1971)
 - E.g. due to plasticity, roughness, compressive residual stresses

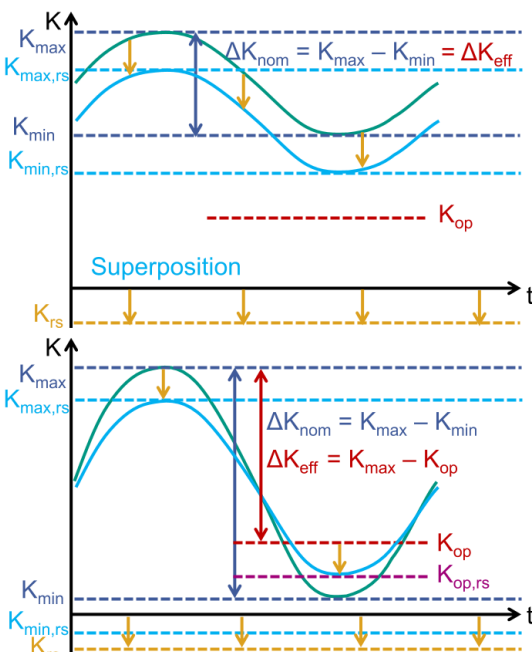


- Effective threshold $\Delta K_{th,eff}$**
 → Dependent on work hardening

- Further effects of residual stresses?



Effects of residual stresses



- „Residual stress intensity“ K_{rs}
 - Weight function / numerical determination (FE)
 - No closure, both with res. stress
 - Local load ratio (R_{eff}) affected, but not ΔK_{eff}

$\Delta K_{eff} = \Delta K_{nom}$

$R_{eff} = \frac{K_{min,rs}}{K_{max,rs}} \neq R_{nom}$
 - Closure effect with res. stress
 - Both ΔK_{eff} and R_{eff} are affected

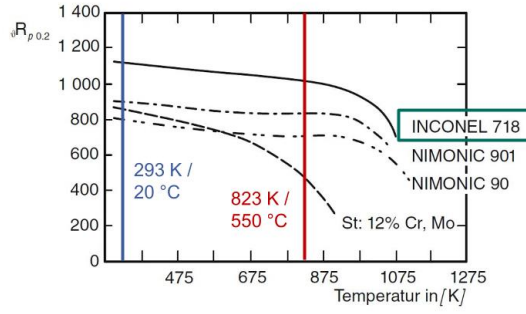
$\Delta K_{eff} = K_{max} - K_{op} \neq \Delta K_{nom}$

$R_{eff} = \frac{K_{op,rs}}{K_{max,rs}} \neq R_{nom}$
- Numerical and experimental methods are required!

Material: Alloy „Inconel“ 718

Chemical composition (mass %)									
Ni	Fe	Cr	Mo	Ti	Nb	Al	Co	Mn	C
Basis	18,80	18,40	2,91	0,99	5,28	0,58	0,24	0,07	0,03

- Heat treatment: ASTM B637
 - γ'' -precipitation hardening with two step tempering:
 - 955 °C (1h)
 - 720 °C (8h)
 - 620 °C (8h)
 - Mean γ -grain size: app. 19 μm
- Micro hardness: app. 460 HV 0,1
- Tests at 20 °C and 550 °C
 - Mechanical properties [1]



[1] Bräunling, W.: Flugzeugtriebwerke, Springer 2015

Mechanical surface treatments (Support by OSK Kiefer, Malsch)



- Goal: Variation of profiles of residual stresses and work hardening (Measure: Micro hardness)

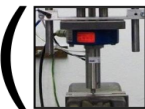
- Application of:



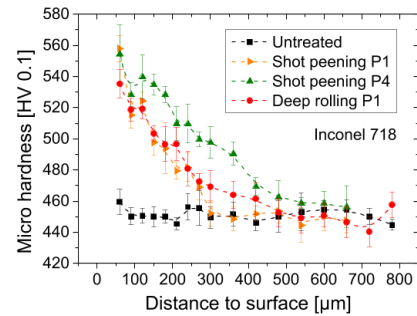
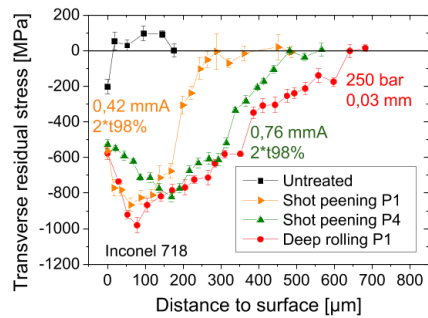
Shot peening: Cut wire G3 Ø 0,8 / S170; 0.21 ~ 0.76 mmA intensity; 100 ~ 300 % coverage



Deep rolling: hard metal Ø 6.35; 200 ~ 250 bar pressure; 0.03 ~ 0.04 mm stepover distance



Piezo peening: Hard metal Ø 5; 36 µm stroke; 500 impacts/s; 0.25 mm stepover distance



9

22.10.2019

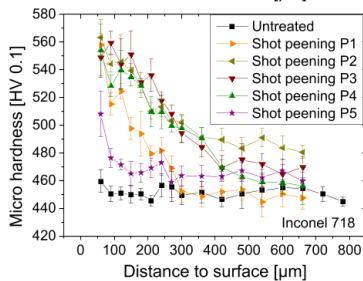
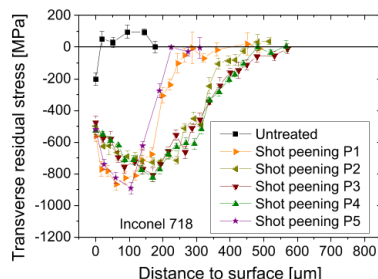
Alexander Klumpp: Influence of mechanical surface treatments on propagation and opening behavior of physically short cracks in Inconel 718



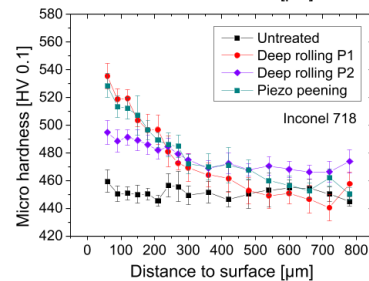
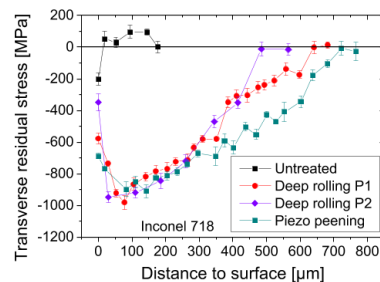
(Print version: All results of surface treatments)



- Shot peening



- Deep rolling / piezo peening



10

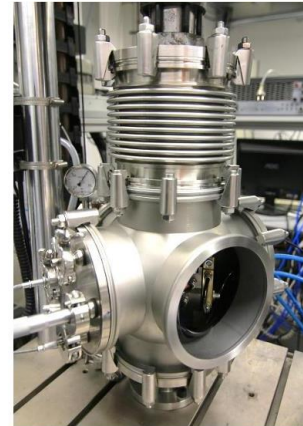
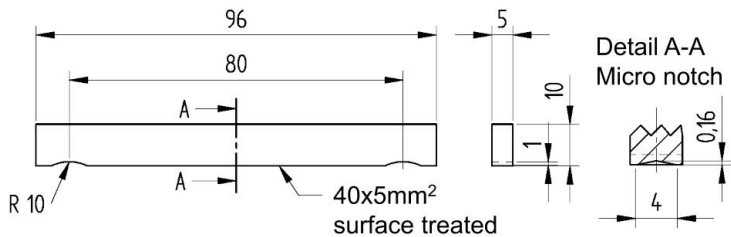
22.10.2019

Alexander Klumpp: Influence of mechanical surface treatments on propagation and opening behavior of physically short cracks in Inconel 718



Experimental procedure

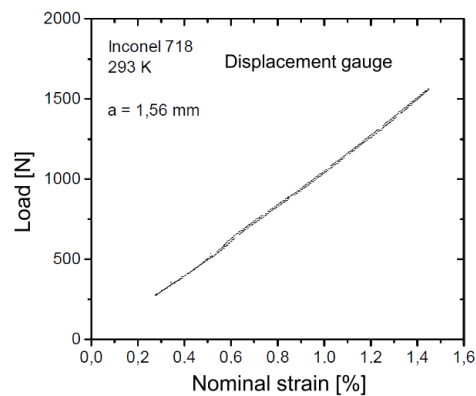
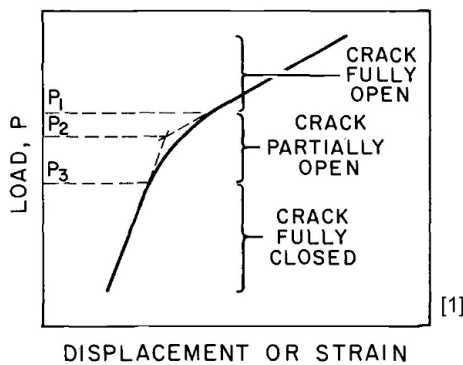
- Linear electro motor based test bench (Instron)
 - Fine vacuum to avoid oxidation
- Specimen geometry for 3P-bending



- Crack growth and opening tests
 - Load ratios: $R_{nom} = 0,01 / 0,5 / 0,7$
 - Test temperatures: 20 °C; 550 °C
 - Captured crack length: 0,25 mm ~ 1,60 mm
 - Necessary: Measurements with very high resolution

Determination of crack opening loads: Classic procedure: *Specimen compliance*

- Principle: Increasing stiffness due to crack closure
- Actual record for a long crack (1,56 mm)



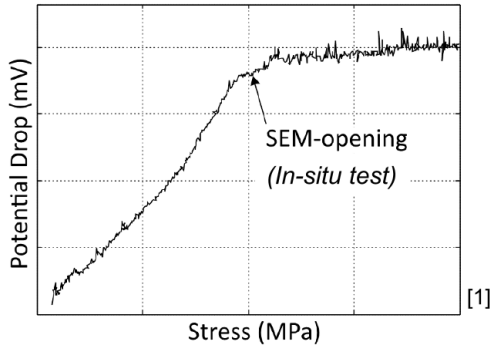
- Resolution is not sufficient for measurements on short cracks after mechanical surface treatments!

[1] Allison, J. E.; Ku, R. C.; Pompetzki, M. A.: A Comparison of Measurement Methods and Numerical Procedures for the Experimental Characterization of Fatigue Crack Closure. In: *Mechanics of Fatigue Crack Closure*, ASTM International, 1988

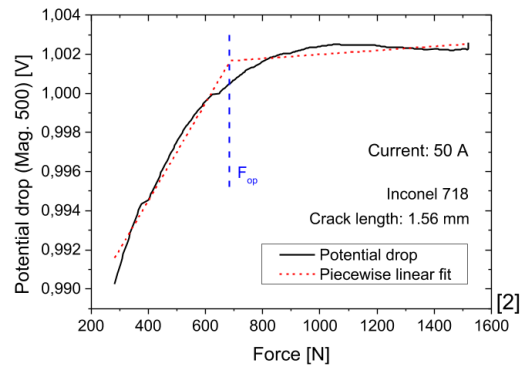
Determination of crack opening loads: Classic procedure: *Potential drop method*



- Plateau formation of electrical voltage due to crack opening



- Suitable for long cracks; no proper resolution for short cracks



- Other methods: DIC, Eddy, Ultrasonic, ISDG (Laser), Barkhausen
- Get the maximum out of the potential drop method

[1] Andersson, M. et al.: Experimental and numerical investigation of crack closure measurements with electrical potential drop technique. *International Journal of Fatigue* 28 (2006), Nr. 9, S. 1059–1068

[2] Klumpp, A. et al.: Influence of work-hardening on fatigue crack growth, effective threshold and crack opening behavior in the nickel-based superalloy Inconel 718. In: *International Journal of Fatigue* 116 (2018), S. 257–267

13

22.10.2019

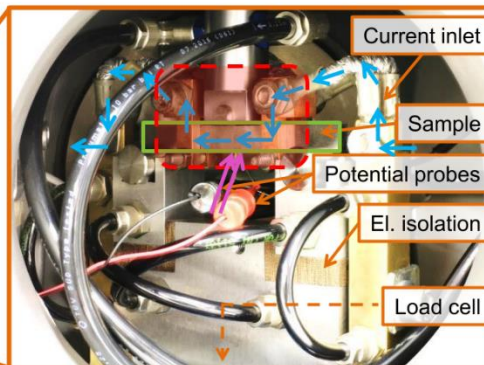
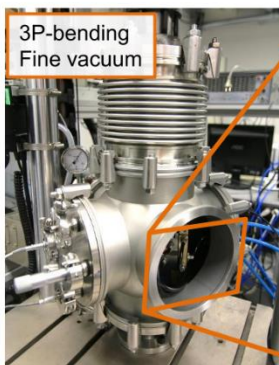
Alexander Klumpp: Influence of mechanical surface treatments on propagation and opening behavior of physically short cracks in Inconel 718



The „elevated current potential drop method“



- Principle:
 - Extremely high currents (>300 A) → reduction of disturbance and noise
 - Setting of test temperature directly by Ohmic losses
 - Potential probes as near as possible to the crack → maximum sensitivity



- 305 A for 823 K
- Prismatic, for low gradients ∇T
- Distance 0.9 mm
- „hot area“ $T(x,t) \approx \text{const.}$; controlled by infrared pyrometer


→ Necessary: Extensive preliminary studies

14

22.10.2019

Alexander Klumpp: Influence of mechanical surface treatments on propagation and opening behavior of physically short cracks in Inconel 718

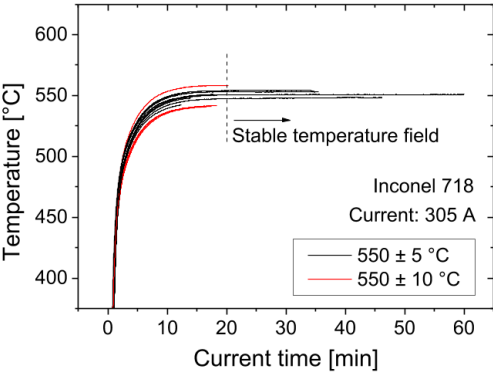




KIT
Karlsruher Institut für Technologie

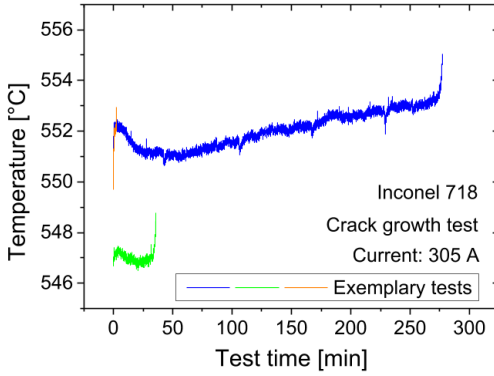
Reproducibility of test temperature

■ Statistical deviations



Inconel 718
Current: 305 A

■ Warming during tests





Inconel 718
Crack growth test
Current: 305 A

→ Reproducible and nearly constant test temperatures

→ Numerical error analyses regarding temperature, work hardening influence and probe positions: *Compromises are necessary*

→ *Measurement of crack opening loads becomes feasible*

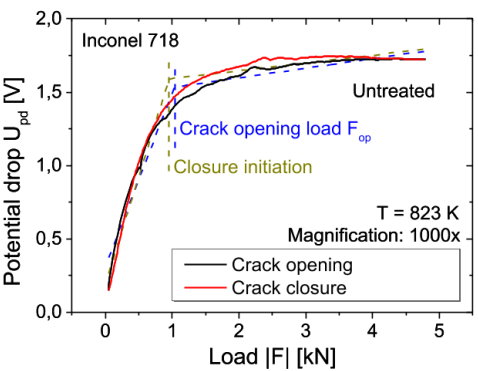
15 22.10.2019
Alexander Klumpp: Influence of mechanical surface treatments on propagation and opening behavior of physically short cracks in Inconel 718




KIT
Karlsruher Institut für Technologie

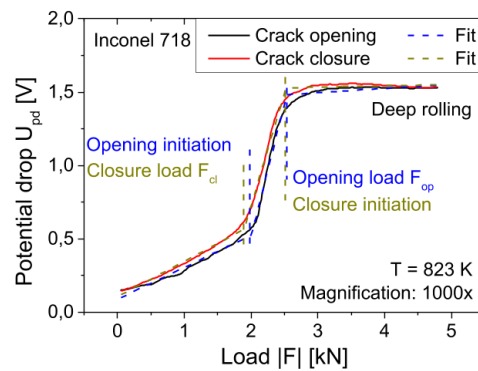
Determination of crack opening loads

■ Untreated state



Inconel 718
Untreated
T = 823 K
Magnification: 1000x

■ Deep rolled state




Inconel 718
Deep rolling
T = 823 K
Magnification: 1000x

■ Bilinear fit, equal to [1]

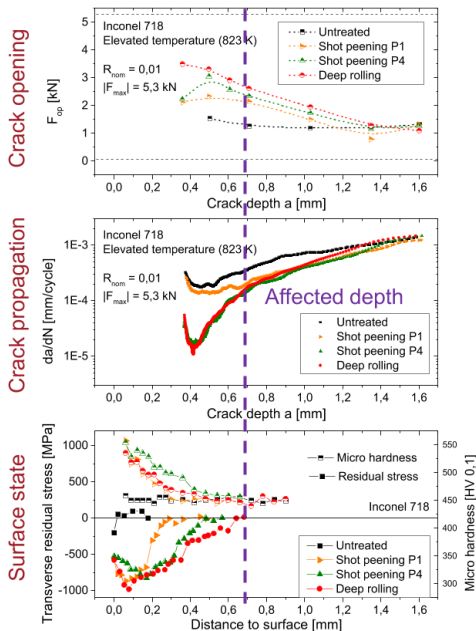
■ Trilinear fit

■ Significant effect of surface treatment:
 „complete“ / „incomplete“ crack closure may occur

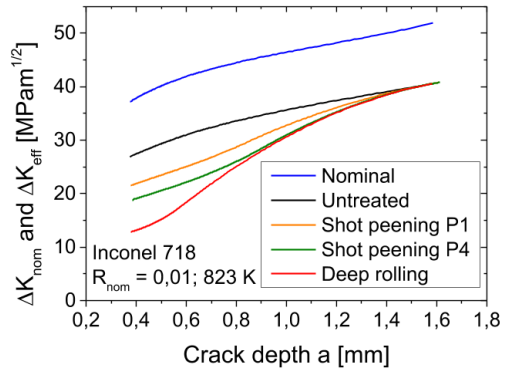
[1] Andersson, M. et al.: Experimental and numerical investigation of crack closure measurements with electrical potential drop technique. *International Journal of Fatigue* 28 (2006), Nr. 9, S. 1059–1068

16 22.10.2019
Alexander Klumpp: Influence of mechanical surface treatments on propagation and opening behavior of physically short cracks in Inconel 718


Correlation opening - growth



■ Correlation between a , ΔK_{nom} , ΔK_{eff} (by means of FEM)



■ Qualitative correlation exists:
 $F_{op} \uparrow \rightarrow \Delta K_{eff} \downarrow \rightarrow da/dN \downarrow$

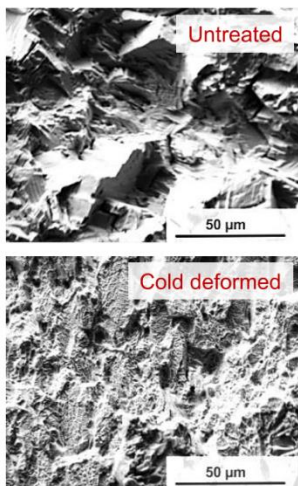
17

22.10.2019

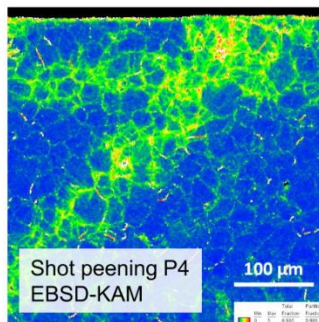
Alexander Klumpp: Influence of mechanical surface treatments on propagation and opening behavior of physically short cracks in Inconel 718

Discussion: Uncertainties during determination of crack driving forces

■ Contribution of roughness-induced crack closure

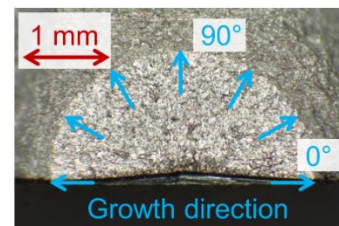


■ Localization of deformation (shear bands)



Credits: A. Kauffmann, IAM-WK

■ Main challenge: Surface cracks after surface treatments



→ Further measures are necessary for clearer results

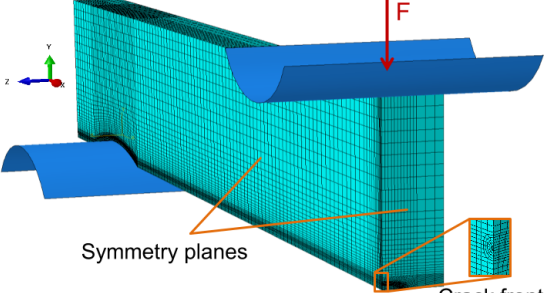
18

22.10.2019

Alexander Klumpp: Influence of mechanical surface treatments on propagation and opening behavior of physically short cracks in Inconel 718

Validation approach: FEM load analysis

■ Quarter model; evaluation of K using „contour integral“ method

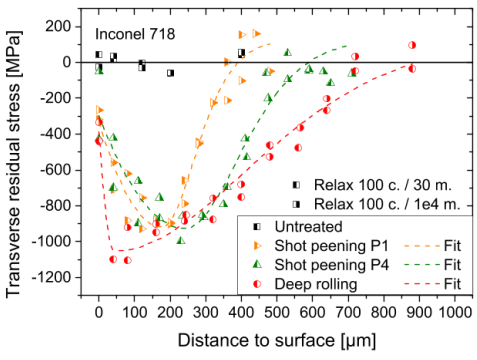


Symmetry planes

Crack front with contours

Approx. 100000x C3D20R
10 discrete models


■ Relaxed (cyclic-thermal) residual stresses as initial condition



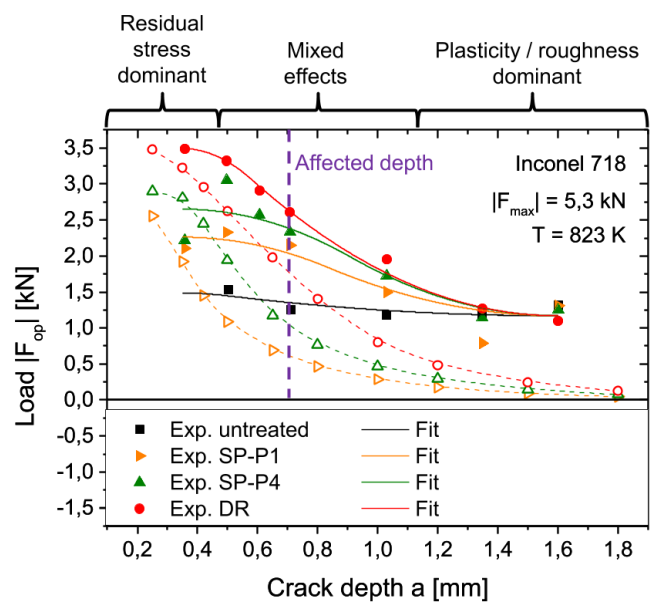
Transverse residual stress [MPa]

Distance to surface [µm]

→ Determination of crack opening loads by using residual stress profiles approximately prevailing at crack initiation

19
22.10.2019
Alexander Klumpp: Influence of mechanical surface treatments on propagation and opening behavior of physically short cracks in Inconel 718


Validation and discussion: Prediction of crack opening in the crack center




Load $|F_{op}|$ [kN]

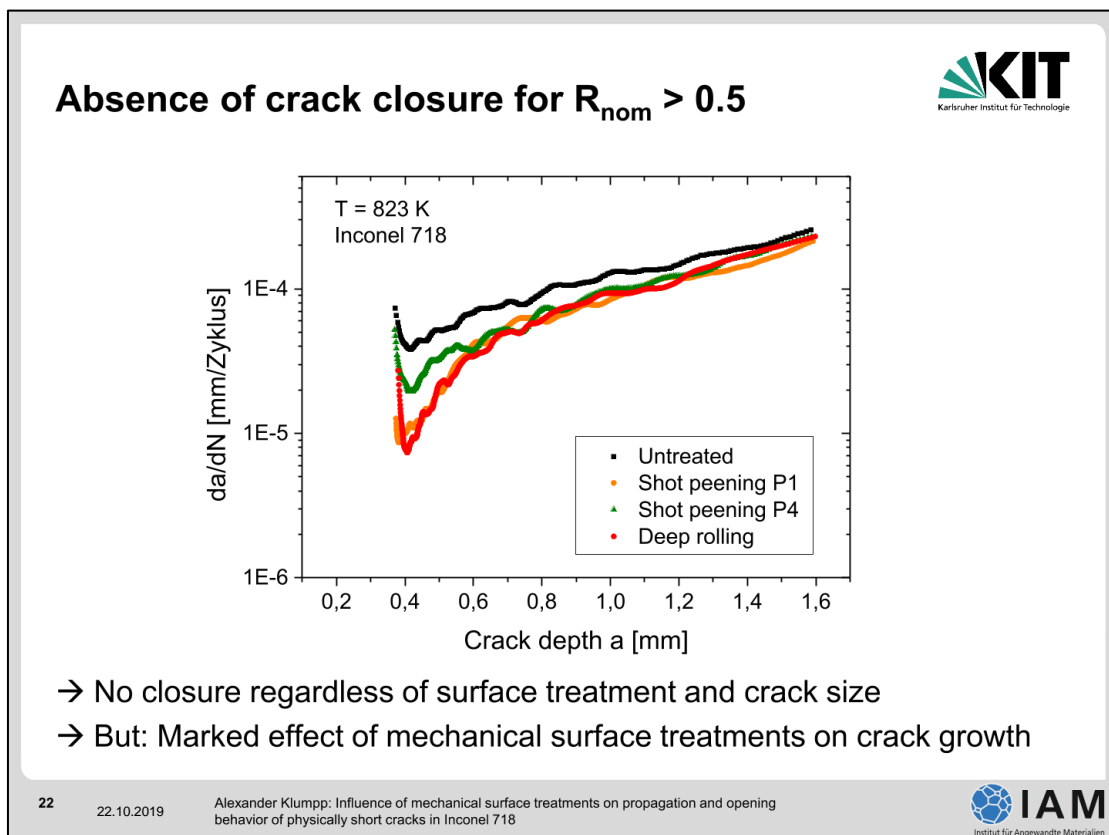
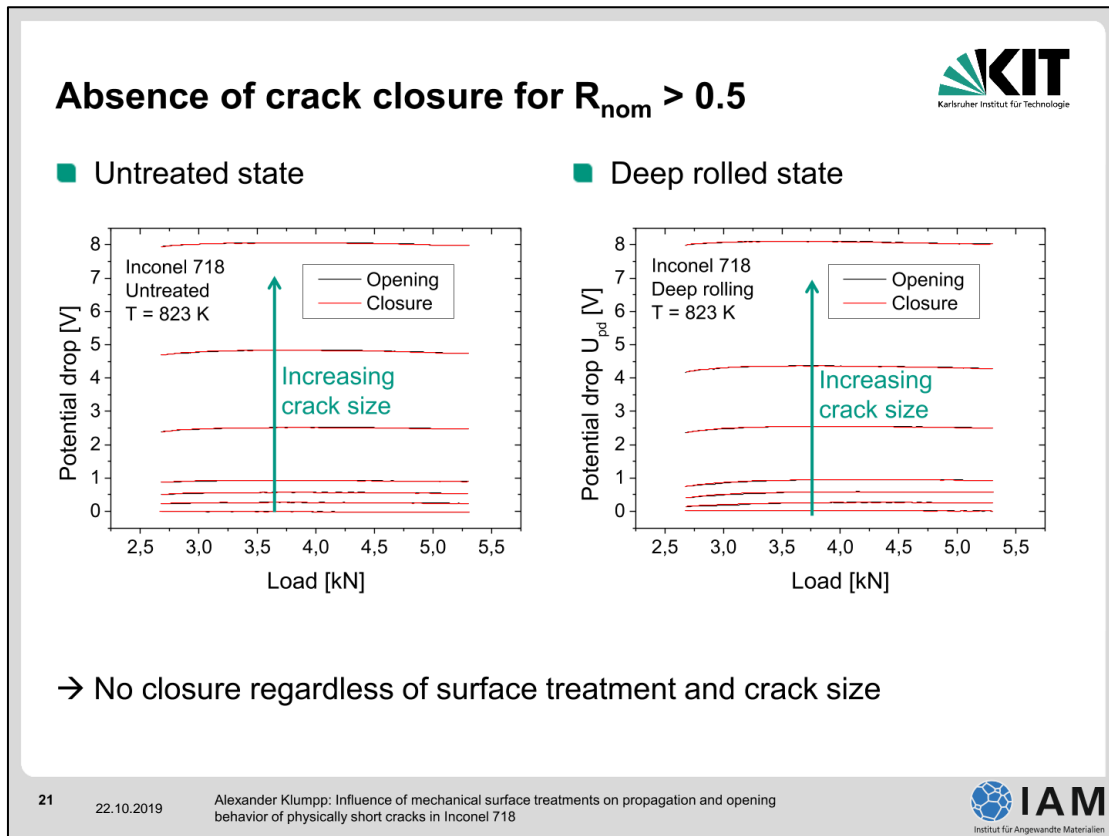
Crack depth a [mm]

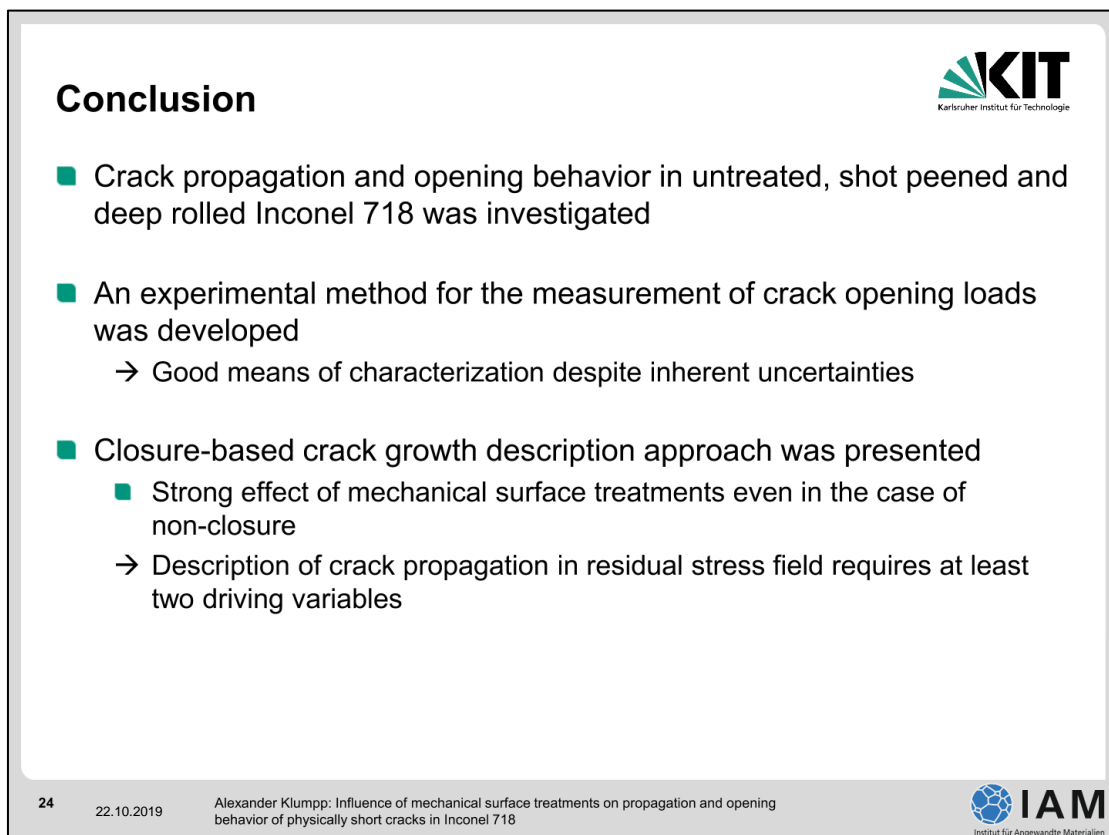
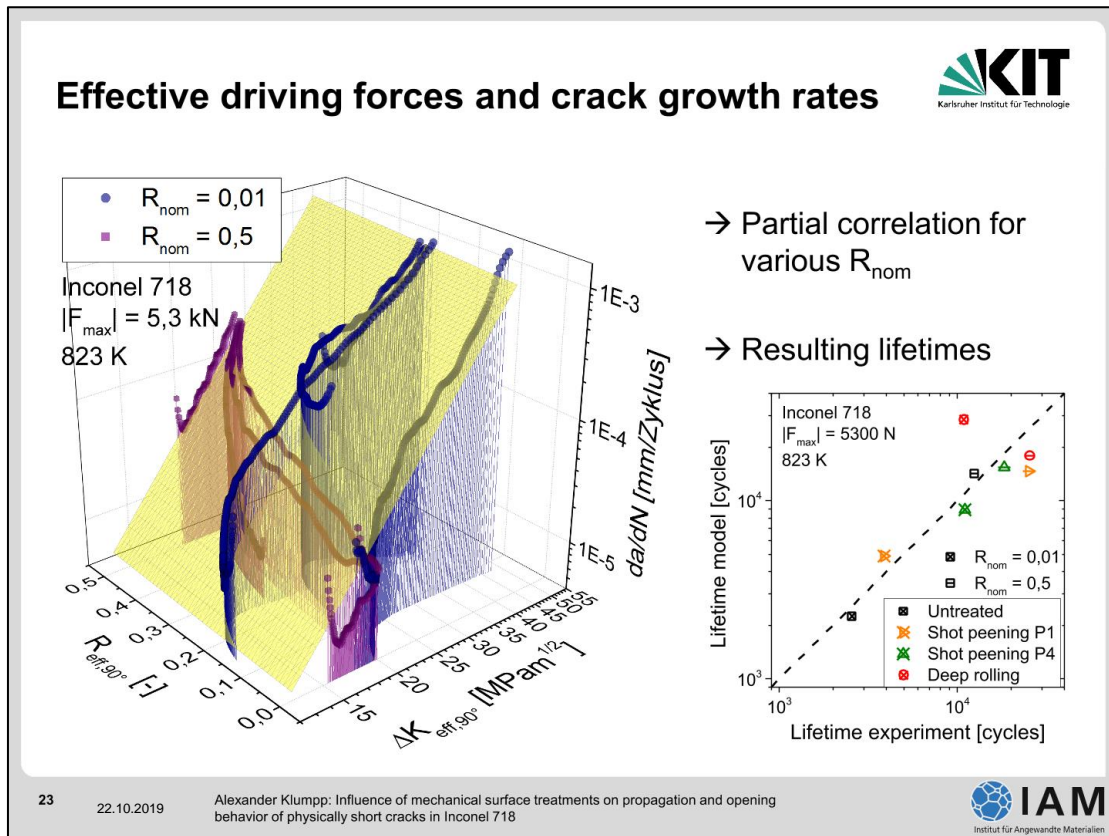
■ Coincidence for very short cracks

■ Increasing deviation with crack depth

→ Explanation:
multicausal crack closure; no prediction possible by means of simple elastic FE analysis!

20
22.10.2019
Alexander Klumpp: Influence of mechanical surface treatments on propagation and opening behavior of physically short cracks in Inconel 718




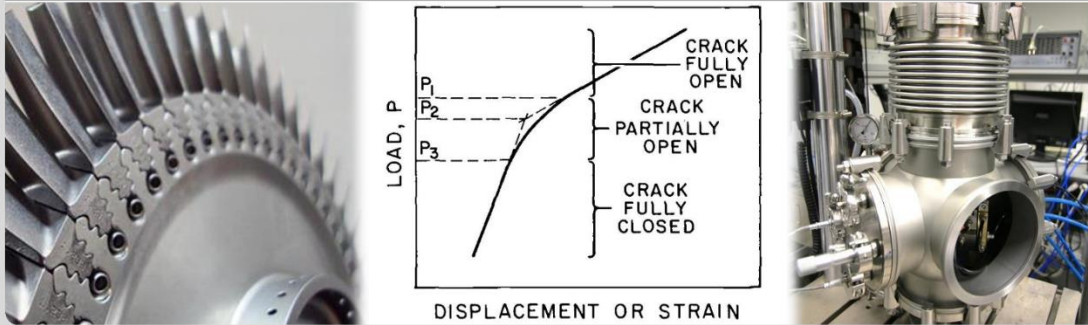




Thank you.



Institut für Angewandte Materialien - Werkstoffkunde



KIT – Die Forschungsuniversität in der Helmholtz-Gemeinschaft

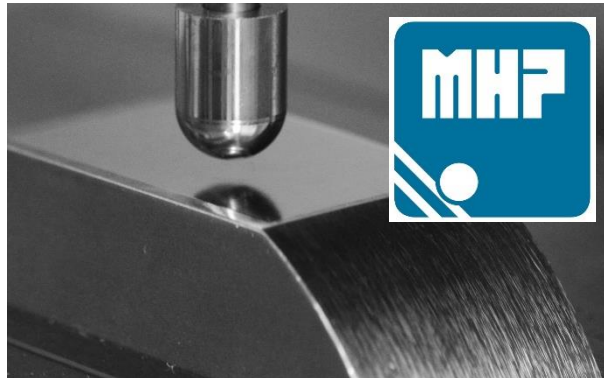


www.kit.edu

Controlled Pneumatic Needle Peening – New Peening Technology for Aerospace Applications

Holger Polanetzki

MTU Aero Engines GmbH





Controlled Pneumatic Needle Peening New Peening Technology for Aerospace Applications

Symposium – Mechanische Oberflächenbehandlung 2019
8th Workshop Machine Hammer Peening
Karlsruhe 22. und 23. Oktober

22. Oktober 2019 Holger Polanetzki

Pneumatic Needle Peening

Contents


Contents

- ▶ Objectives
- ▶ Technology Description
- ▶ Experimental Procedure
- ▶ Results
 - ▶ Surface Roughness
 - ▶ Residual Stress Distribution
 - ▶ Fatigue Testing
- ▶ Application
- ▶ Conclusion
- ▶ Acknowledgement

Pneumatic Needle Peening

2

© MTU Aero Engines AG. The information contained herein is proprietary to the MTU Aero Engines group companies.




Objective


- Develop new technique that could fulfill requirements:
 - Comparable or better results than conventional shot peening
 - Surface Finish
 - Residual Stress Distribution
 - Fatigue Life
 - Acceptable on Rotating Parts
 - Small head for better accessibility
 - No risk of Foreign Object Damage (FOD)
 - Very reproducible process
 - No operator influence

Pneumatic Needle Peening 3


© MTU Aero Engines AG. The information contained herein is proprietary to the MTU Aero Engines group companies.



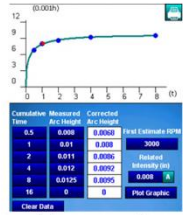
SPIKER® Features




Different Heads and End Caps for different Geometries




Each needle monitored in real time



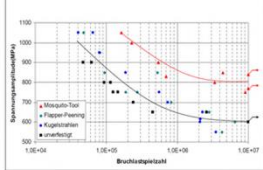
Interface guides operator, record process parameters and makes intensity calculations



Standoff distance maintained at all times



Portable unit for easy transportation




Comparable or better results than flapper or conventional peening



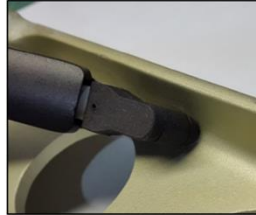
Save Data to USB key for quick reporting

Pneumatic Needle Peening 4

© MTU Aero Engines AG. The information contained herein is proprietary to the MTU Aero Engines group companies.




SPIKER® 4 Needle Linear Head with 3 End Caps

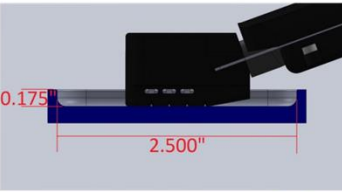
Needles	S230 tip (0.60mm), Tungsten Carbide, 4 needles
End Caps	3 included end caps: Flat surface, Corner radius down to 0.09" (2.3mm) and edge radius
Sensors	Individual tracking for each needle
Input	Proprietary air and electrical input
Maintenance	Replaceable needles and end caps
Intensity range	0.004A - 0.016A – Inch (0.10A - 0.40 mA)
Pressure range	5 - 60 PSI (0.34 – 4.08 bar)

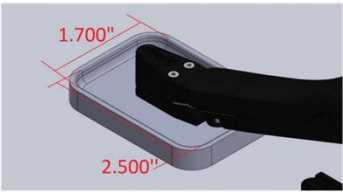
Pneumatic Needle Peening 5

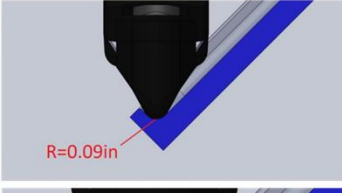
© MTU Aero Engines AG. The information contained herein is proprietary to the MTU Aero Engines group companies.

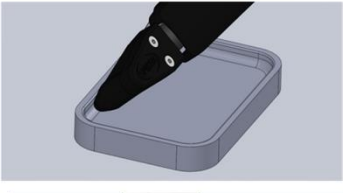


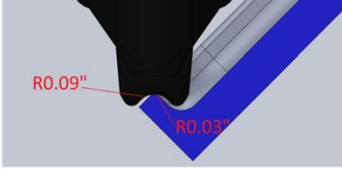
SPIKER® - Radius 0.09 requirements interchangeable caps














Pneumatic Needle Peening 6

© MTU Aero Engines AG. The information contained herein is proprietary to the MTU Aero Engines group companies.



SPIKER® 1 needle Corner Head

- Used on corner, pocket, radius
- Tool in contact with surface enables accurate intensity and repeatability
- Can meet radius of 0.09 inch
- Reach intensity between 4A to 16A



Pneumatic Needle Peening

© MTU Aero Engines AG. The information contained herein is proprietary to the MTU Aero Engines group companies.

7



SPIKER® Performance Testing

- Test program was performed at Technology University Clausthal in Germany under Prof. Dr. L. Wagner's supervision
- Testing was done under the leadership of MTU Aero Engines AG
- Testing looked at surface roughness, residual stress distribution and fatigue life

Pneumatic Needle Peening

© MTU Aero Engines AG. The information contained herein is proprietary to the MTU Aero Engines group companies.

8

MTU
Aero Engines

Experimental Procedure

- Peening Equipment



CNC Conventional Peening



Controlled Rotary Flapper Peening using the FlapSpeed® Controller



Controlled Needle Peening using the Spiker® tool

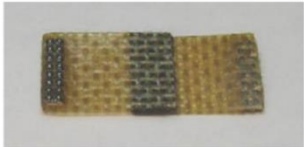
Pneumatic Needle Peening

© MTU Aero Engines AG. The information contained herein is proprietary to the MTU Aero Engines group companies.


MTU
Aero Engines

Experimental Procedure


- Controlled Rotary Flapper Peening



Flap

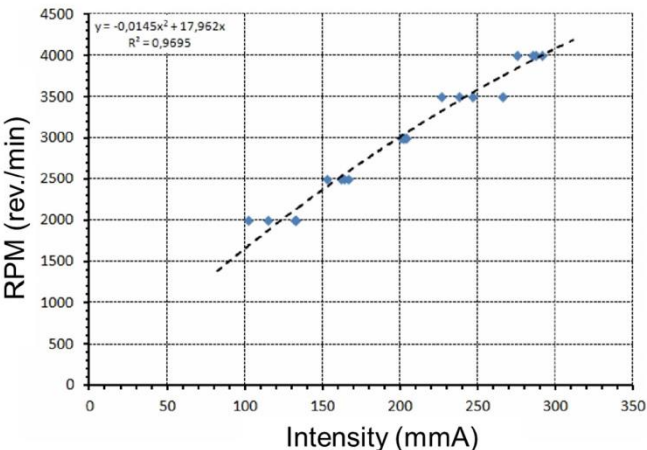


Mandrel



Magnetic Block

Almen Intensity vs. RPM Curve




The graph shows a strong positive correlation between Almen Intensity (mA) and RPM (rev./min). The data points are fitted with a quadratic equation: $y = -0,0145x^2 + 17,962x$ with $R^2 = 0,9695$.

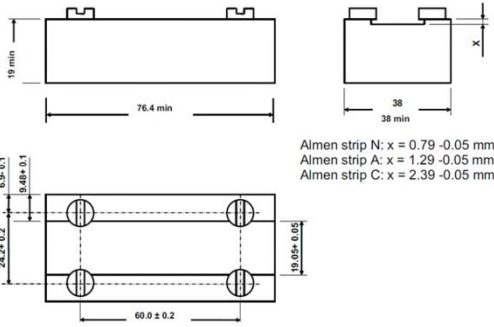
Intensity (mA)	RPM (rev./min)
100	2000
110	2000
120	2000
130	2000
150	2500
160	2500
180	3000
200	3000
220	3500
230	3500
240	3500
250	3500
260	3500
270	4000
280	4000
290	4000

Pneumatic Needle Peening

© MTU Aero Engines AG. The information contained herein is proprietary to the MTU Aero Engines group companies.

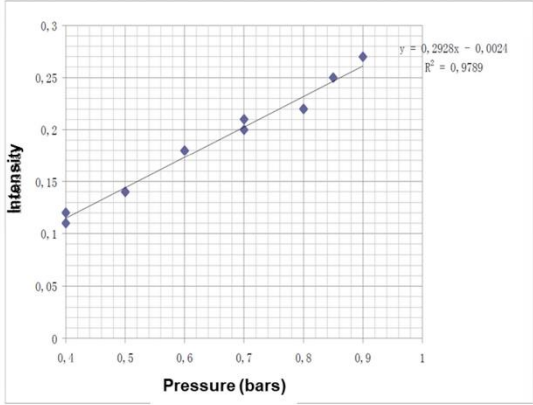


Experimental Procedure




Almen strip holder for
 Controlled Pneumatic Needle Peening and Forming
 (all dimensions are in millimeter)

Almen Intensity vs. Pressure Curve




Pneumatic Needle Peening 11

© MTU Aero Engines AG. The information contained herein is proprietary to the MTU Aero Engines group companies.

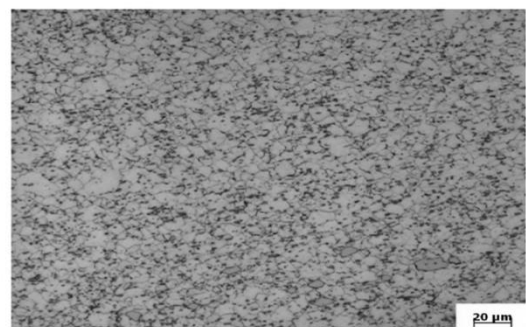


Experimental Procedure

- **Material**



Ti-6Al-2Sn-4Zr-6Mo
 • Near-β-Alloy
 Lamellar Microstructure



DA718
 Nickelbase-Superalloy

Pneumatic Needle Peening 12

© MTU Aero Engines AG. The information contained herein is proprietary to the MTU Aero Engines group companies.

MTU
Aero Engines

Experimental Procedure

- Coupon Design**

Flat Specimen for:

- Roughness measurement
- Residual stress measurement
- Metallographic Examination

Flat-Bar Bending Test
 Specimen for Cyclic Bending Test

Pneumatic Needle Peening

© MTU Aero Engines AG. The information contained herein is proprietary to the MTU Aero Engines group companies.

13

MTU
Aero Engines

Experimental Procedure

- Specimen Holder**

Specimen Holder

Specimen

Flexible fastener for assemble / disassemble of the specimen

surface area of strengthening

Pneumatic Needle Peening

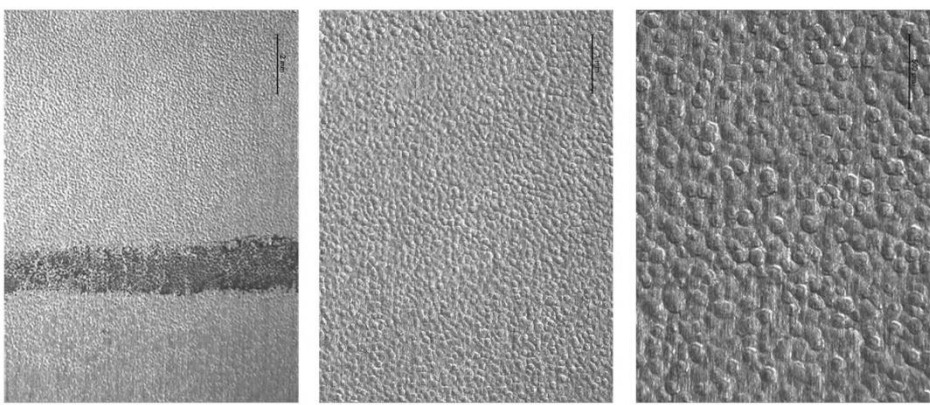
© MTU Aero Engines AG. The information contained herein is proprietary to the MTU Aero Engines group companies.

14

MTU
Aero Engines

Results

- **Surface Finish: A strip, 0.006-0.008A Intensity**



10x
20x
50x

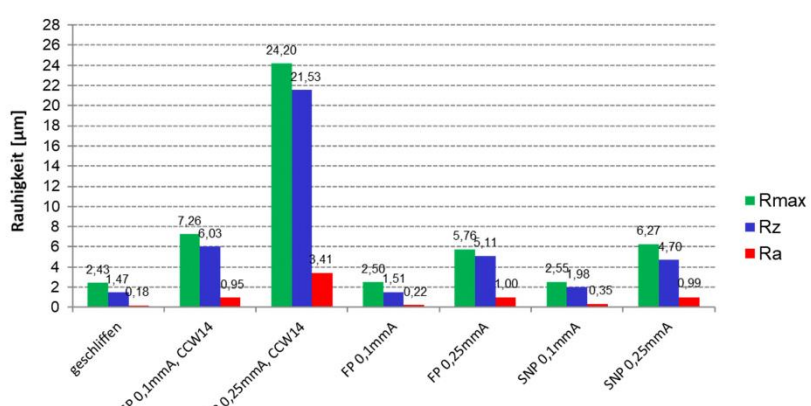
Pneumatic Needle Peening

© MTU Aero Engines AG. The information contained herein is proprietary to the MTU Aero Engines group companies. 15

MTU
Aero Engines

Results

- **Surface Roughness Ti-6246**

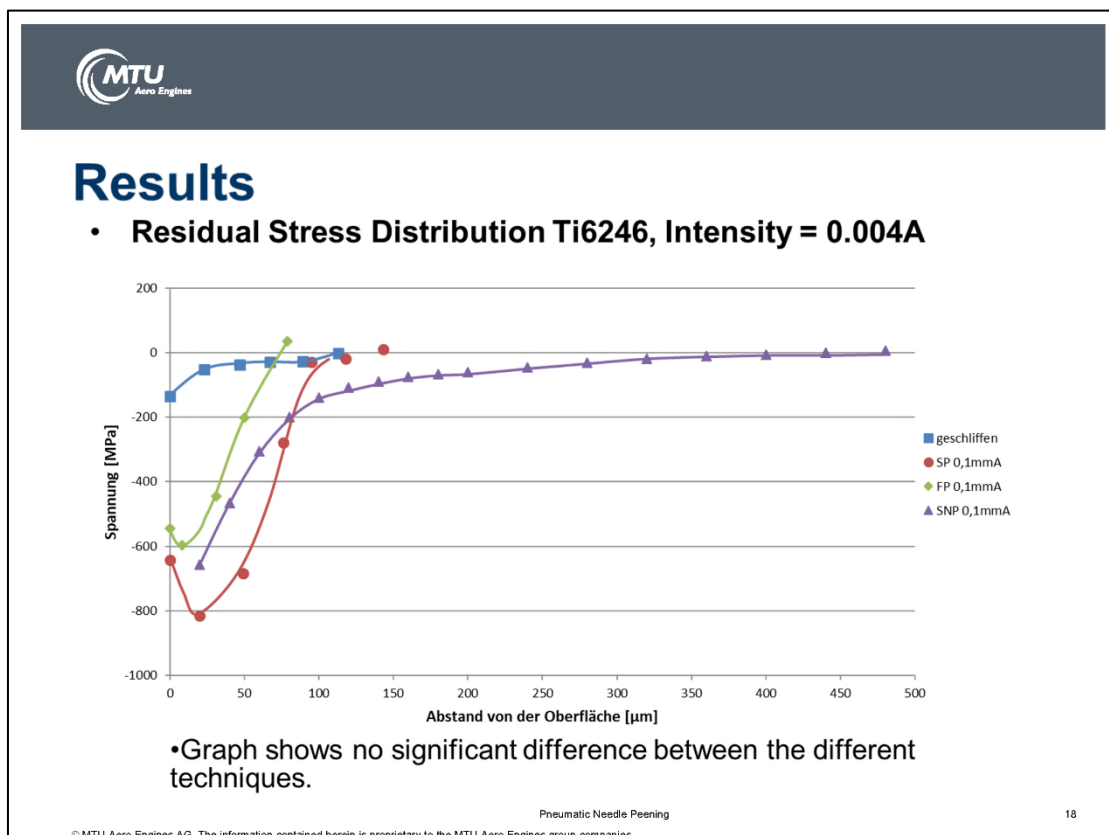
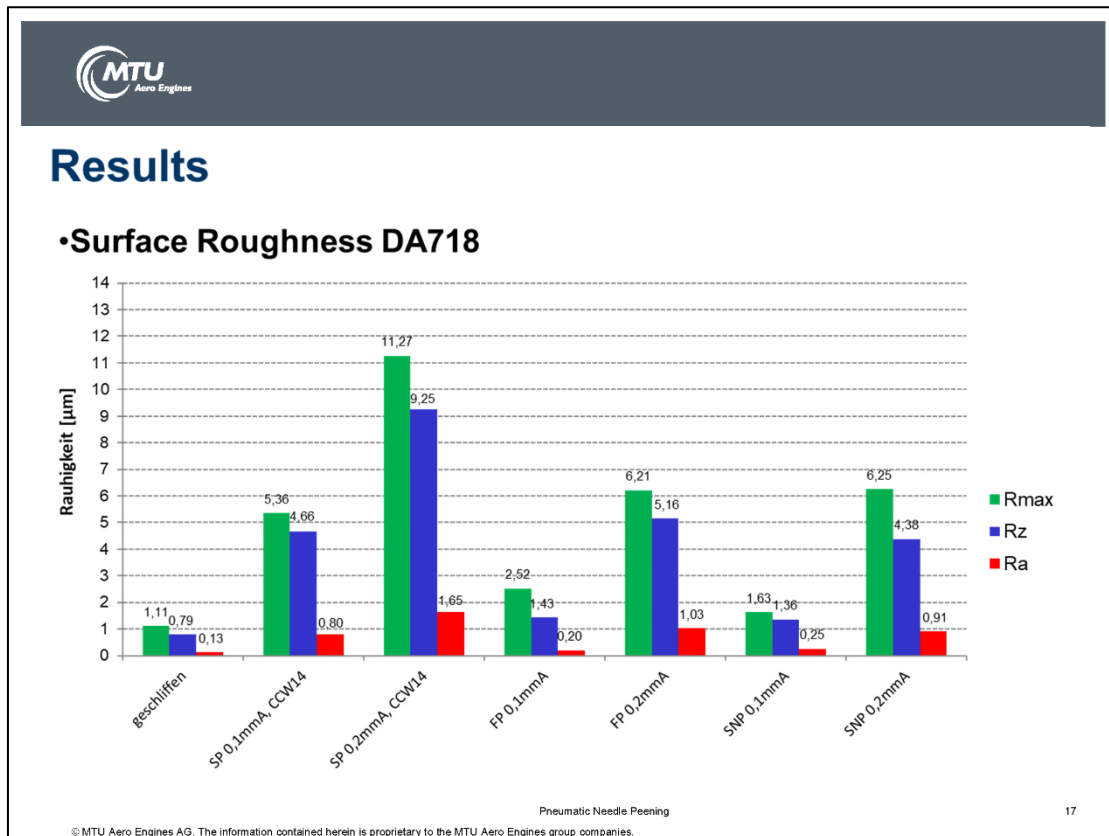


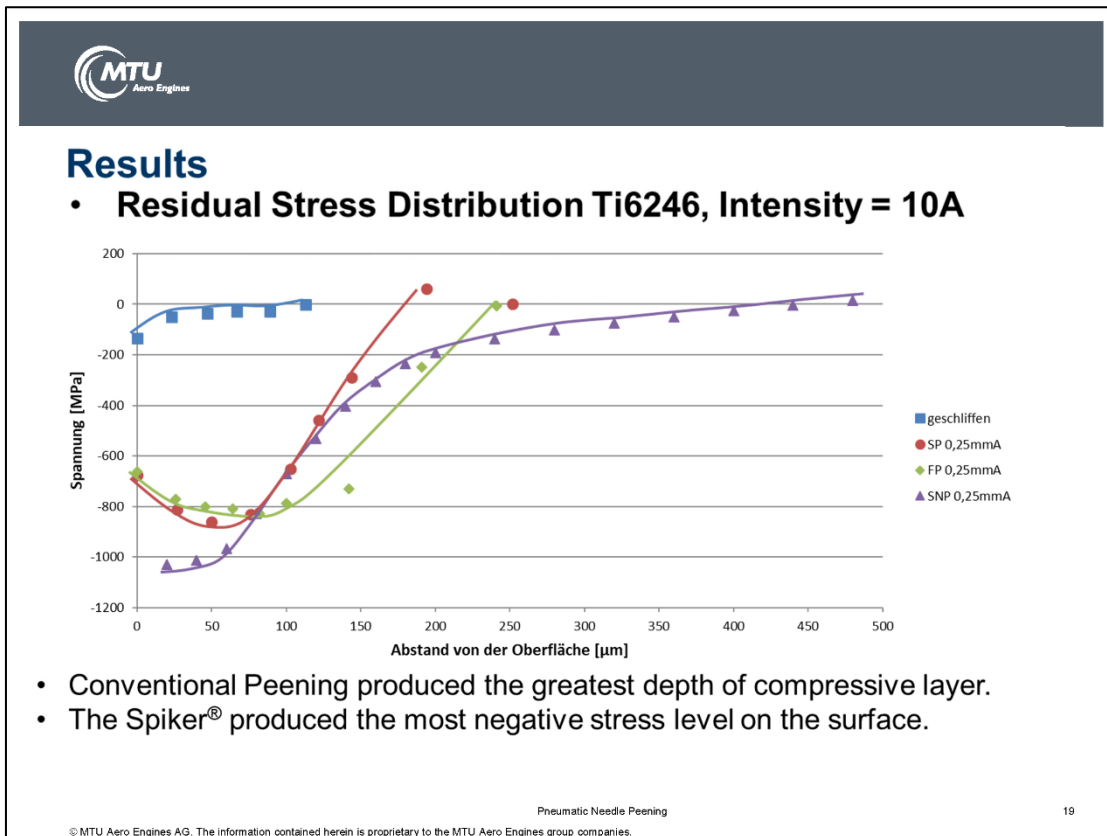
Treatment	Rmax [µm]	Rz [µm]	Ra [µm]
geschliffen	2,43	1,47	0,18
SP 0,1mmA, CCW14	7,26	6,03	0,95
SP 0,25mmA, CCW14	24,20	21,53	3,41
FP 0,1mmA	2,50	1,51	0,22
FP 0,25mmA	5,76	5,11	1,00
SNP 0,1mmA	2,55	1,98	0,35
SNP 0,25mmA	6,27	4,76	0,99

- Roughness rises with Intensity.
- Roughness achieved by the Flapper Peening is an order of magnitude lower than Shot Peening.
- Pneumatic needle peening tool gives roughness in the same scale as Flapper Peening.

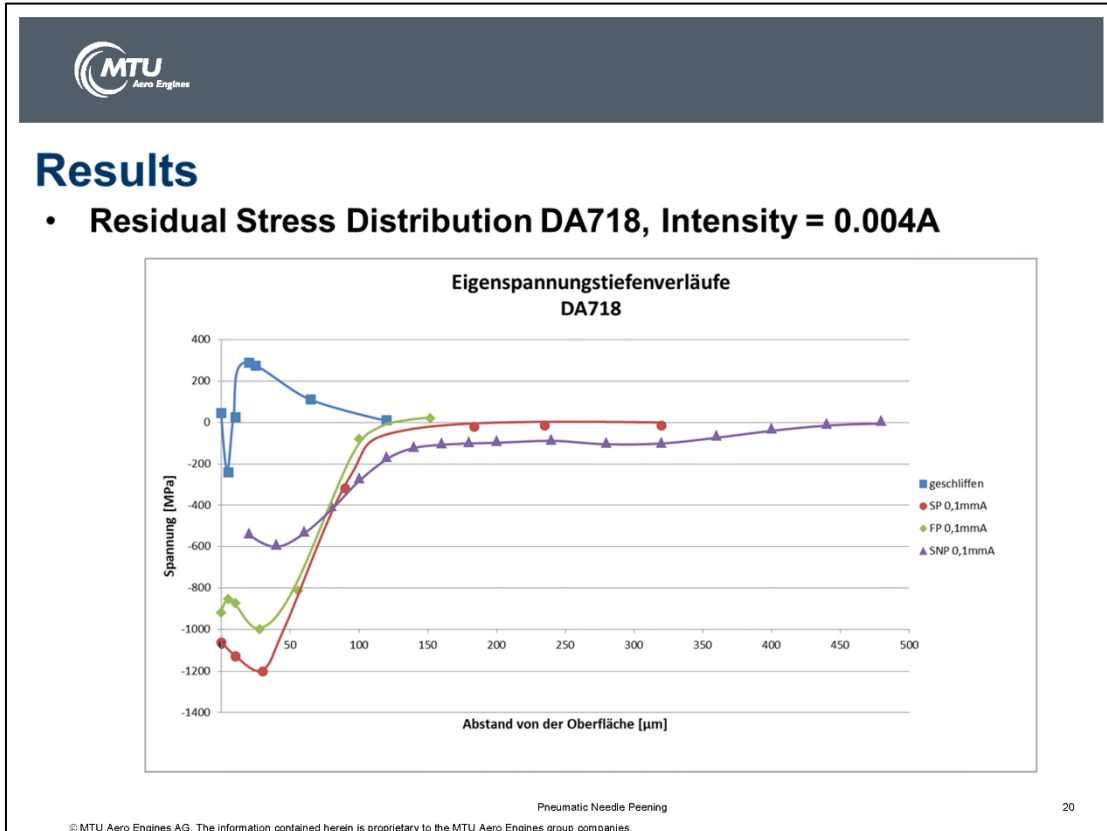
Pneumatic Needle Peening

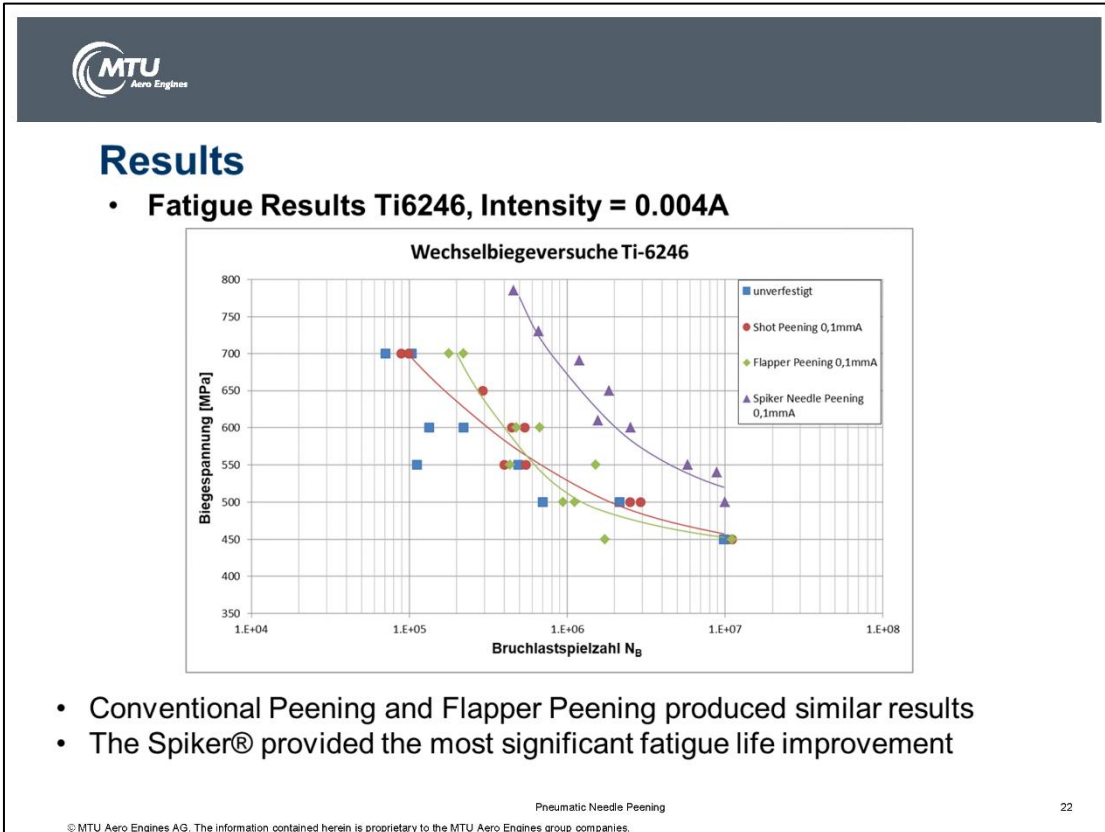
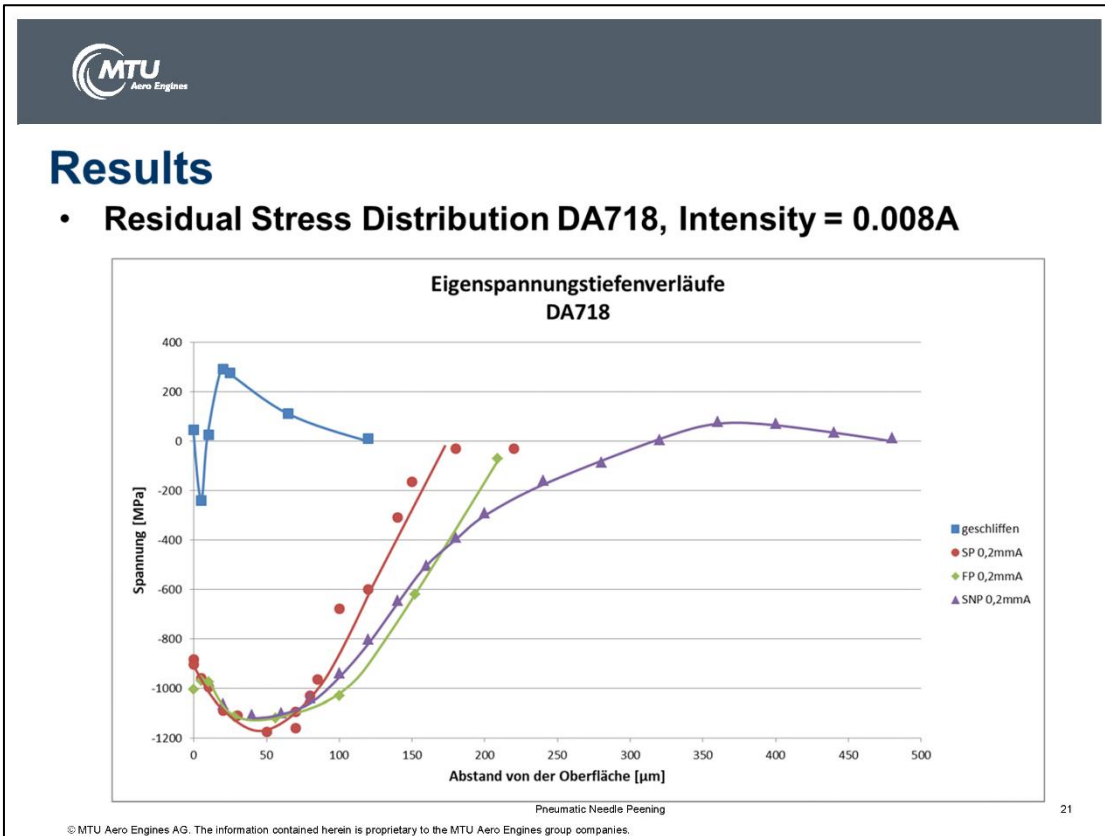
© MTU Aero Engines AG. The information contained herein is proprietary to the MTU Aero Engines group companies. 16



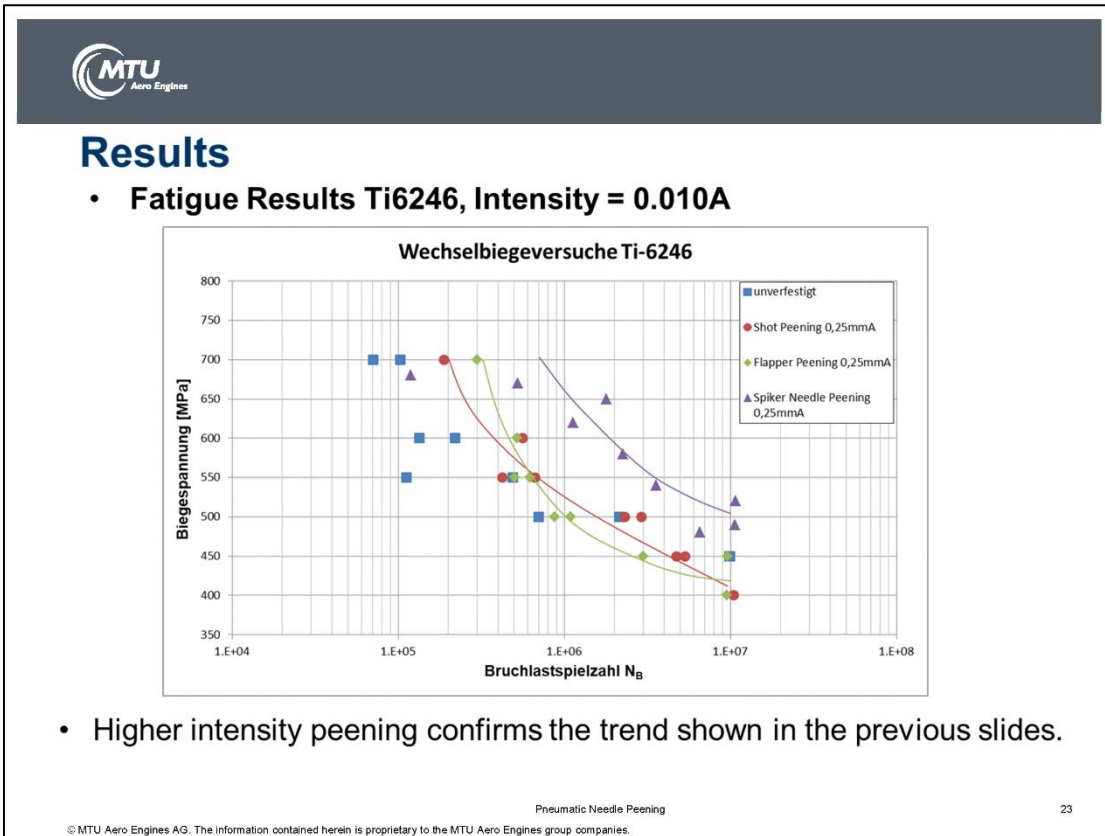


- Conventional Peening produced the greatest depth of compressive layer.
- The Spiker[®] produced the most negative stress level on the surface.

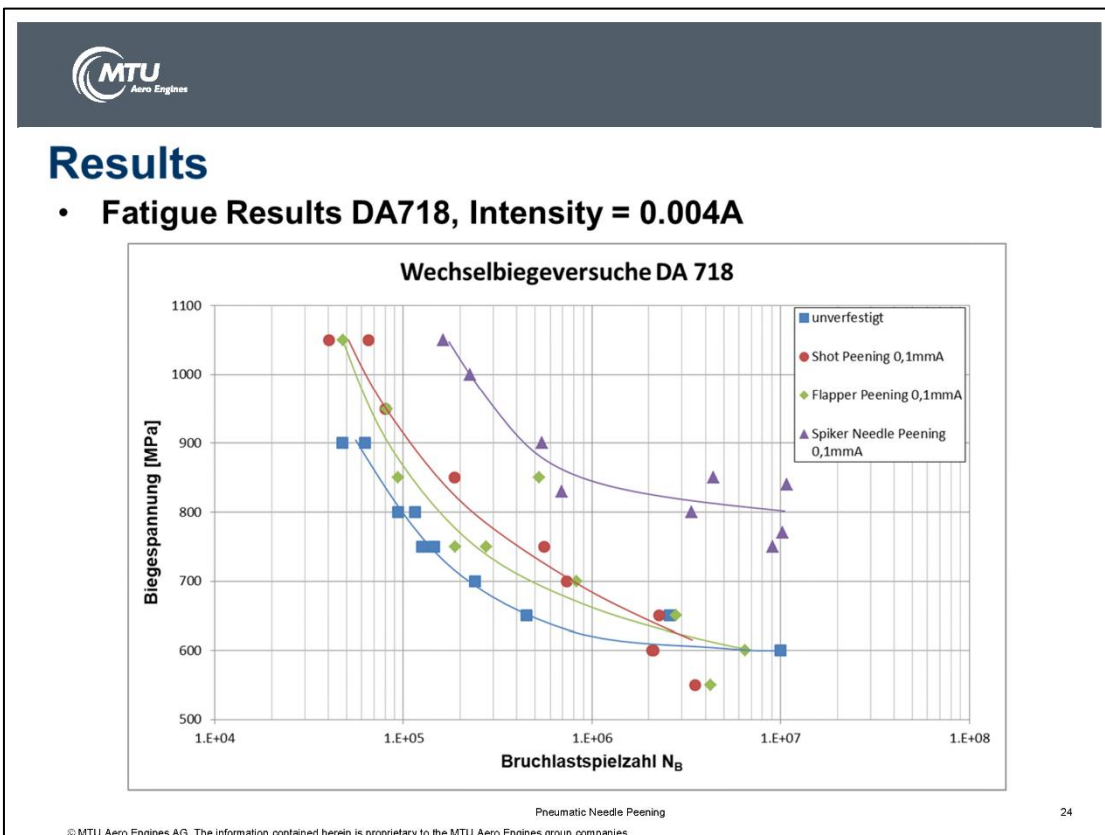


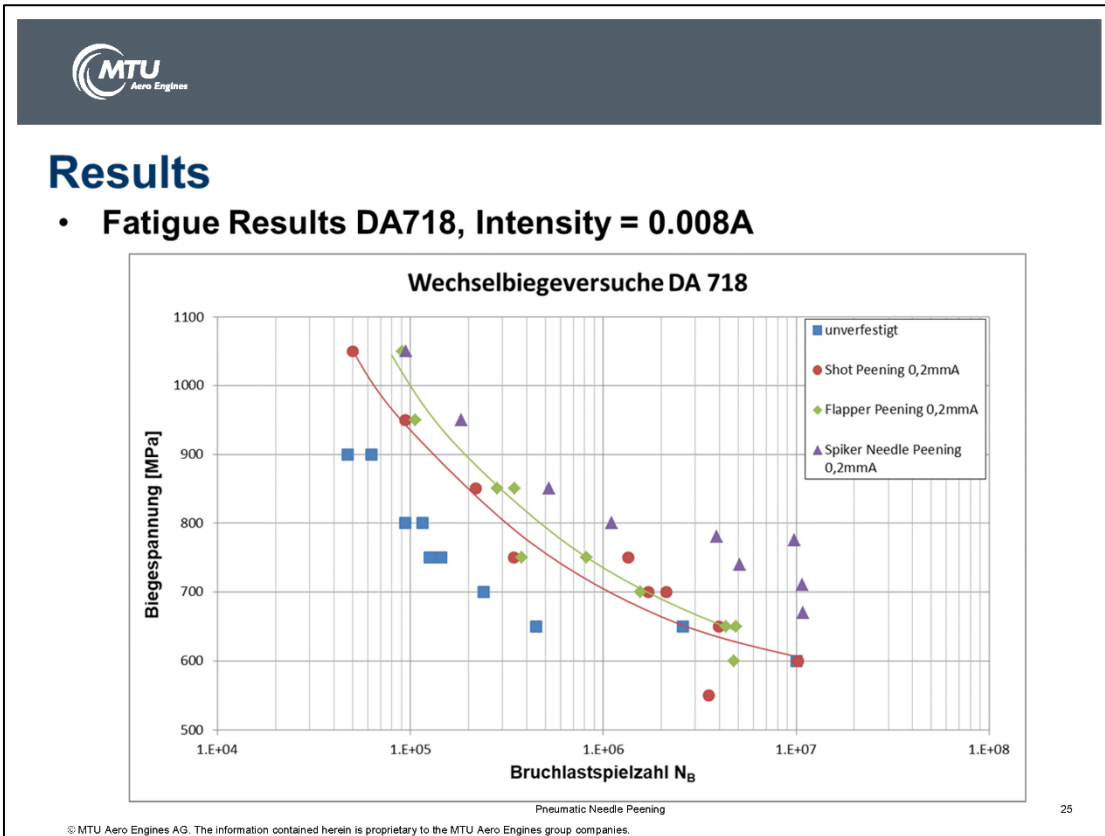



- Conventional Peening and Flapper Peening produced similar results
- The Spiker® provided the most significant fatigue life improvement




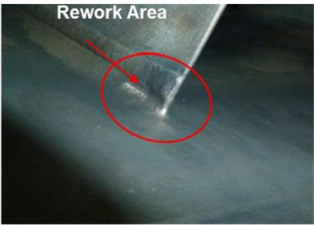
- Higher intensity peening confirms the trend shown in the previous slides.








Spiker® Applications

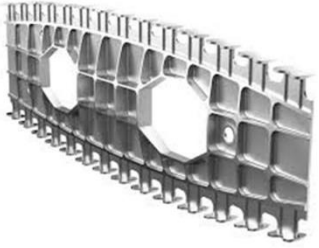



Rework Area

V2500 Turbine Exhaust Case
Save of 40 man hours




CF6-80 HPT Blades
Tip-Repair



Bulhead Pockets and difficult to reach geometries

Pneumatic Needle Peening

© MTU Aero Engines AG. The information contained herein is proprietary to the MTU Aero Engines group companies. 27



Specification

**AMS 2545 Controlled Pneumatic Needle Peening,
Straightening and Forming**
Issued 2017 – 11

Nadcap Checklist AC7117/6 for Needle Peening

Ballot for Approval 2019 - 07

Pneumatic Needle Peening

© MTU Aero Engines AG. The information contained herein is proprietary to the MTU Aero Engines group companies. 28



Conclusion

- **In this study, the new Spiker[®] Needle Peening Tool has shown:**
 - A Surface Finish that is equivalent to flapper peening and usually better than conventional peening
 - Residual Stress Distribution that can be deeper on the surface than conventional or flapper peening
 - Fatigue Life that are equivalent and often much better than conventional or flapper peening
 - Easy application on aero-engine components with significant cost saving potential

Pneumatic Needle Peening

29

© MTU Aero Engines AG. The information contained herein is proprietary to the MTU Aero Engines group companies.



Acknowledgement

- Prof. Dr. L. Wagner and his employees at the institute of material technology at the University of Technology Clausthal for their support and realization of the scientific investigations.
- Mr. Norbert Huber and Götz Lebküchner for their support and helpful consultation during the development of the head for the Spiker[™] tool

Pneumatic Needle Peening

30

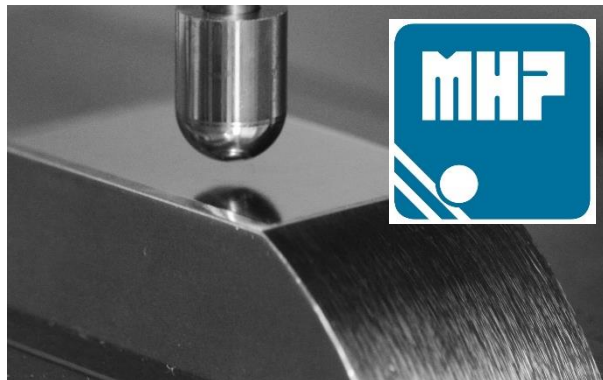
© MTU Aero Engines AG. The information contained herein is proprietary to the MTU Aero Engines group companies.

Experimental analysis of the surface integrity of stainless steel modified by robot based machine hammer peening

Lars Uhlmann

Laboratory for Machine Tools and Production Engineering WZL

RWTH Aachen University





Experimental analysis of the surface integrity of stainless steel modified by robot based machine hammer peening

Thomas Bergs, Lars Uhlmann*, Robby Mannens, Daniel Trauth

Laboratory for Machine Tools and Production Engineering (WZL) of RWTH Aachen

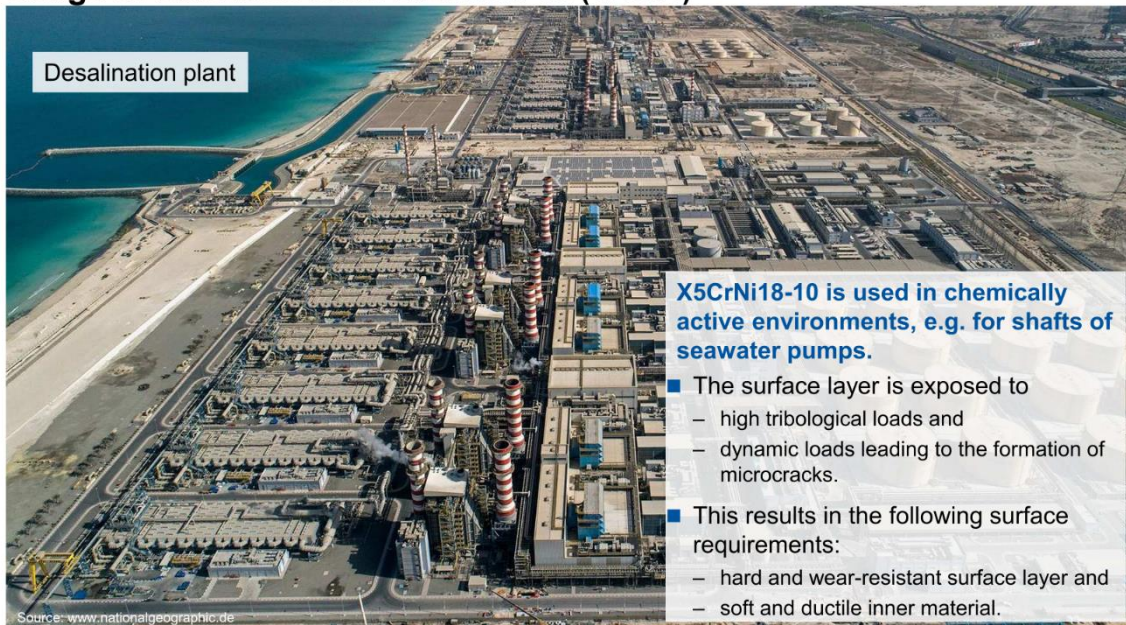
Symposium Mechanical Surface Treatment 2019,
Karlsruhe, 22.10.2019

© WZL/Fraunhofer IPT



Motivation

Usage of stainless steel X5CrNi18-10 (1.4301)



X5CrNi18-10 is used in chemically active environments, e.g. for shafts of seawater pumps.

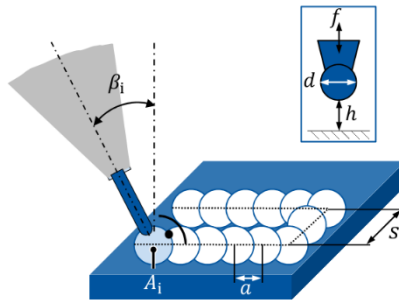
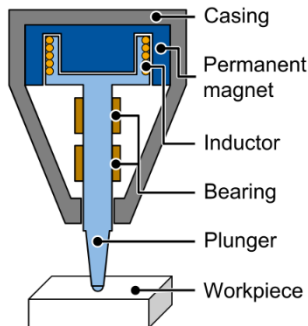
- The surface layer is exposed to
 - high tribological loads and
 - dynamic loads leading to the formation of microcracks.
- This results in the following surface requirements:
 - hard and wear-resistant surface layer and
 - soft and ductile inner material.

Source: www.nationalgeographic.de
© WZL/Fraunhofer IPT



Slide 2

Introduction Machine hammer peening (MHP)



Process parameter	Symbol
Impact angle	β_i
Stepover distance	s
(Hammer) head diameter	d
Hammering frequency	f
Stroke	h
Projected area of indentation	A_i
Distance of indentations	a

(acc. to VDI 3416)

- Work hardening and compressive residual stresses are induced into the surface layer.
- Surface of the specimen may be structured or smoothed.

Source: [VDI18]

© WZL/Fraunhofer IPT



Slide 3

Agenda

- 1 Introduction
- 2 Experimental set-up**
- 3 Surface integrity of peened surfaces
- 4 Description model for the Vickers hardness
- 5 Summary and outlook

© WZL/Fraunhofer IPT



Slide 4

Experimental set-up

Processing of X5CrNi18-10 with a robot based MHP system

Experimental design		MHP system adapted to an industrial robot	
Full factorial experimental design with variation of the factors:			
Head diameter d [mm]	6	12	
Stroke h [mm]	0.3	1.2	
Distance of indentation a [mm]	0.05	0.4	
Impact angle β_i [°]	0	30	
In addition:			
Experiment with multiple processing ($n = 5$): $d = 6$ mm; $h = 1.2$ mm; $a = 0.05$ mm; $\beta_i = 0^\circ$			
Center point experiment: $d = 8$ mm; $h = 0.75$ mm; $a = 0.225$ mm; $\beta_i = 15^\circ$			
n : number of processing			

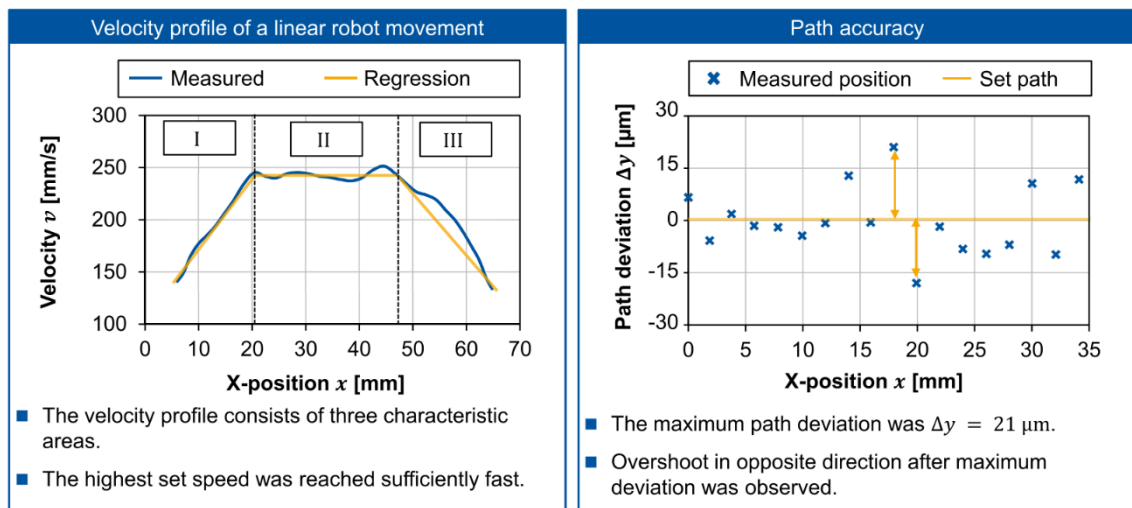
© WZL/Fraunhofer IPT



Slide 5

Experimental set-up

Robot based machine hammer peening



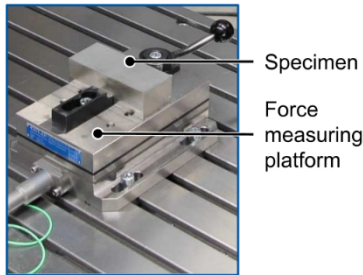
Consideration of the robot acceleration is necessary. The high path accuracy is reached due to a high robot stiffness.

© WZL/Fraunhofer IPT

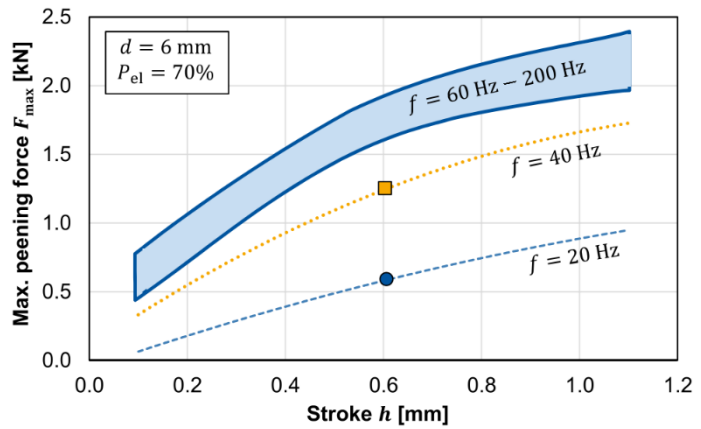


Slide 6

Experimental set-up Peening force



- The specimen was fixed by clamping.
- MHP at the center of the specimen to ensure a direct force application.
- Specimen (42CrMo4) was treated by MHP in advance to the tests.



f : hammer frequency, d : head diameter, P_{el} : percentage of electrical power

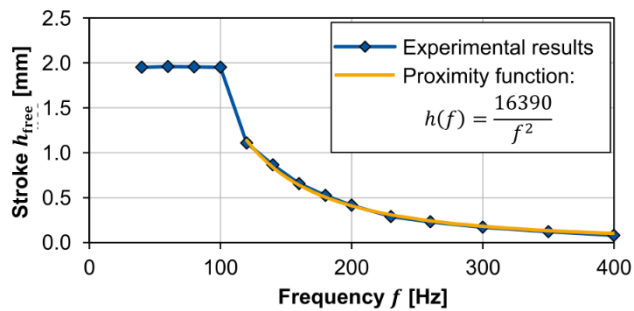
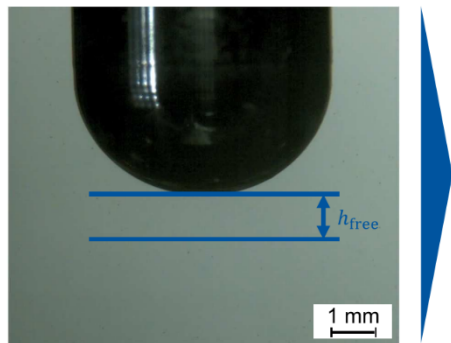
Up to a frequency of 60 Hz the maximum force rises with frequency. Between 60 Hz and 200 Hz the maximum force does not vary much. Results qualitatively in accordance with TRAUTH [TRAU16].

© WZL/Fraunhofer IPT



Slide 7

Experimental set-up Limitation of the adjustable stroke by the frequency (Video)



- Free stroke decreases with increasing frequency.
- The stroke may not be greater than the free stroke.
- Restriction of the combination of the stroke and the frequency exists.
- For frequencies smaller or equal $f = 100$ Hz the stroke may be $h < 1.955$ mm. For $f = 200$ Hz the stroke may only be $h < 0.416$ mm.

© WZL/Fraunhofer IPT



Slide 8

Agenda

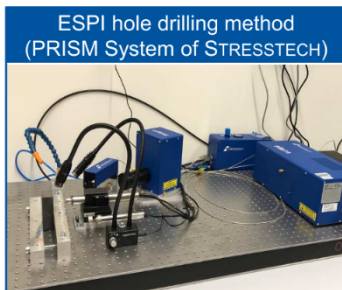
- 1 Introduction
- 2 Experimental set-up
- 3 Surface integrity of peened surfaces**
- 4 Description model for the Vickers hardness
- 5 Summary and outlook

© WZL/Fraunhofer IPT



Slide 9

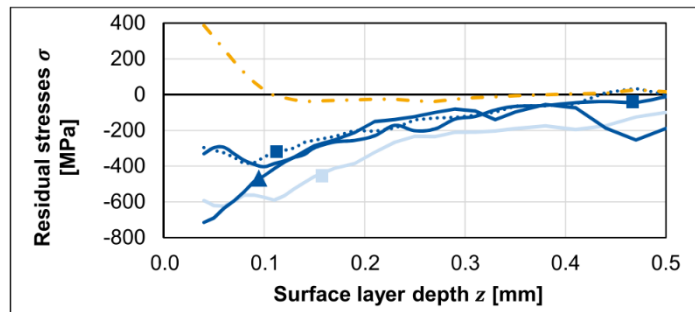
Surface integrity of peened surfaces Evaluation of the residual stresses



- Removing material results in a new stress equilibrium achieved by deformation.
- Deformation is measured by using optical interferometry.
- Removed stress is calculated from measured displacement.

Source: www.stresstech.com

© WZL/Fraunhofer IPT

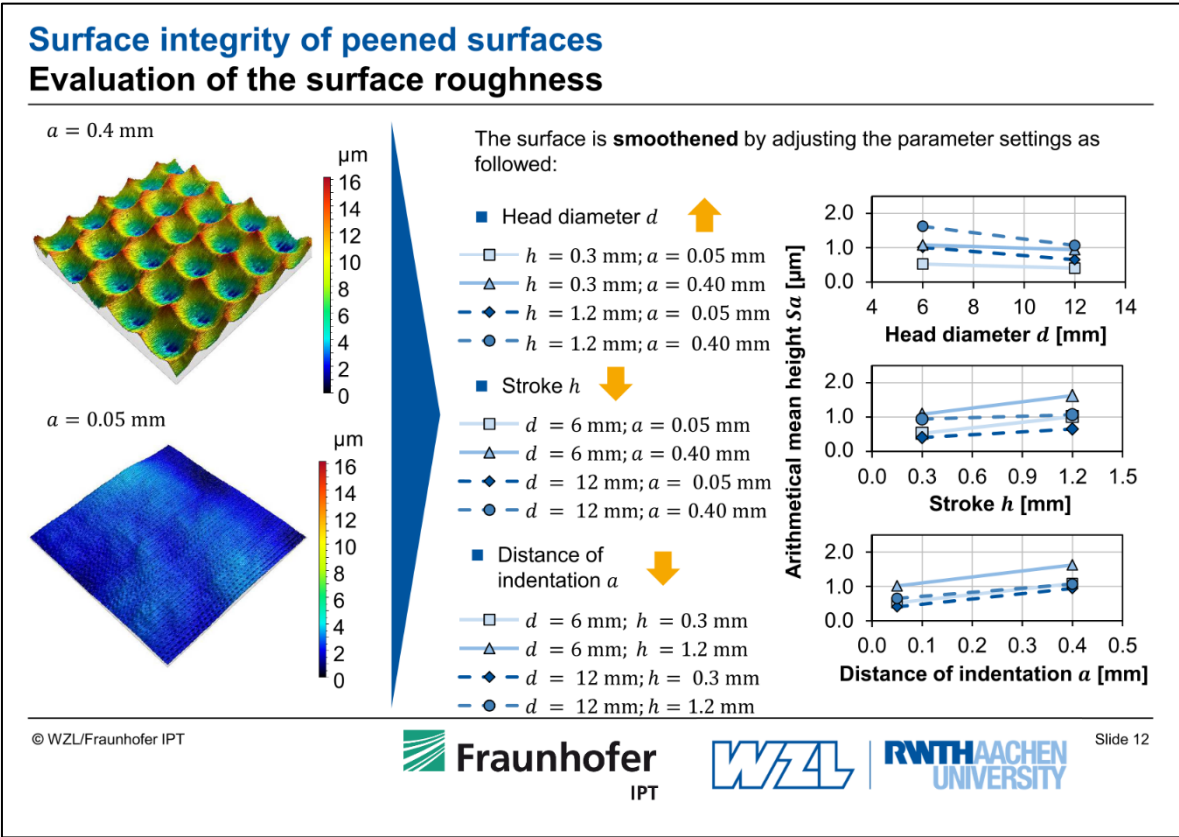
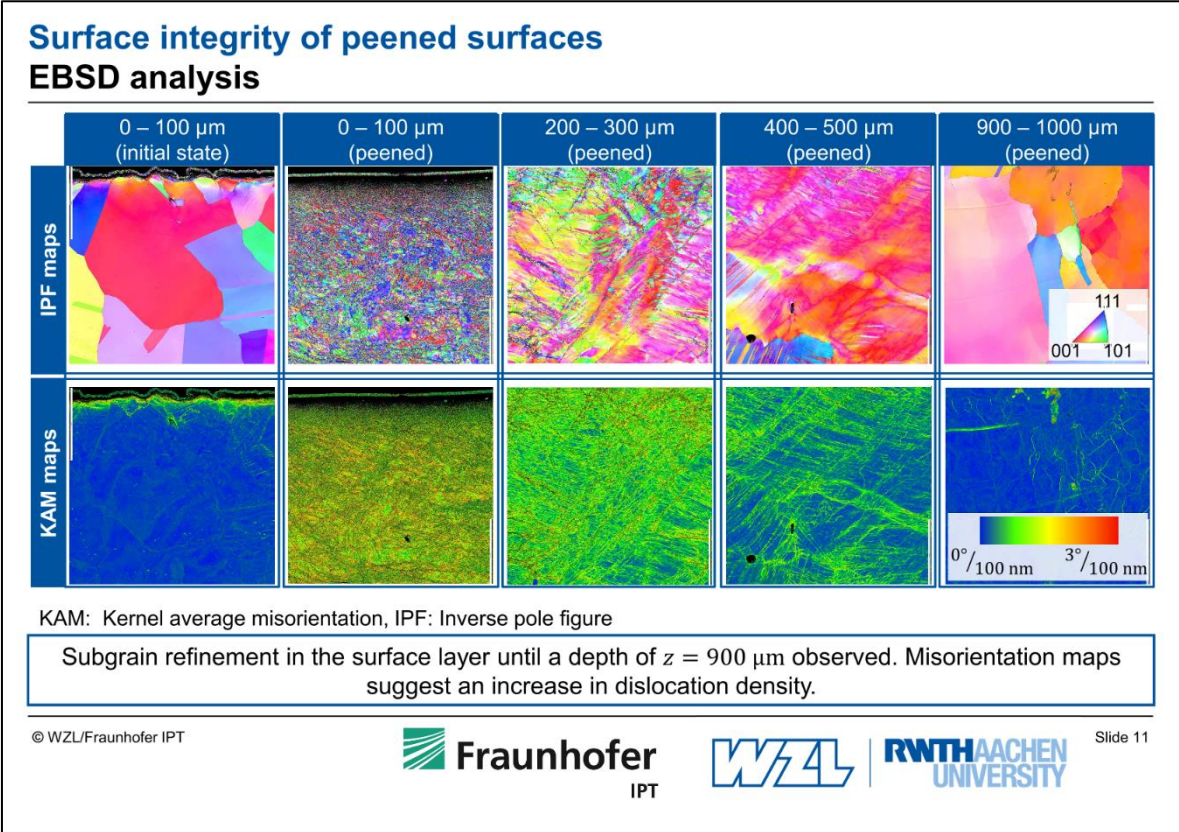


- Initial state
- Line type: — $d = 6$ mm $d = 12$ mm
- Line color: — $h = 0.3$ mm — $h = 1.2$ mm
- Symbol: ■ $a = 0.40$ mm ▲ $a = 0.05$ mm

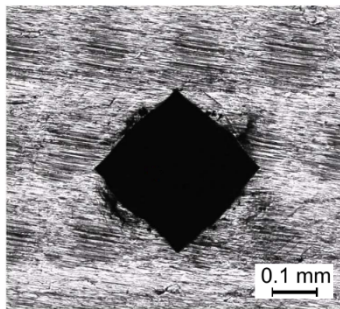
- Raising the stroke results in inducing compressive residual stresses into a deeper surface layer depth.
- Decreasing the distance of indentation a results in higher compressive residual stresses until a depth of $z \approx 0.11$ mm.



Slide 10

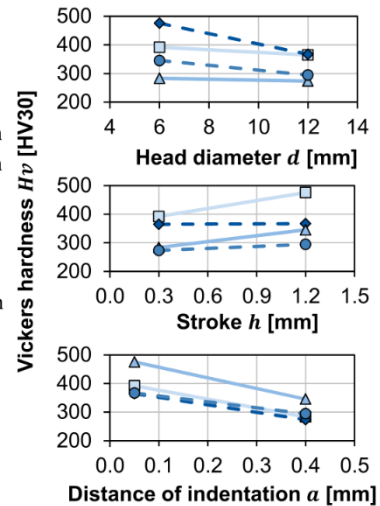


Surface integrity of peened surfaces Evaluation of the surface hardness



Work hardening is influenced by the investigated process parameters as followed:

- **Head diameter d** ↓
 - $h = 0.3 \text{ mm}; a = 0.05 \text{ mm}$
 - △ $h = 0.3 \text{ mm}; a = 0.40 \text{ mm}$
 - ◆ $h = 1.2 \text{ mm}; a = 0.05 \text{ mm}$
 - $h = 1.2 \text{ mm}; a = 0.40 \text{ mm}$
- **Stroke h** ↑
 - $d = 6 \text{ mm}; a = 0.05 \text{ mm}$
 - △ $d = 6 \text{ mm}; a = 0.40 \text{ mm}$
 - ◆ $d = 12 \text{ mm}; a = 0.05 \text{ mm}$
 - $d = 12 \text{ mm}; a = 0.40 \text{ mm}$
- **Distance of indentation a** ↓
 - $d = 6 \text{ mm}; h = 0.3 \text{ mm}$
 - △ $d = 6 \text{ mm}; h = 1.2 \text{ mm}$
 - ◆ $d = 12 \text{ mm}; h = 0.3 \text{ mm}$
 - $d = 12 \text{ mm}; h = 1.2 \text{ mm}$



© WZL/Fraunhofer IPT



Slide 13

Agenda

- 1 Introduction
- 2 Experimental set-up
- 3 Surface integrity of peened surfaces
- 4 Description model for the Vickers hardness
- 5 Summary and outlook

© WZL/Fraunhofer IPT



Slide 14

Description model for the Vickers hardness

Developing the description model

Equation of a description model acc. to KLOCKE

$$\hat{y}(x, t, u, \dots) = c_0 \cdot x^{c_1} \cdot t^{c_2} \cdot u^{c_3} \dots ()^0$$

\hat{y} : Quality feature
 x, t, u : Input variables
 c_0, c_1, c_2, c_3 : Coefficients of the regression model

$$\widehat{HV}(d, h, a, \beta_i) = c_0 \cdot d^{c_1} \cdot h^{c_2} \cdot a^{c_3} \cdot \beta_i^{c_4}$$

\widehat{HV} : Vickers hardness as quality feature
 d : Hammer diameter
 h : Stroke
 a : Distance of Indentation
 β_i : Impact angle
 c_0, c_1, c_2, c_3 : Coefficients of the regression model

- The regression model was developed from the friction model of FILZEK and LUDWIG.
- KLOCKE extendet the existing model to be suitable for general use. Therefore the model is suitable to be used to describe the behavior of the Vickers hardness after MHP.
- The experimental parameters and results served as data to determine the coefficients of the regression model c_0, c_1, c_2 and c_3 .
- The parameters and results of the center point experiment was not used to determine the coefficients of the regression model. Instead they were used for the validation.

Source: [KLOC15], [FILZ13]

© WZL/Fraunhofer IPT



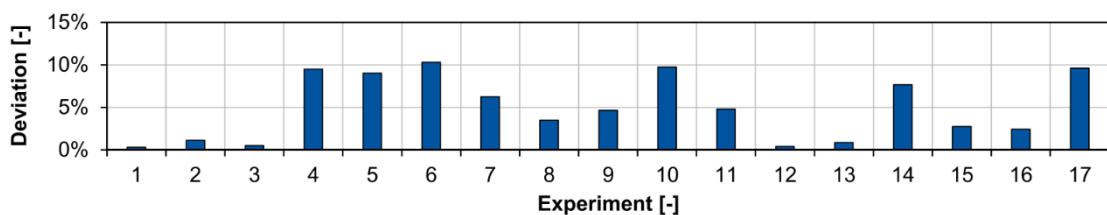
Slide 15

Description model for the Vickers hardness

Accuracy of the description model

$$\widehat{HV}(d, h, a, \beta_i) = 2.19 \cdot d^{-0.393} \cdot h^{0.227} \cdot a^{-0.285} \cdot \beta_i^{1.057}$$

\widehat{HV} : Vickers hardness as quality feature
 d : Hammer diameter
 h : Stroke
 a : Distance of Indentation
 β_i : Impact angle



The Vickers hardness of the center point experimental measurement and the model prediction deviates by 9.6 %. The highest deviation of the model and the measured value is 10.3 %.

© WZL/Fraunhofer IPT



Slide 16

Agenda

- 1 Introduction
- 2 Experimental set-up
- 3 Surface integrity of peened surfaces
- 4 Description model for the Vickers hardness
- 5 Summary and outlook**

© WZL/Fraunhofer IPT



Slide 17

Summary and outlook

Conclusions from the investigations

Summary

- The positioning accuracy of the industrial robot is high during MHP.
- Grain refinement due to MHP was observed up to a depth of $z \approx 900 \mu\text{m}$.
- Compressive residual stresses of maximal $\sigma = -820 \text{ Mpa}$ were induced.
- The linear description model has a high prediction accuracy with a maximum deviation of 7.6 % within the considered process room.

Outlook

- Investigation of the cause-effect relations between process parameters, grain refinement and dislocation density.
- Developing an accurate description model for the roughness by extending the linear description model to a quadratic model.
- Improving a finite element model to support the experimental results by predicting the dislocation density and grain size.



© WZL/Fraunhofer IPT



Slide 18

Your contact persons



Chair of Manufacturing Technology
Laboratory for Machine Tools and Production Engineering WZL of RWTH Aachen
Campus-Boulevard 30
D-52074 Aachen



Lars Uhlmann, M.Sc. M.Sc.


Research Associate

 0 241/ 80 27428
 l.uhlmann@wzl.rwth-aachen.de



Robby Mannens, M.Sc. RWTH

Research Associate

 0 241/ 80 28244
 r.mannens@wzl.rwth-aachen.de

© WZL/Fraunhofer IPT



Slide 19

Bibliography

- [FILZ13] Filzek, J.; Ludwig, M.: Berücksichtigung der Reibung in der FEM-Simulation. In: Umformen, Schneiden, Verbinden im Leichtbau. Machbarkeit - Produktivität - Qualität ; Tagungsband des 33. EFB-Kolloquiums Blechverarbeitung 2013 am 16. und 17. April 2013 in Fellbach. (Reihe: Tagungsband / Europäische Forschungsgesellschaft für Blechverarbeitung e.V. T 36). Aufl. Hannover: EFB, 2013
- [KLOC15] Klocke, F.; Trauth, D.; Shirobokov, A.; Mattfeld, P.: FE-analysis and in situ visualization of pressure-, slip-rate-, and temperature-dependent coefficients of friction for advanced sheet metal forming. Development of a novel coupled user subroutine for shell and continuum discretization. In: The International Journal of Advanced Manufacturing Technology, 81. Jg., 2015, Nr. 1-4, S. 397-410
- [VDI18] VDI 3416 (2018): Maschinelles Oberflächenhämmern

© WZL/Fraunhofer IPT



Slide 20

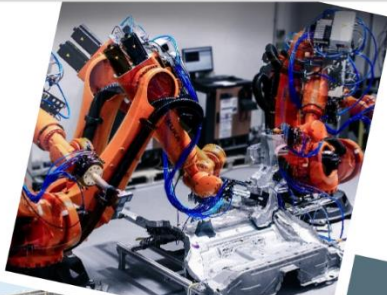
Analyses of technical and true overlap in hammer peening operations

Eric Segebade

wbk Institute of Production Science

Karlsruhe Institute of Technology





ANALYSES OF TECHNICAL AND TRUE OVERLAP IN HAMMER PEENING OPERATIONS

E. Segebade, A. Hilligardt, V. Schulze



KIT – The Research University in the Helmholtz Association

www.wbk.kit.edu

MOTIVATION METHODS TECHNICAL KINEMATIC TRUE COMPARISON OUTLOOK

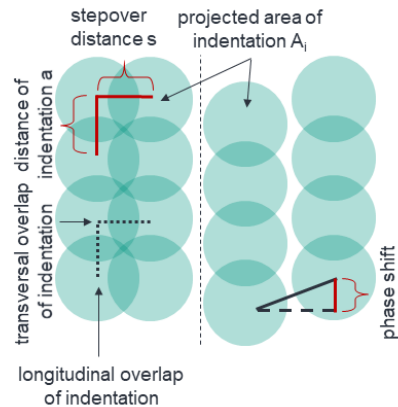
MOTIVATION

What is overlap?

- Overlap of indentations in hammer peening operations defines the resulting percentage overlap of surface.
- It is the main factor to control in order to reach defined treatment intensities or surface textures.

As per the definition in VDI 3416:

- Percentage overlap of surface $o_s = \sum A_i / A_{total}$
- In the following: "Technical Overlap"
- "...it has to be mentioned, that o_s can reach values of $\geq 100\%$, even if not all of the surface was hit at least once."



- Technical Overlap is not accurate for complex indentation shapes.
- Is it accurate for simple indentation shapes?

METHODS

Technical overlap vs. kinematic overlap vs. true overlap

Technical overlap

Simple calculation of area of indentation:

- Calculate secant
 - $s = \sqrt{i_{depth} * (d - i_{depth})}$
- Calculate area of indentation
 - $A_i = (s/2)^2 * \pi$
- Calculate α_s
 - $\alpha_s = n * A_i / A_{total}$

Kinematic overlap

Numerical calculation in Matlab:

- Load .stl geometry
- Create master-indentation (dixel)
- Create translation matrix
- Calculate new surface with (w) and without (w/o) consideration of former indentations

True overlap

Full thermo-mechanical FEM:

Material model

- Voce-Kocks-Vöhringer (AISI 4140)

Body boundary conditions

- 5 x 5 x 5 mm elastic body
- 0.5 x 0.5 x 0.1 mm elastic-plastic body
- Rigid tool, constant Temperature: RT

Surface element edge length

- 0.005 mm, no remeshing

Tool movement

- Position & velocity based

- Kinematic overlap w/o consideration of former indentations and technical overlap should be the same.
- Elasto-plastic FE-simulation result should be closest to the truth and higher than kinematic overlap (w).

3

22.10.2019

Prof. Dr.-Ing. J. Fleischer, Prof. Dr.-Ing. G. Lanza, Prof. Dr.-Ing. habil. V. Schulze

TECHNICAL OVERLAP

Exemplary calculation

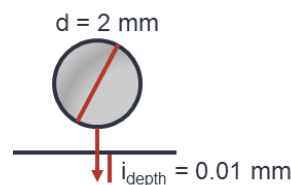
Technical overlap

Simple calculation of area of indentation:

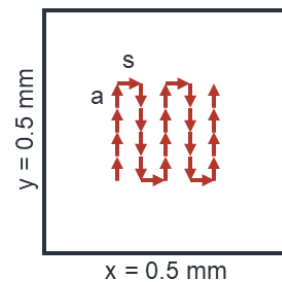
- Calculate secant
 - $s = \sqrt{i_{depth} * (d - i_{depth})}$
- Calculate area of indentation
 - $A_i = (s/2)^2 * \pi$
- Calculate α_s
 - $\alpha_s = n * A_i / A_{total}$

Example:

- Ball diameter $d = 2$ mm,
- $A_{total} = 0.5 \times 0.5$ mm = 0.25 mm²
- $n = 25$ (5 * 5 indentations)
- $a = s = 0.05$ mm



5 x 5 indentations



- $A_i = 0.029$ mm², $\alpha_s = 5 \times 5 \times A_i / A_{total} = 6.252$
- Technical overlap in our example totals 625.2% as per VDI 3416.

4

22.10.2019

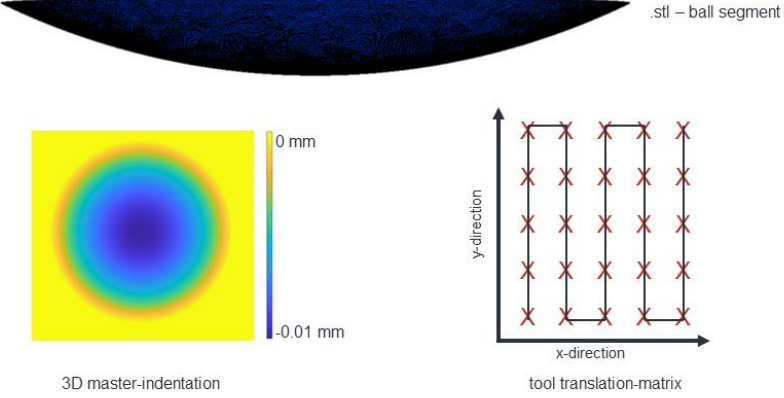
Prof. Dr.-Ing. J. Fleischer, Prof. Dr.-Ing. G. Lanza, Prof. Dr.-Ing. habil. V. Schulze

MOTIVATION METHODS TECHNICAL **KINEMATIC** TRUE COMPARISON OUTLOOK

KINEMATIC OVERLAP
 Exemplary calculation

Kinematic overlap
 Numerical calculation in Matlab:


- Load .stl geometry
- Create master-indentation (dexel)
- Create translation matrix
- Calculate overlap with and without consideration of former indentations



stl – ball segment

3D master-indentation

tool translation-matrix

5 22.10.2019 Prof. Dr.-Ing. J. Fleischer, Prof. Dr.-Ing. G. Lanza, Prof. Dr.-Ing. habil. V. Schulze 

MOTIVATION METHODS TECHNICAL **KINEMATIC** TRUE COMPARISON OUTLOOK

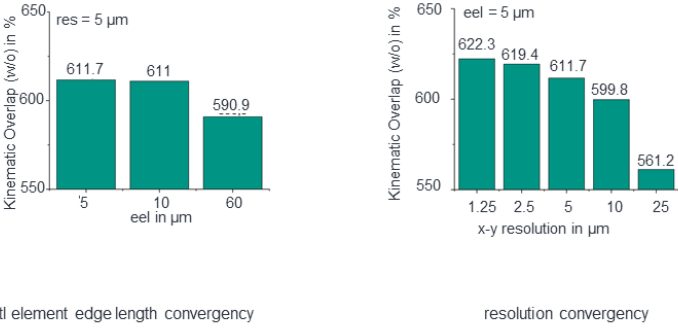
KINEMATIC OVERLAP
 Exemplary calculation

Kinematic overlap
 Numerical calculation in Matlab:

- Load .stl geometry
- Create master-indentation (dexel)
- Create translation matrix
- Calculate overlap with and without consideration of former indentations

Main sources of errors

- .stl element edge length (eel)
- x-y surface resolution (res)




Kinematic Overlap (w/o) in %

eel in μm	Kinematic Overlap (w/o) in %
5	611.7
10	611
60	590.9

stl element edge length convergency


x-y resolution in μm	Kinematic Overlap (w/o) in %
1.25	622.3
2.5	619.4
5	611.7
10	599.8
25	561.2

resolution convergency

6 22.10.2019 Prof. Dr.-Ing. J. Fleischer, Prof. Dr.-Ing. G. Lanza, Prof. Dr.-Ing. habil. V. Schulze 

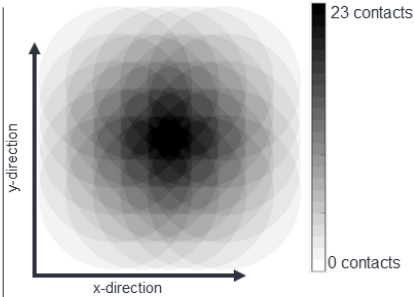
MOTIVATION METHODS TECHNICAL **KINEMATIC** TRUE COMPARISON OUTLOOK

KINEMATIC OVERLAP
 Exemplary calculation

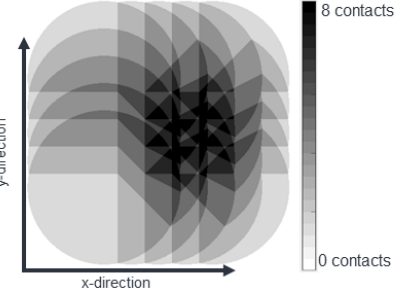


Kinematic overlap
 Numerical calculation in Matlab:

- Load .stl geometry
- Create master-indentation (dexel)
- Create translation matrix
- Calculate overlap with and without consideration of former indentations
 - eel = 5 μ m
 - res = 1.25 μ m




Kinematic Overlap (w/o)
 without consideration of former indentations
 $\rightarrow \sigma_s = 622.3\%$



Kinematic Overlap (w)
 with consideration of former indentations
 $\rightarrow \sigma_s = 252.7\%$


- Kinematic overlap w/o consideration of former indentations ~ technical overlap (622.3% vs. 625.2%)
- Kinematic overlap considering former indentations is significantly lower: 252.7%
- Maximum number of tool contacts is also very different (23 w/o vs. 8 w)

7 22.10.2019 Prof. Dr.-Ing. J. Fleischer, Prof. Dr.-Ing. G. Lanza, Prof. Dr.-Ing. habil. V. Schulze



MOTIVATION METHODS TECHNICAL **TRUE** COMPARISON OUTLOOK

TRUE OVERLAP
 Exemplary calculation



True overlap
 Full thermo-mechanical FEM:

Material model

- Voce-Kocks-Vöhringer (AISI 4140)

Body boundary conditions

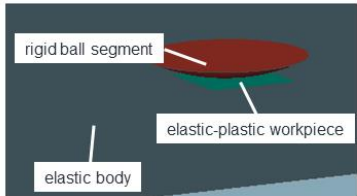
- 5 x 5 x 5 mm elastic body
- 0.5 x 0.5 x 0.1 mm elastic-plastic body
- Rigid tool, constant Temperature: RT

Surface element edge length

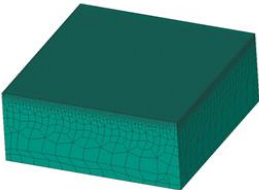
- 0.005 mm, no remeshing

Tool movement

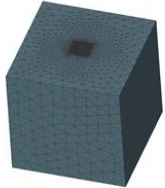
- Position & velocity based




Model setup:
 Workpiece comprised of "glued"
 elastic and elasto-plastic bodies.



Elasto-plastic body:
 Persistent hexmesh comprised of 26k elements
 with 10.2k nodes on relevant surface.




Elastic body:
 Persistent tetmesh comprised
 of 38k elements.



Rigid body:
 Persistent surface mesh comprised
 of 65k tri-facets.

8 22.10.2019 Prof. Dr.-Ing. J. Fleischer, Prof. Dr.-Ing. G. Lanza, Prof. Dr.-Ing. habil. V. Schulze



MOTIVATION METHODS TECHNICAL KINEMATIC **TRUE** COMPARISON OUTLOOK

TRUE OVERLAP
 Exemplary calculation

True overlap
 Full thermo-mechanical FEM:

Material model

- Voce-Kocks-Vöhringer (AISI 4140)

Body boundary conditions

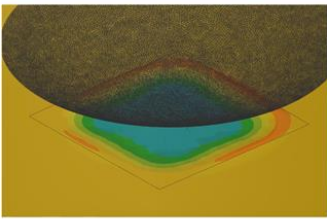
- 5 x 5 x 5 mm elastic body
- 0.5 x 0.5 x 0.1 mm elastic-plastic body
- Rigid tool, constant Temperature: RT

Surface element edge length

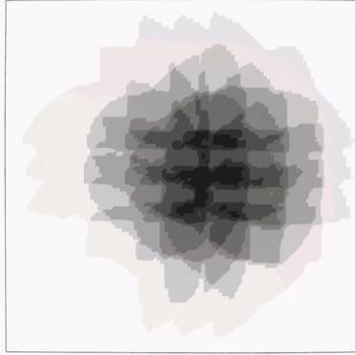
- 5 μm, no remeshing

Tool movement

- Position & velocity based



Animation: tool movement



True Overlap
 → $\alpha_s = 378.5\%$

- Full thermo-mechanical FEM enables calculation of true overlap considering material displacement
- True overlap is significantly lower than technical overlap (378.5% vs. 625.2%)
- True overlap is significantly higher than kinematic overlap considering former indentations (378.5% vs. 252.7%)

9 22.10.2019 Prof. Dr.-Ing. J. Fleischer, Prof. Dr.-Ing. G. Lanza, Prof. Dr.-Ing. habil. V. Schulze **wbk** Institute of Production Science

MOTIVATION METHODS TECHNICAL KINEMATIC TRUE **COMPARISON** OUTLOOK

COMPARISON
 Is technical overlap accurate enough for simple indentation shapes?

Technical overlap
 Simple calculation of area of indentation:

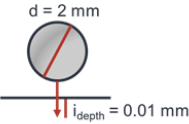
- 625.5%

Kinematic overlap

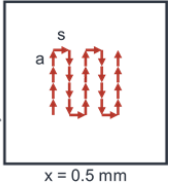
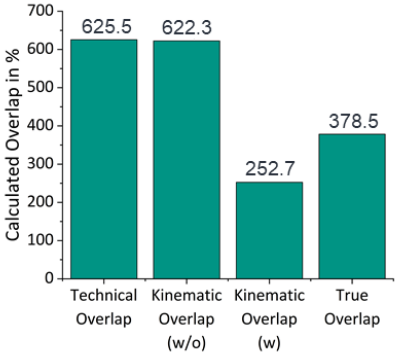
- 622.3% w/o consideration of former indentations
- 252.7% w consideration of former indentations

True overlap

- 378.5% full thermo-mechanical FE-simulation



5 x 5 indentations

Method	Calculated Overlap in %
Technical Overlap	625.5
Kinematic Overlap (w/o)	622.3
Kinematic Overlap (w)	252.7
True Overlap	378.5

Overlap: differences by calculation method

- Technical overlap severely overestimates the contact area!
- True overlap is closer to kinematic overlap (w) than technical overlap.
 → Kinematic overlap (w) features the best time invested vs. accuracy ratio.

10 22.10.2019 Prof. Dr.-Ing. J. Fleischer, Prof. Dr.-Ing. G. Lanza, Prof. Dr.-Ing. habil. V. Schulze **wbk** Institute of Production Science

MOTIVATION METHODS TECHNICAL KINEMATIC TRUE **COMPARISON** OUTLOOK

COMPARISON
 Is kinematic overlap accurate enough for complex indentation shapes?

Technical overlap

- Supposing an area comprised of two half-ovals

Kinematic overlap


- w/o consideration of former indentations
- w consideration of former indentations

True overlap

- Thermo-mechanical FE-Simulation

$r_k = 0.4 \text{ mm}$
 $r_\beta = 0.04 \text{ mm}$
 $\beta = 90^\circ$
 $\gamma = -7^\circ$
 $\alpha = 7^\circ$

5 x 5 indentations
 $y = 0.5 \text{ mm}$
 $x = 0.5 \text{ mm}$
 $a = s = 0.05 \text{ mm}$
 $i_{\text{depth}} = 0.01 \text{ mm}$

11 22.10.2019 Prof. Dr.-Ing. J. Fleischer, Prof. Dr.-Ing. G. Lanza, Prof. Dr.-Ing. habil. V. Schulze 

MOTIVATION METHODS TECHNICAL KINEMATIC TRUE **COMPARISON** OUTLOOK

COMPARISON
 Exemplary calculation

Technical overlap

Simple calculation of area of indentation:

- Calculate half-ovals area:
 - $A_i = (a_1 * b_1 + a_2 * b_2) * \pi / 2$
- Calculate Overlap
 - $o_s = n * A_i / A_{\text{total}}$
- Technical Overlap = 144.5%

Kinematic overlap

Numerical calculation in Matlab:

- Load .stl geometry
- Create master-indentation (dixel)
- Create translation matrix
- Calculate new surface with and without consideration of former indentations

True overlap

Full thermo-mechanical FEM:

Material model

- Voce-Kocks-Vöhringer (AISI 4140)

Body boundary conditions

- 5 x 5 x 5 mm elastic body
- 0.5 x 0.5 x 0.1 mm elastic-plastic body
- Rigid tool, constant Temperature: RT


Surface element edge length

- 0.005 mm, no remeshing

Tool movement

- Position & velocity based

- Kinematic overlap (w/o) and technical overlap should be the same.
- Elasto-plastic FE-simulation result should be closest to the truth and higher than kinematic overlap (w).

12 22.10.2019 Prof. Dr.-Ing. J. Fleischer, Prof. Dr.-Ing. G. Lanza, Prof. Dr.-Ing. habil. V. Schulze 

MOTIVATION METHODS TECHNICAL KINEMATIC TRUE **COMPARISON** OUTLOOK

COMPARISON
 Is kinematic overlap accurate enough for complex indentation shapes?

Technical overlap
 Simple calculation of area of indentation:

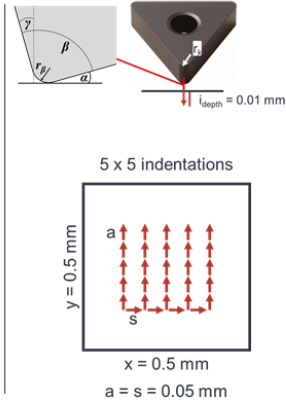
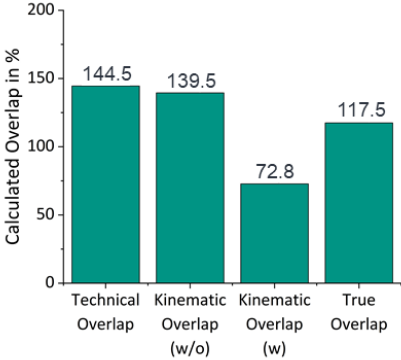
- 144.5%

Kinematic overlap

- 139.5% w/o consideration of former indentations
- 72.8% w consideration of former indentations

True overlap

- 117.5% full thermo-mechanical FE-simulation

Overlap: differences by calculation method

- Technical overlap is harder to calculate for complex indentation shapes.
- Analogous to simple indentation shapes, kinematic overlap (w/o) is closest to technical overlap.
 → Kinematic overlap (w) is less accurate for the indentation shape we analyzed!

13 22.10.2019 Prof. Dr.-Ing. J. Fleischer, Prof. Dr.-Ing. G. Lanza, Prof. Dr.-Ing. habil. V. Schulze

wbk Institute of Production Science

MOTIVATION METHODS TECHNICAL KINEMATIC TRUE **COMPARISON** OUTLOOK

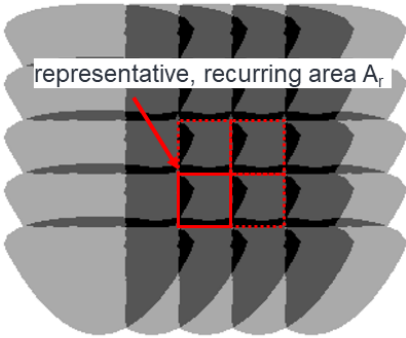
VDI 3416 EXTENSION?
 Considering deterministic surface topographies produced by hammer peening

Deterministic, recurring surface topographies

- Depend on all process parameters (distance of indentation, stepover distance, indenter shape etc.)
- Result in calculable technical and kinematic percentage overlap of surface

Representative percentage of overlap σ_r

- Calculated as per VDI within A_r
- Allows comparison of processes or process parameters without defining arbitrary areas or including peripheral phenomenon in the calculation



14 22.10.2019 Prof. Dr.-Ing. J. Fleischer, Prof. Dr.-Ing. G. Lanza, Prof. Dr.-Ing. habil. V. Schulze

wbk Institute of Production Science



OUTLOOK

We did

- Calculate overlap of indentations in different ways considering arbitrary indentation shapes

We found

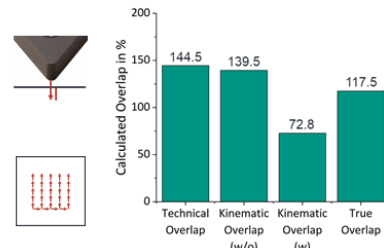
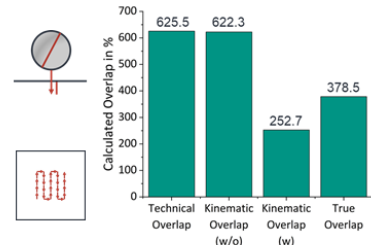
- Technical overlap is neither accurate, nor comparable regardless of indentation shape
- All overlap values calculated so far require knowledge of the surface area considered

We propose

- Extension of VDI 3416 considering deterministic surfaces: *representative percentage of overlap o_r*

What comes next

- Compare calculated overlap and surface topography with experimental results using different indentation shapes
- Refine tool movement in FE-simulation and in kinematic calculations (e.g. acceleration & energy based)



Thank you for your kind attention!

Eric Segebade M.Sc.
 Research Associate
 Tel.: +49 1523 9502615
 E-Mail: eric.segebade@kit.edu

wbk Institut of Produktionstechnik
 Kaiserstraße 12
 76131 Karlsruhe
<https://www.wbk.kit.edu/>

Influence of the process parameters on the penetration behaviour of ceramic particles in Composite Peening

Michael Seitz

IAM-WK – Institute for Applied Materials

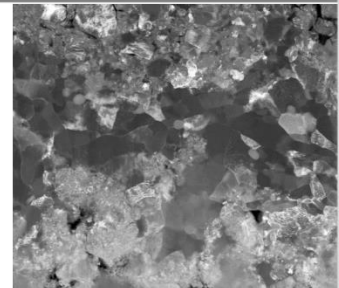
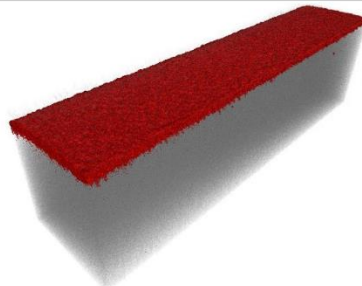
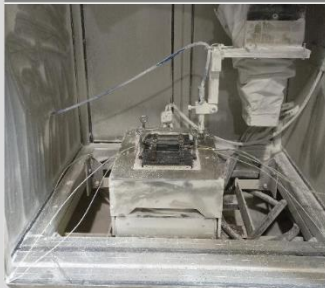
Karlsruhe Institute of Technology



Influence of the process parameters on the penetration behaviour of ceramic particles in Composite Peening

Symposium **Mechanische Oberflächenbehandlung 2019, Karlsruhe**
Michael Seitz
 Hybrid and Lightweight Materials

Institute for Applied Materials (IAM-WK)



KIT – Die Forschungsuniversität in der Helmholtz-Gemeinschaft



www.kit.edu

Motivation Composite Peening

Metal Matrix Composites (MMC)

- Improvement of specific properties, for instance by particle reinforcement
- Strengthening of the surface layer
- Functionally graded materials (FGM)

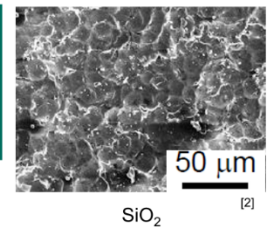
Micro Shot Peening

- Surface strengthening process
- Increase in fatigue strength
- Lower roughness compared to shot peening
- Ceramic blasting particles < 100 µm
- Embedment of blasting particles [2]



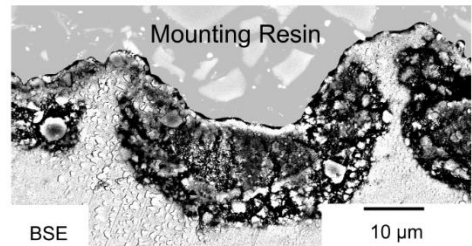
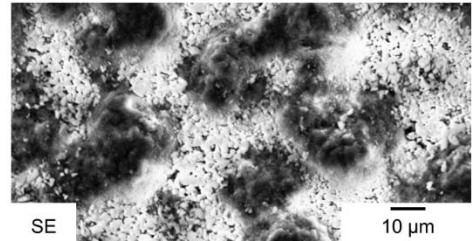
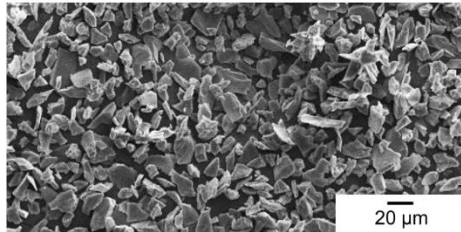
Composite Peening

- Manufacturing of a metal matrix composite by peening process
- Introduction of particles without liquid phase



Motivation
Penetration behaviour

- Observation from current research [3-5]
 - After composite peening a hill-valley profile is formed
 - The ceramic particles are mainly located in the valleys
 - Penetration depth is up to 30 µm
 - Particles are significantly smaller than their initial size



What happens to the blasting particles during the composite peening process?

3

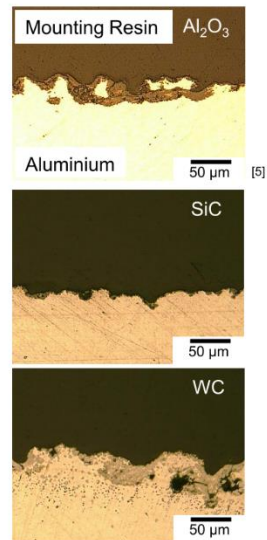
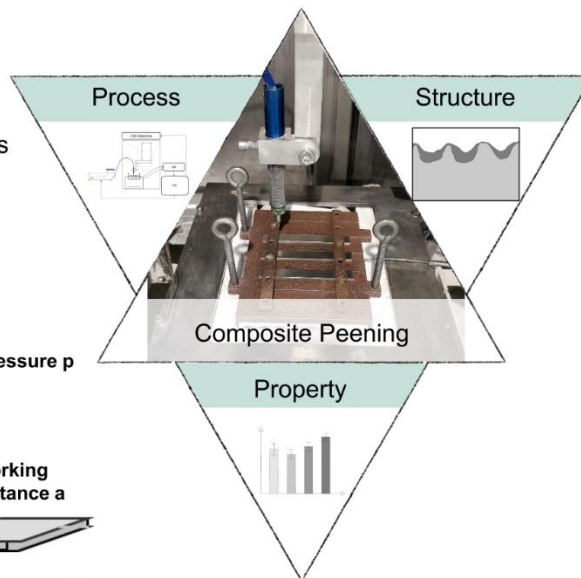
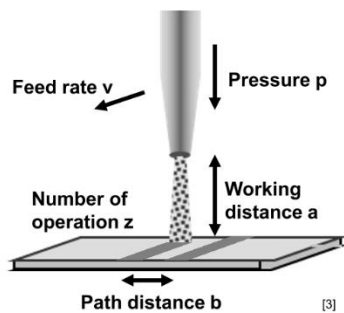
23.10.2019

Michael Seitz – Influence of the process parameters on the penetration behaviour of ceramic particles in Composite Peening

[3] Seitz et al., 2017
 [4] Seitz et al., 2019
 [5] Seitz et al., 2019

Agenda

- Manufacturing
- Penetration behaviour
 - Deep Impact in Metals
 - Solid Particle Erosion
 - Composite Peening
- Conclusion



4

23.10.2019

Michael Seitz – Influence of the process parameters on the penetration behaviour of ceramic particles in Composite Peening

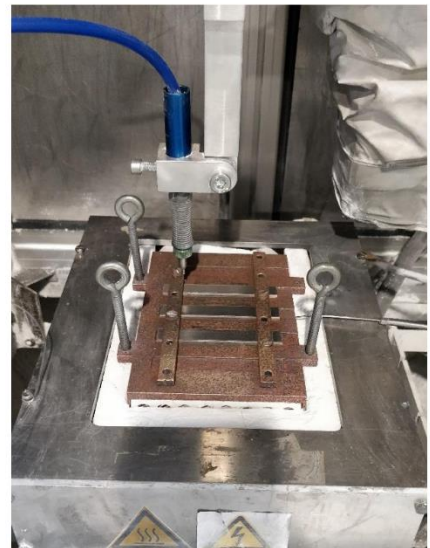
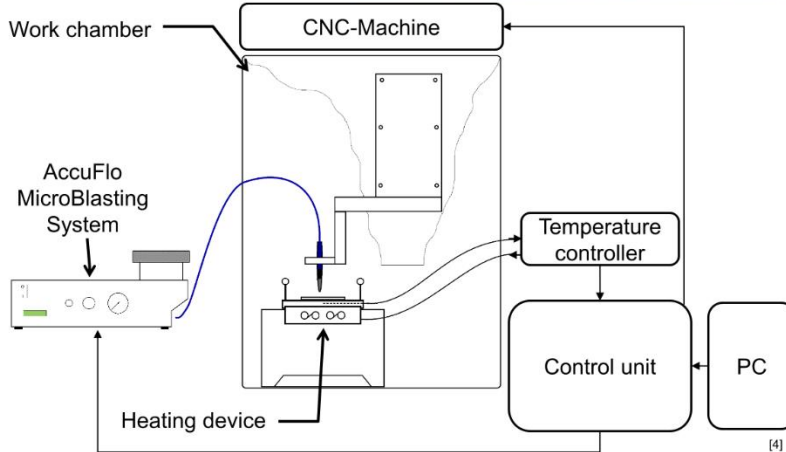
Manufacturing

5

23.10.2019

Michael Seitz – Influence of the process parameters on the penetration behaviour of ceramic particles in Composite Peening

Manufacturing Experimental setup

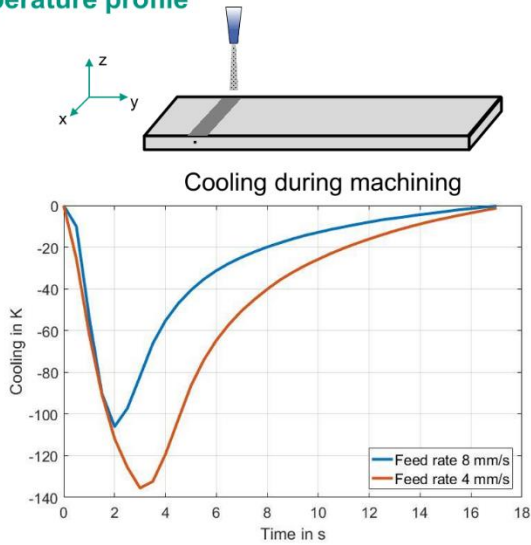


6

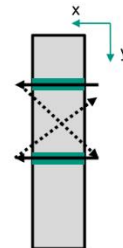
23.10.2019

Michael Seitz – Influence of the process parameters on the penetration behaviour of ceramic particles in Composite Peening

Manufacturing Temperature profile



Higher velocity
 Dwell time between machining operations



Symmetrical machining

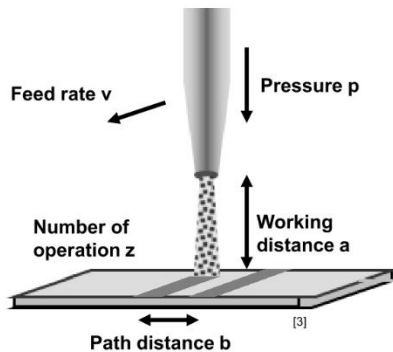
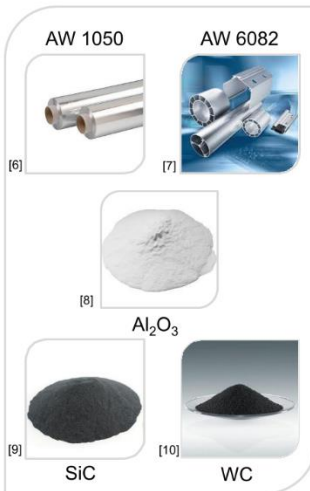
7

23.10.2019

Michael Seitz – Influence of the process parameters on the penetration behaviour of ceramic particles in Composite Peening

Manufacturing Process parameters for Composite Peening

[6] Esska GmbH [9] Haussen GmbH
 [7] Gerhardt AluTechnik GmbH [10] H.C. Starck GmbH
 [8] Bierther Submikron GmbH



Working distance (mm)	Path distance (mm)	Feed rate (mm/s)	Angle (°)
10	1	8	90

Pressure (bar)	Number of operation (-)	Temperature (T/T _s)
4; 7	2; 4; (10)	0,8; 0,9; 0,95

	1,28 – 1,81	mm
	28 – 81	%
	0,033 – 0,047	mmN
Mass flow rate	8,2 – 14,8	g/min

100.000.000 Particles/mm²

8

23.10.2019

Michael Seitz – Influence of the process parameters on the penetration behaviour of ceramic particles in Composite Peening

Deep Impact in Metals

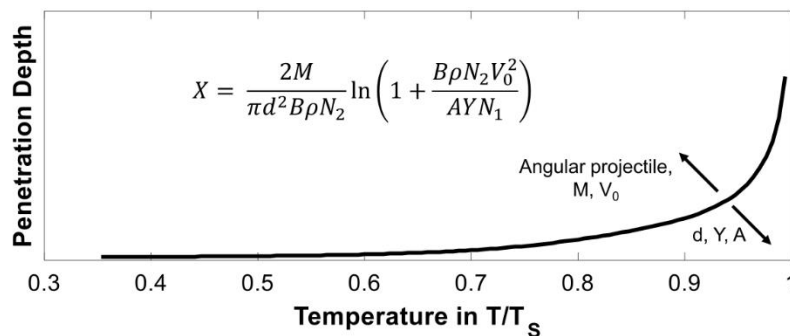
9

23.10.2019

Michael Seitz – Influence of the process parameters on the penetration behaviour of ceramic particles in Composite Peening

Deep Impact in Metals Determination of the penetration depth

- „Deep penetration of a non-deformable projectile with different geometrical characteristics“ [11]
 - Single particle impact
 - Penetration depth depends on momentum conservation, geometry of the projectile and dynamic-cavity expansion.



Particle properties

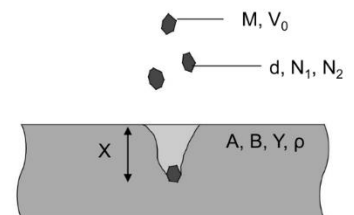
- M Mass of the projectile
- d Diameter of the projectile
- N_1, N_2 Projectile Shape

Target properties

- A, B Material constants
- ρ Density
- Y Yield strength

Process properties

- V_0 Velocity of the projectile
- X Penetration depth



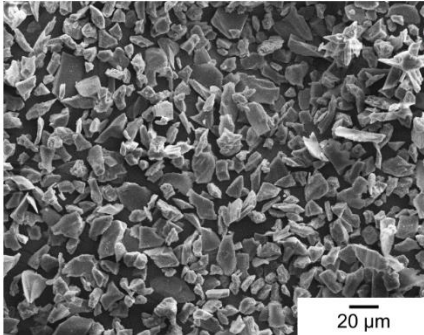
10

23.10.2019

Michael Seitz – Influence of the process parameters on the penetration behaviour of ceramic particles in Composite Peening

[11] Chen et al., 2002

Deep Impact in Metals Particle properties

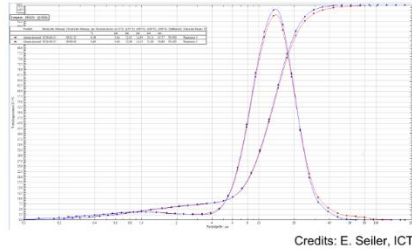


■ Shape and Size

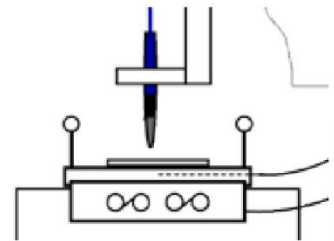
- Fracturing of the particles during processing?
- Average Diameter and size distribution

- Before Peening: 12.8 +/- 0.2 µm
- After Peening: 12.2 +/- 0.1 µm

10 %	90 %
5.38 µm	20.47 µm



➔ **No significant reduction in grain size**



$$X = \frac{2M}{\pi d^2 B \rho N_2} \ln \left(1 + \frac{B \rho N_2 V_0^2}{A Y N_1} \right)$$

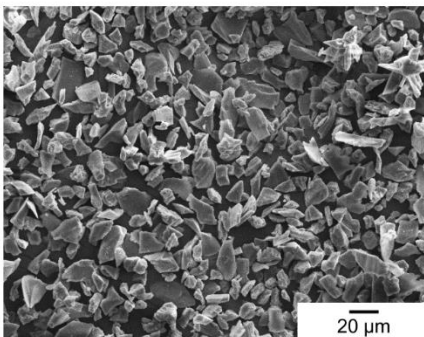
11

23.10.2019

Michael Seitz – Influence of the process parameters on the penetration behaviour of ceramic particles in Composite Peening

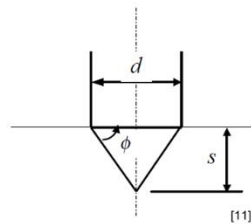


Deep Impact in Metals Particle properties



■ Shape and Size

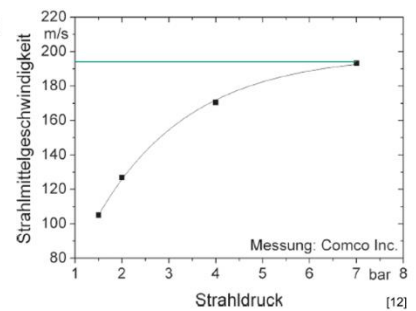
- Angular Shape
- Conical nose geometry
 - N1 = 1.30
 - N2 = 0.13



- Calculated weight of a particle
 - M = 1.9 ng (double cone)

10 %	90 %
0.2 ng	8.9 ng

- Velocity of the particles
 - V_{7bar} = 195 m/s



$$X = \frac{2M}{\pi d^2 B \rho N_2} \ln \left(1 + \frac{B \rho N_2 V_0^2}{A Y N_1} \right)$$

12

23.10.2019

Michael Seitz – Influence of the process parameters on the penetration behaviour of ceramic particles in Composite Peening

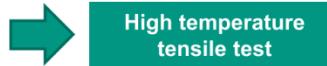
[12] Weingärtner et al., 2015



Deep Impact in Metals

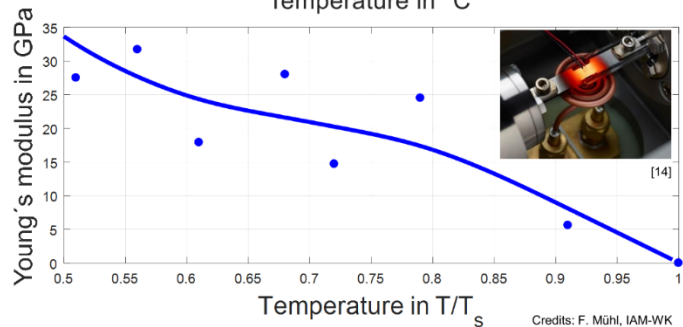
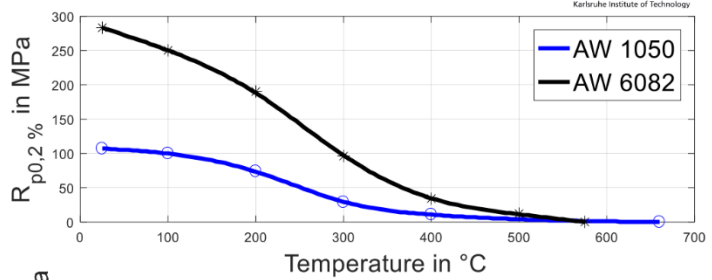
Target properties

- Certain material properties depend on the process temperature during composite peening
 - Yield Strength
 - Young's modulus



- $B = 1.041$ for Aluminium [13]
- $\rho_{Al} = 2.7 \text{ g/cm}^3$

$$X = \frac{2M}{\pi d^2 B \rho N_2} \ln \left(1 + \frac{B \rho N_2 V_0^2}{A Y N_1} \right)$$



13

23.10.2019

Michael Seitz – Influence of the process parameters on the penetration behaviour of ceramic particles in Composite Peening

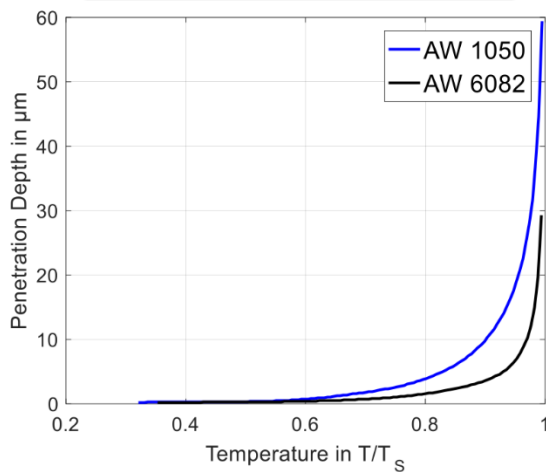
[13] Forrestal et al., 1988
 [14] TA Instruments, Inc



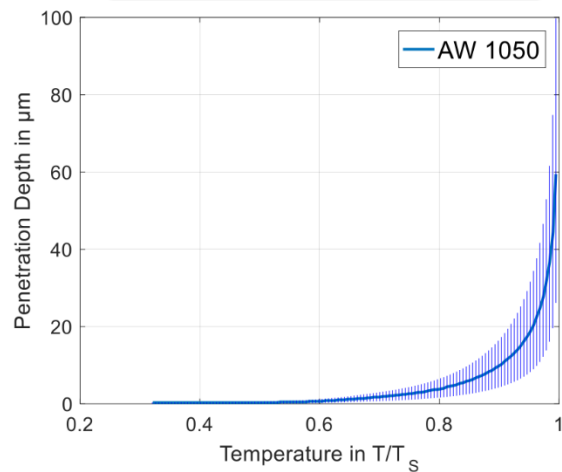
Deep Impact in Metals

Penetration depth

Influence of the target material



Influence of the projectile size




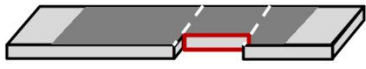
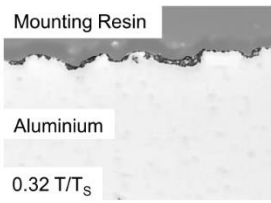
14

23.10.2019

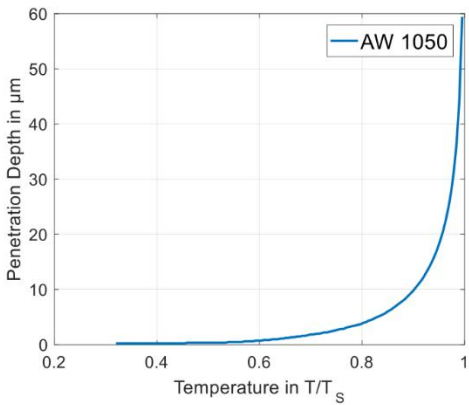
Michael Seitz – Influence of the process parameters on the penetration behaviour of ceramic particles in Composite Peening



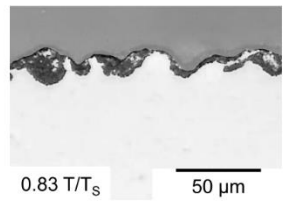
Deep Impact in Metals Penetration depth

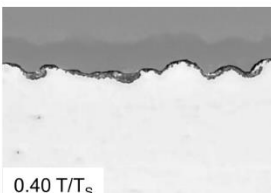
Mounting Resin
Aluminium
0.32 T/T_s



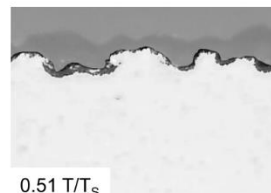
Penetration Depth in µm
Temperature in T/T_s
— AW 1050



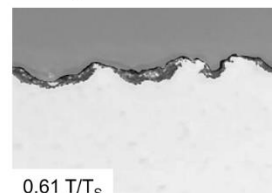
0.83 T/T_s 50 µm



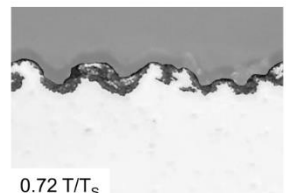
0.40 T/T_s



0.51 T/T_s




0.61 T/T_s





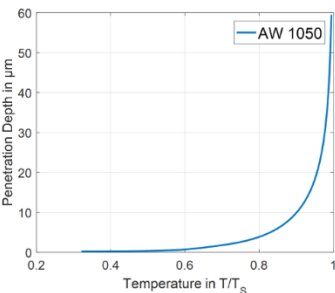
0.72 T/T_s

15 23.10.2019 Michael Seitz – Influence of the process parameters on the penetration behaviour of ceramic particles in Composite Peening

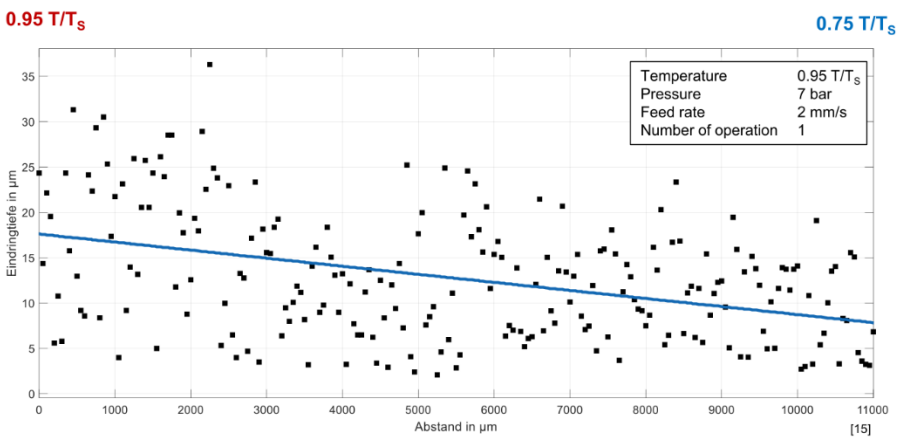


Deep Impact in Metals Penetration depth

- Penetration depth along a blasting path
- Cooling from 0.95 T/T_s to 0.75 T/T_s






Penetration Depth in µm
Temperature in T/T_s
— AW 1050



Eindringtiefe in µm
Abstand in µm
Temperature 0.95 T/T_s
Pressure 7 bar
Feed rate 2 mm/s
Number of operation 1

16 23.10.2019 Michael Seitz – Influence of the process parameters on the penetration behaviour of ceramic particles in Composite Peening [15] Scherr, BA, 2018



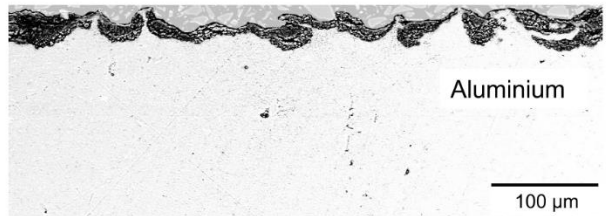
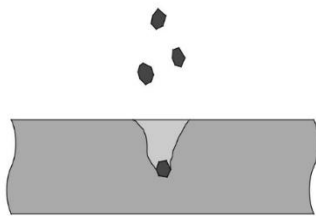
Solid Particle Erosion (SPE)

17

23.10.2019

Michael Seitz – Influence of the process parameters on the penetration behaviour of ceramic particles in Composite Peening

Solid Particle Erosion Composite Peening

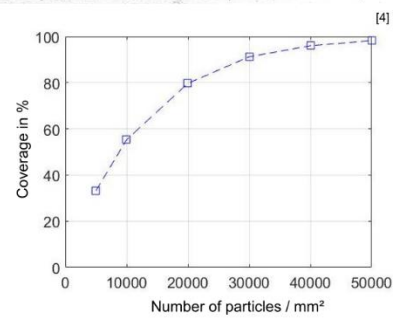


- Difference: Single particle impact – Composite Peening
- During compound blasting, ~ 100 million particles / mm² hit the surface.



Multiple Particle Impact

- Similar to Solid Particle Erosion



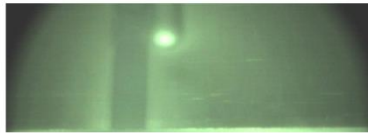
18

23.10.2019

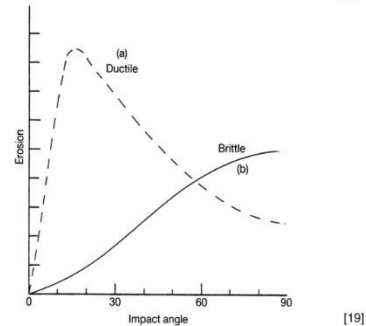
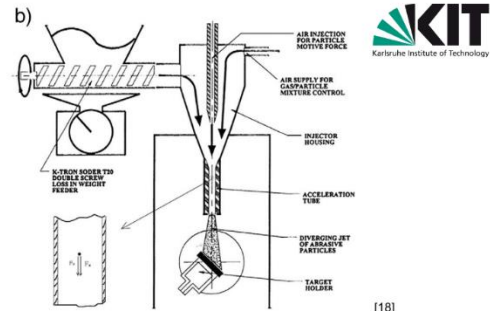
Michael Seitz – Influence of the process parameters on the penetration behaviour of ceramic particles in Composite Peening

Solid Particle Erosion Overview

- Field of research since WW II [16]
 - Power plant vessel
 - Pneumatic transportation systems
 - Helicopter rotor blades
- Occurs when granular particles hit a material surface
- Impact angle is an important factor in SPE
 - Maximum erosion of brittle materials at 90°
 - Maximum erosion of ductile materials at 15° - 45°
- Kinetic energy is mainly converted into elastic-plastic deformation and fracture energy
- Luminescence can also be observed [17]



Composite Peening,
 Al_2O_3 & AW 1050



19

23.10.2019

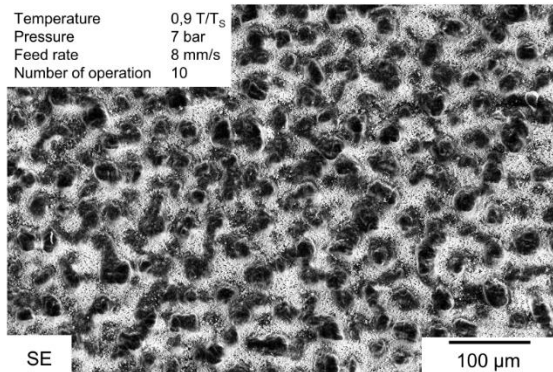
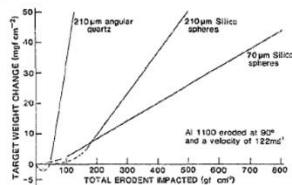
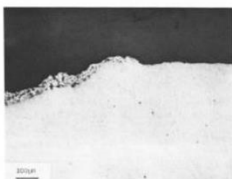
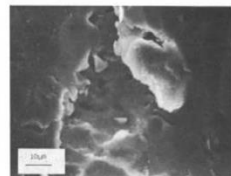
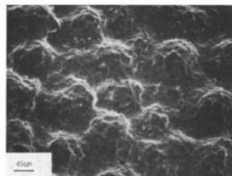
Michael Seitz – Influence of the process parameters on the penetration behaviour of ceramic particles in Composite Peening

[16] Kleis et al., 2008 [19] Hutchings, 1992
 [17] Thiessen, 1967
 [18] Deng et al., 2008



Solid Particle Erosion Aluminium

- With aluminium, no erosion rate can be observed at an impact angle of 90° because blasting particles are embedded [16]
- SPE at AW 1100 showed a hill-valley profile and embedded particles [20]



Temperature 0,9 T/T_s
 Pressure 7 bar
 Feed rate 8 mm/s
 Number of operation 10

20

23.10.2019

Michael Seitz – Influence of the process parameters on the penetration behaviour of ceramic particles in Composite Peening

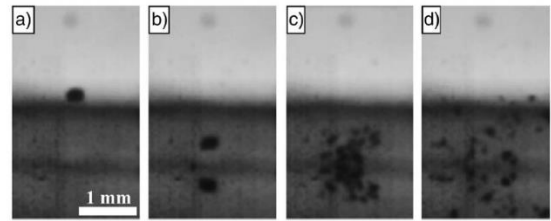
[20] Brown et al., 1983



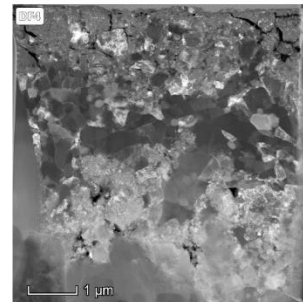
Solid Particle Erosion Particle Fracturing

- Several authors have proven that particles fracture on impact (according to Bousser [21])
 - Wada presents the thesis that particles fragment upon impact when the hardness of the particles \leq hardness target material [23]
 - Particle toughness is also important
- After Composite Peening, nanoscale aluminium oxide particles can be found in the surface layer

➔ Multiple impacts cause the particles to fracture



Sand particle on tungsten carbide surface [22]



21 23.10.2019

Michael Seitz – Influence of the process parameters on the penetration behaviour of ceramic particles in Composite Peening

[21] Bousser et al., 2014
[22] Celotta et al., 2007
[23] Wada, 1992

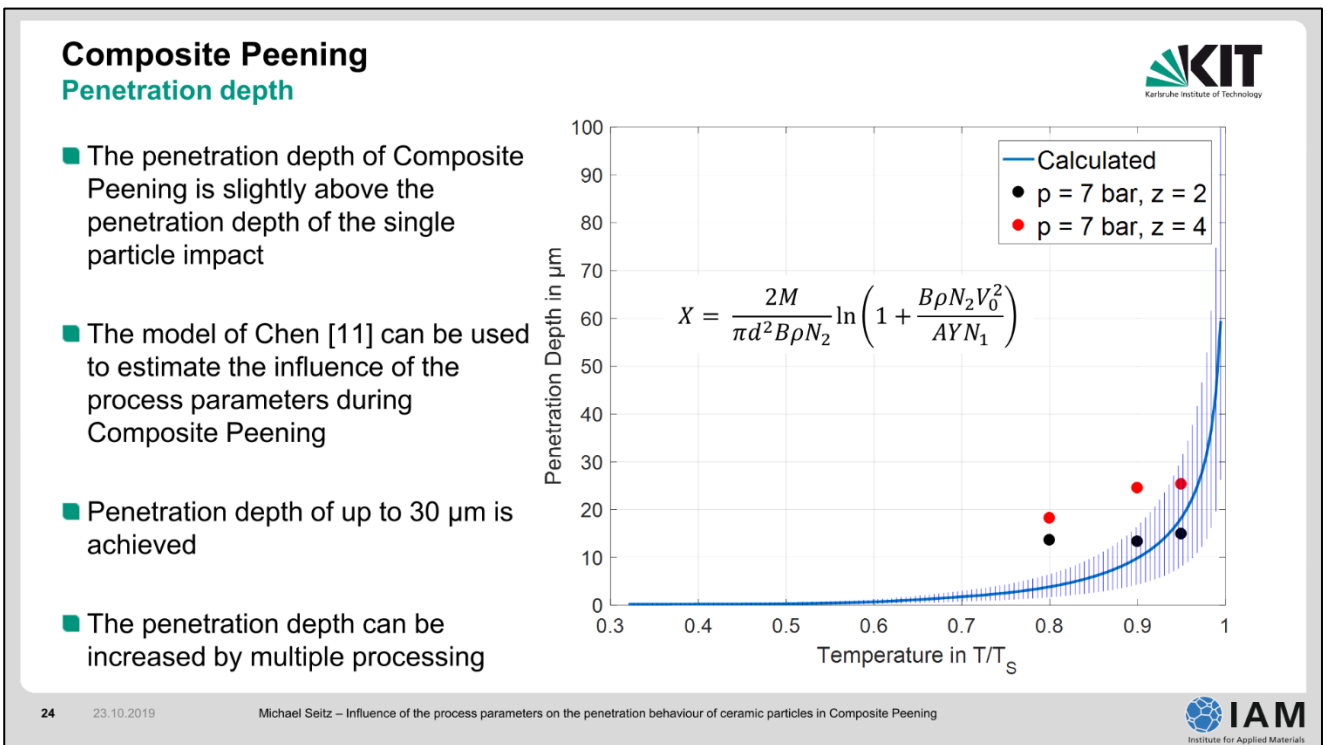
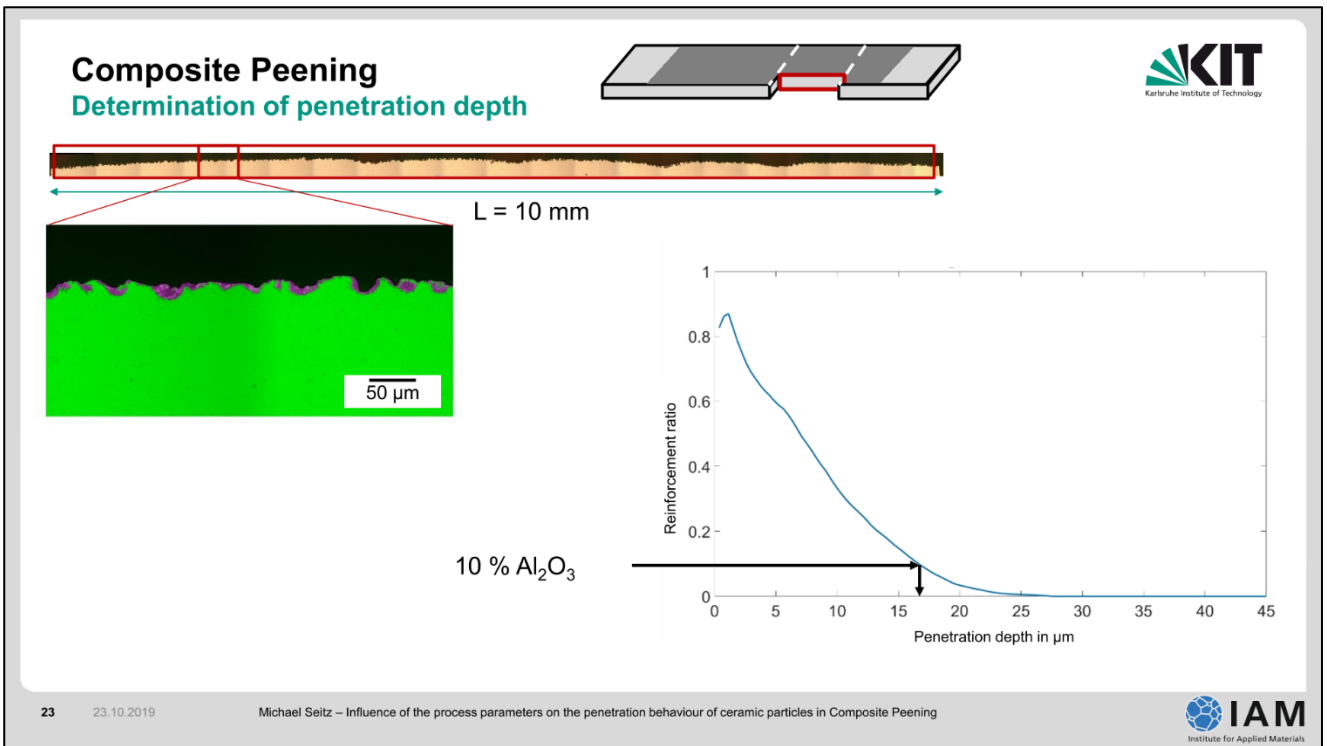


Composite Peening

22 23.10.2019

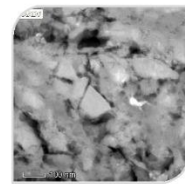
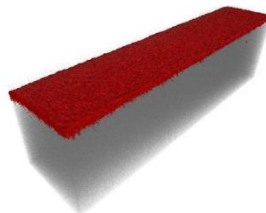
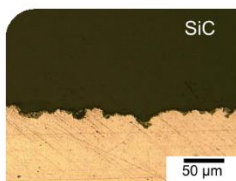
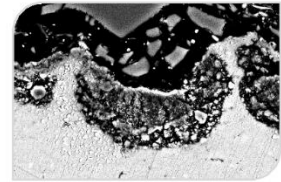
Michael Seitz – Influence of the process parameters on the penetration behaviour of ceramic particles in Composite Peening





Conclusion & Outlook

- Estimation of penetration depth during compound peening based on a ballistic model
- Influence of individual process parameters on the penetration depth
- Correlation between Composite Peening and Solid Particle Erosion
- Adaptation of the model to other material combinations
 - WC and SiC as blasting particles

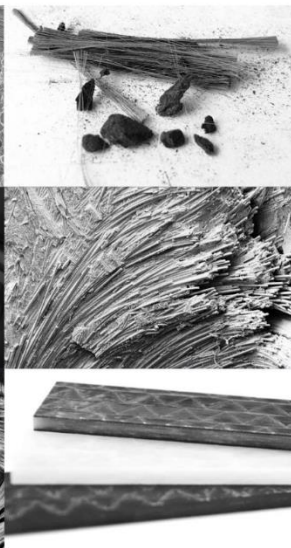


25

23.10.2019

Michael Seitz – Influence of the process parameters on the penetration behaviour of ceramic particles in Composite Peening

Thank you for your attention!

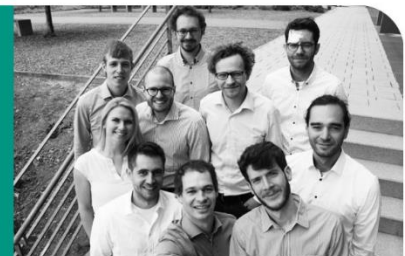


Michael Seitz

Karlsruhe Institute of Technology
Institute for Applied Materials
IAM-WK
Hybrid and Lightweight Materials

Kaiserstr. 12
Building. 10.96, office 113
76131 Karlsruhe, Germany
+49 721 608-47450

Michael.Seitz@kit.edu



The authors would like to thank the German Research Foundation (DFG) for the financial support.



WE4273/15-1

26

23.10.2019

Michael Seitz – Influence of the process parameters on the penetration behaviour of ceramic particles in Composite Peening

References

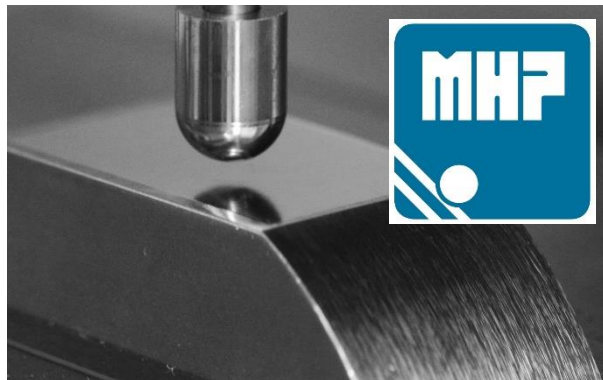
- [1] K. M. Gupta, Materials Science, Metallurgy and Engineering Materials, Umesh Publications, New Delhi, (2012).
- [2] Ando, M., Kitano, H., Usami, H., Endo, T. Applicability of fine particle peening on surface modification of aluminum alloy. In: The 10th International Conference On Shot Peening procedure, pp. 223-227 (2008).
- [3] Seitz, M., Reeb, A., Klumpp, A., Weidenmann, K. A. Composite Peening - A Novel Processing Technology for Graded Reinforced Aluminium Matrix Composites. Key Engineering Materials, 742, 137-144 (2017).
- [4] Seitz, M., Weidenmann, K. A. Influence of the Process Parameters on the Penetration Depth of the Reinforcing Phase During Composite Peening for the Production of Functionally Graded Metal Matrix Composites. Key Engineering Materials, 809, 73-78 (2019).
- [5] Seitz, M., Weidenmann, K. A. Investigations on Composite Peened Aluminium. In: International Conference on Advanced Surface Enhancement, pp. 10-18 (2019).
- [11] Chen, X. W., Li, Q. M. Deep penetration of a non-deformable projectile with different geometrical characteristics. International Journal of Impact Engineering, 27.6, pp. 619-637 (2002).
- [12] Weingärtner, R., Hoffmeister, J., Schule, V. Mechanische Oberflächenbearbeitung durch das Mikrostrahlen. Journal of Heat Treatment and Materials, 70.2, pp. 59-65 (2015).
- [13] Forrestal, M. J., Okajima, K., Luk, V. K. Penetration of 6061-T651 aluminum targets with rigid long rods. Trans ASME J Appl Mech, 55, pp. 755-760 (1988).
- [15] Scherr, T. Einfluss der Verbundstrahlparameter auf die Prozesstemperatur und Eindringtiefe. IAM-WK, Bachelorarbeit, (2018).
- [16] Kleis, I., Kulu, P. Solid particle erosion: occurrence, prediction and control. Springer Science & Business Media, 2007.
- [17] Thiessen, P. A. Physikalisch-chemische Untersuchungen tribomechanischer Vorgänge. Grundlagen der Tribochemie. Akademie-Verlag, pp. 7-23 (1967).
- [18] Deng, T., Bingley, M. S., Bradley, M. S. A., De Silva, S. R. A comparison of the gas-blast and centrifugal-accelerator erosion testers: The influence of particle dynamics. Wear, 265, pp. 945-955 (2008).
- [19] Hutchings, I. M. Transitions, threshold effects and erosion maps. Key Engineering Materials. Trans Tech Publications, 71, pp. 75-92 (1999).
- [20] Brown, R., Kosco, S., Jun, E. J. The effect of particle shape and size on erosion of aluminum alloy 1100 at 90 impact angles. Wear, 88.2, pp.181-193 (1983).
- [21] Bousser, E., Martinu, L., Klemberg-Sapieha, J. E. Solid particle erosion mechanisms of protective coatings for aerospace applications. Surface and Coatings Technology, 257, pp. 165-181 (2014).
- [22] Celotta, D. W., Qureshi, U. A., Stepanov, E. V., Goulet, D. P., Hunter, J., Buckberry, C. H., Hill, R., Sherikar, S. V., Moshrefi-Torbati, M., Wood, R. J. K. Sand erosion testing of novel compositions of hard ceramics. Wear, 263, pp. 278-283 (2007).
- [23] Wada, S. WADA, S. Effects of hardness and fracture toughness of target materials and impact particles on erosion of ceramic materials. Key Engineering Materials. Trans Tech Publications, 71, pp. 51-74 (1992).

Residual stress relaxation in HFMI-treated fillet welds after single overload peaks

Jan Schubnell

Institute for Mechanics of Materials IWM

Fraunhofer



RESIDUAL STRESS RELAXATION IN HFMI-TREATED FILLET WELDS AFTER SINGLE OVERLOAD PEAKS

Symposium Mechanische Oberflächenbehandlung
KIT Karlsruhe, 22.-23.10.2019



Jan Schubnell, Eva Carl, Majid Farajian (IWM)
Stefanos Gkatzogiannis, Peter Knödel, Thomas Ummenhofer (KIT)
Robert Wimpory (HZB)
Hamdollah Eslami (IFS)

1
© Fraunhofer IWM

AGENDA Residual stress relaxation at HFMI-treated fillet welds after single overload peaks

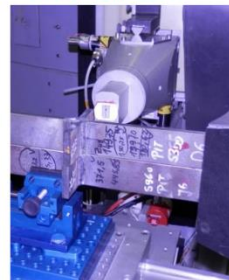
IIW – Document XIII-2829-19

- Motivation
- Experimental set-up
 - Material and weld detail
- Residual stress analysis
 - Experimental study
 - Numerical study
- Conclusion

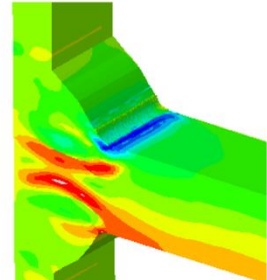
X-ray-diffr.



Neutron-diffr.



FEA

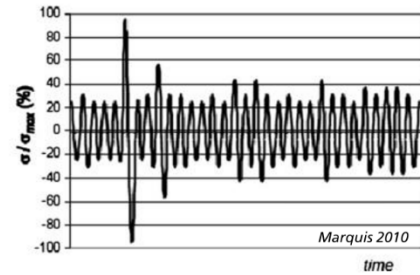
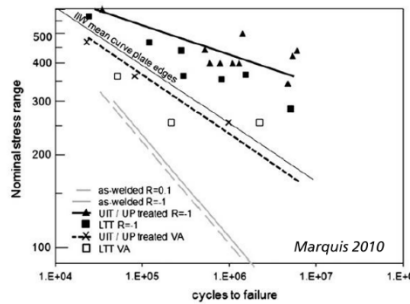


2
© Fraunhofer IWM



Motivation

- Significant fatigue life improvement of HFMI-treated welded joints is statistically proved (*Marquis and Barsoum 2016*) based on numerous studies under constant amplitude (CA) loading
- Studies have shown that the fatigue life benefit decreases at variable amplitude (VA) loading (*Marquis 2010, Leitner et al. 2018*).
- It is assumed that this decrease is strongly related to the compressive residual stress relaxation under high peak stresses



3
 © Fraunhofer IWM



Motivation

- Multiple recommendations exist to limit the RS-relaxation:

$$S_{max}/S_{min} = +/ -0.45f_y \quad \text{Marquis et al. (2013)*} \quad (R < -0.125)$$

$$S_{max}/S_{min} = +/ -0.6f_y \quad \text{Mikkola et al. (2017)} \quad (R = -1)$$

$$S_{max}/S_{min} = +/ -0.8f_y \quad \text{Haagensen and Maddox (2013)**}$$

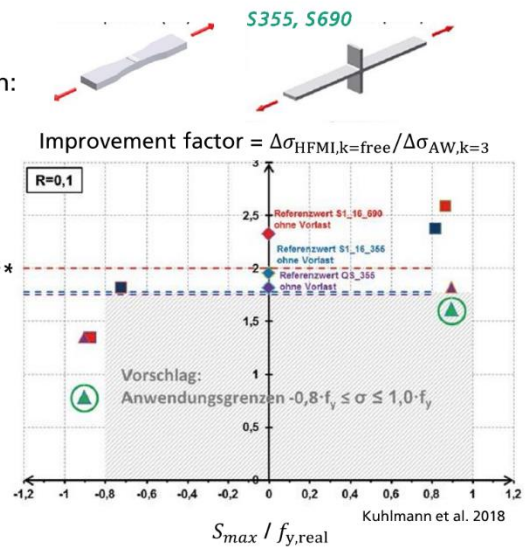
$$S_{min} = -0.8f_y / S_{max} = f_y \quad \text{Kuhlmann et al. (2018)***}$$

Aim: Quantify the compressive residual stress relaxation

S_{max} = Maximum nominal stress, f_y = nominal yield of the base material

R = Stress ratio

*Current IIW-Recommendation (HFMI) / ** Hammer & Needle Peening / *** German DAST guideline (not released yet)

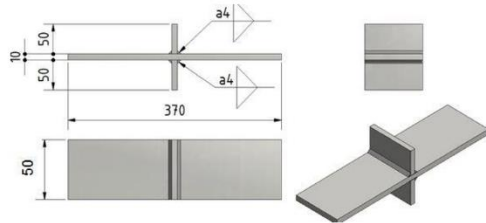


4
 © Fraunhofer IWM



Material and specimen details

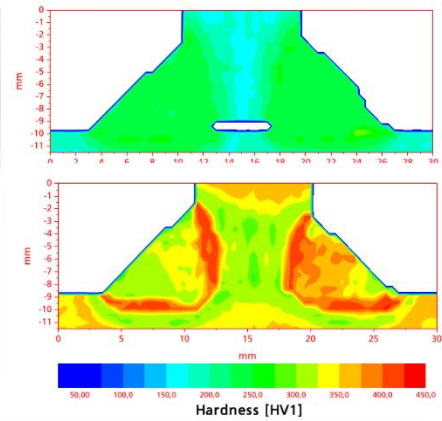
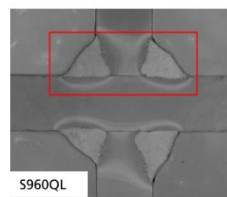
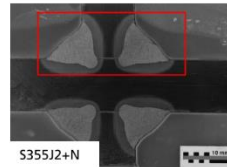
- Steel: **S355J2+N / S960QL**
- Weld detail: Transverse stiffener
- Weld type: Single layer fillet weld*
- Weld process: GMAW (135)*
- HFMI: Pneumatically Impact treatment (PIT)



*J. Schubnell, D. Discher, and M. Farajian, "Static, dynamic and cyclic properties of the heat affected zone for different steel grades," *Mater. Test.*, vol. 61, no. 7, 2019

Materials	Yield strength [MPa]	Ultimate Strength [MPa]	Elongation [%]	Hardness [HV10]
S355J2+N	420	538	25*	169
S960QL	1011	1060	14*	316

*data sheet



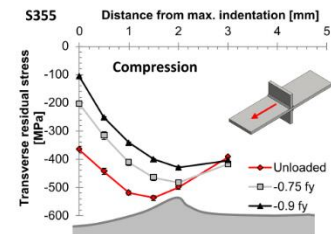
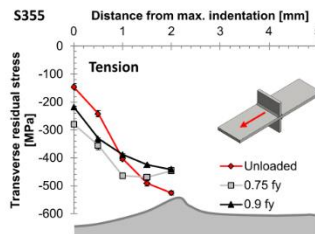
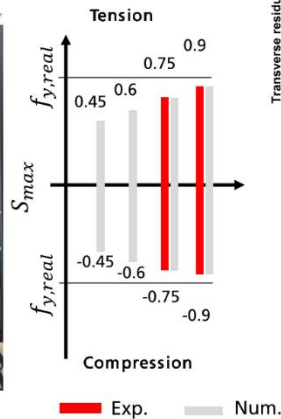
5
© Fraunhofer IWM



Experimental test set-up / residual stress analysis

„Stress peaks“ from VA loading were approximated by single static loads (majority of residual stress relaxation occurs at N=1 (Farajian et al. 2010, Leitner et al. 2018))

Load set-up (IFS)
 PLm 630N



6
© Fraunhofer IWM

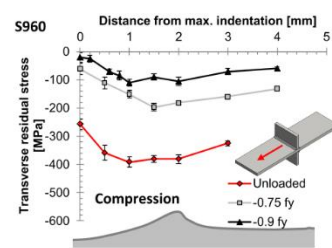
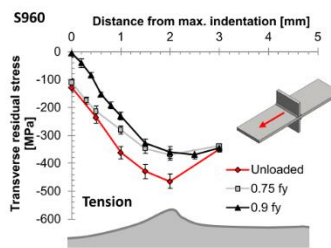
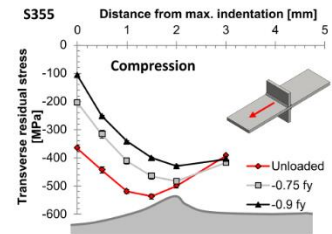
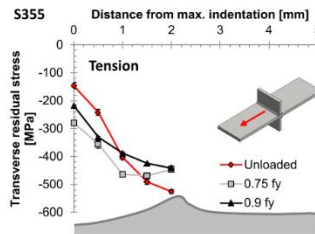
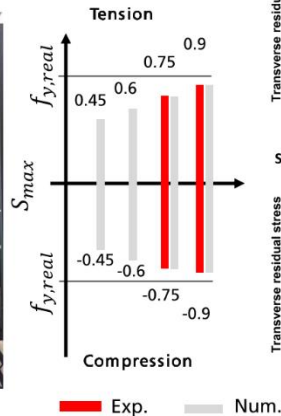


Experimental test set-up / residual stress analysis

„Stress peaks“ from VA loading were approximated by single static loads (majority of residual stress relaxation occurs at N=1 (Farajian et al. 2010, Leitner et al. 2018))

Load set-up (IFS)

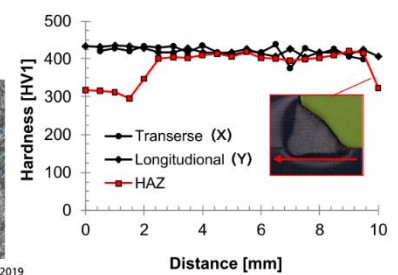
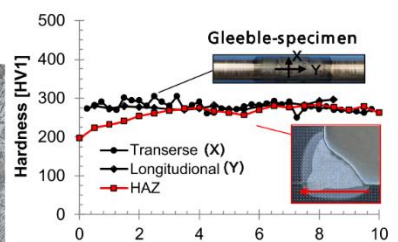
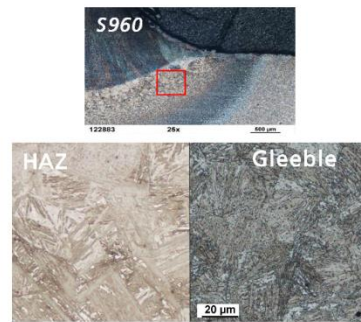
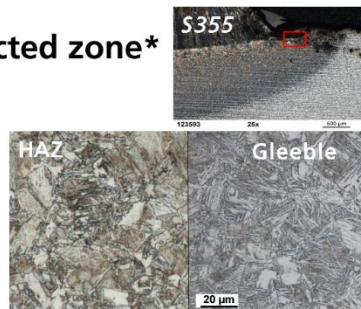
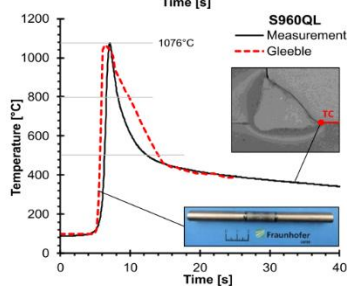
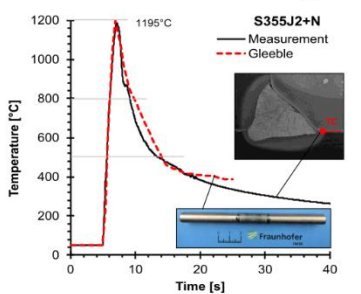
PLm 630N



7
© Fraunhofer IWM



Material modelling: Heat affected zone*



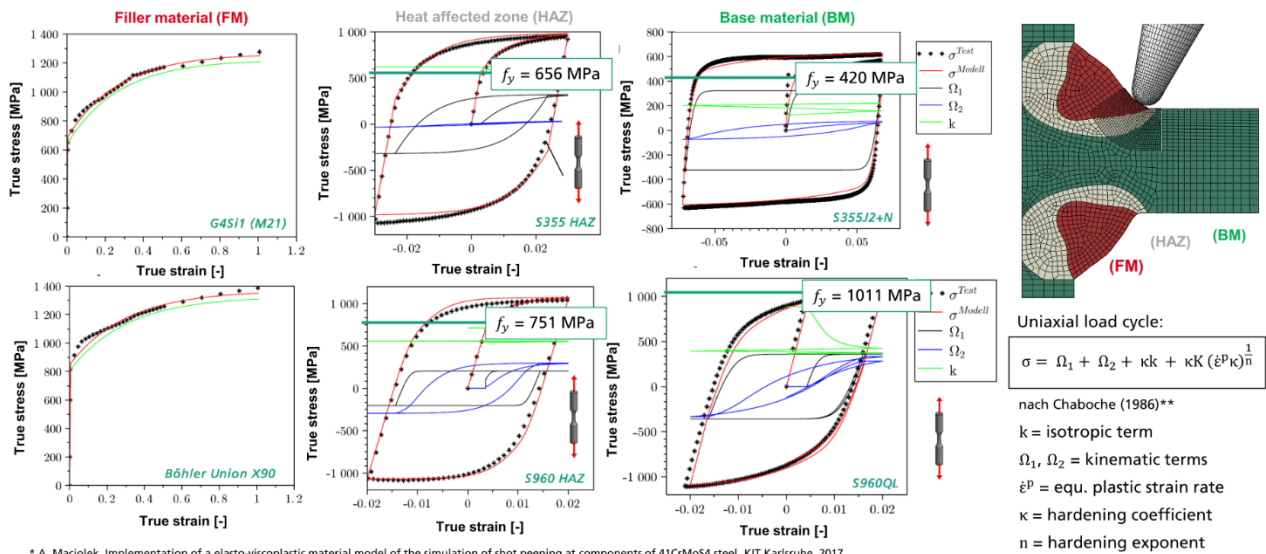
*J. Schubnell, D. Discher, and M. Farajian, "Static, dynamic and cyclic properties of the heat affected zone for different steel grades," Mater. Test., vol. 61, no. 7, 2019

8
© Fraunhofer IWM



Numerical simulation: Constitutive model

(implemented as VUMAT-Subroutine by Maciolek 2017*)



* A. Maciolek, Implementation of an elasto-viscoplastic material model of the simulation of shot peening at components of 41CrMo54 steel, KIT Karlsruhe, 2017.
 ** J.-L. Chaboche, "Time-independent constitutive theories for cyclic plasticity," *Int. J. Plast.*, vol. 2, pp. 149-188, 1986

© Fraunhofer IWM

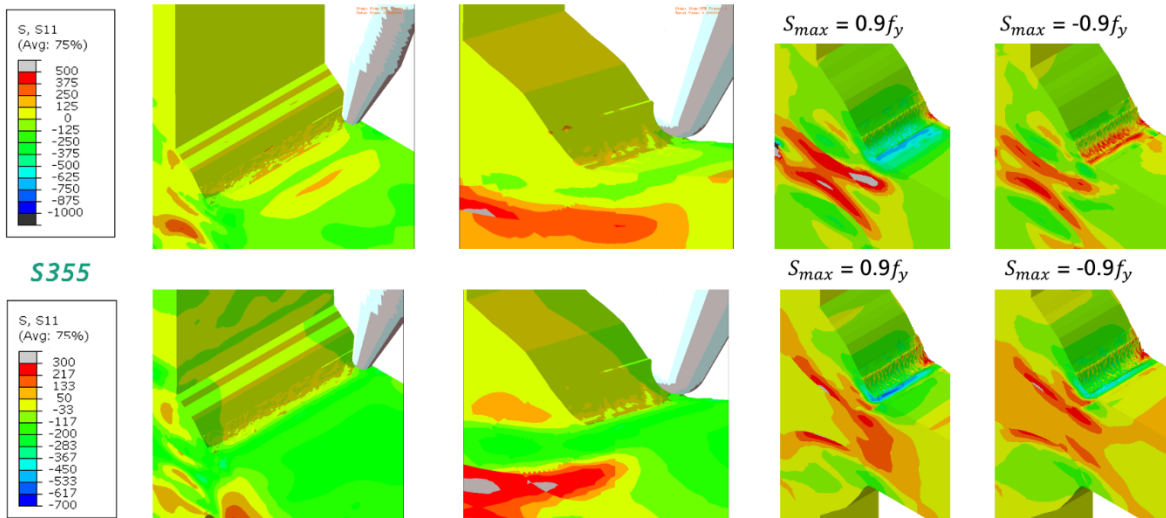


Numerical simulation: Residual stress analysis

Transverse residual stress contour plot

S960

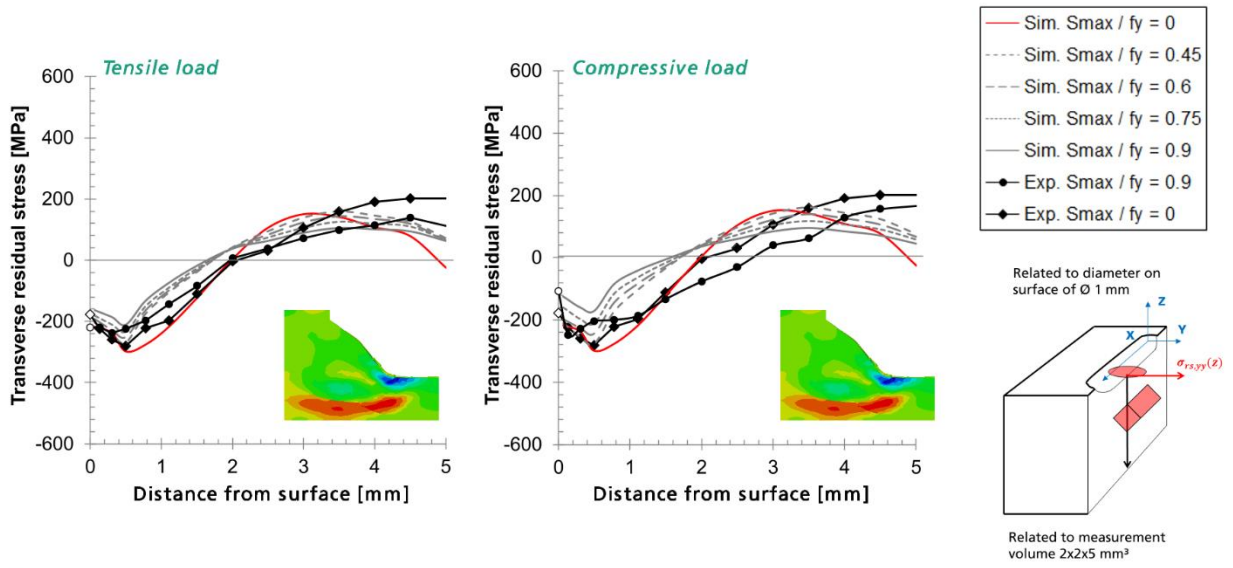
Finite-Element simulation according to Hardenacke et al. (2015), Föhrenbach et. al (2016), Schubnell et al. (2017) and Ernould et. al (2019)



10
© Fraunhofer IWM



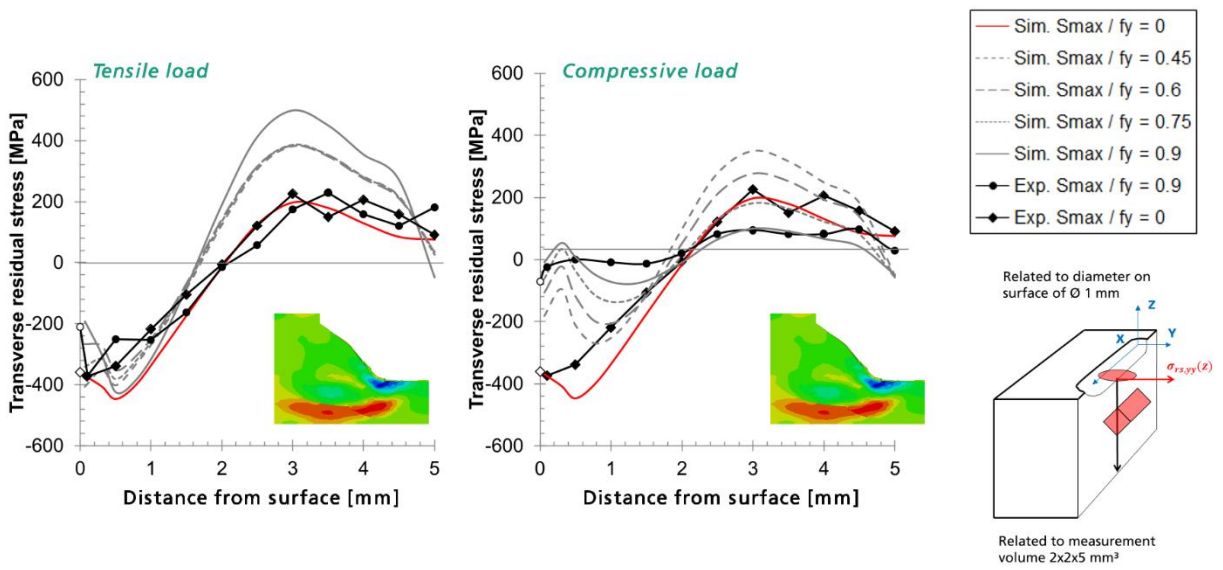
Numerical / Experimental residual stress analysis S355



11
 © Fraunhofer IWM



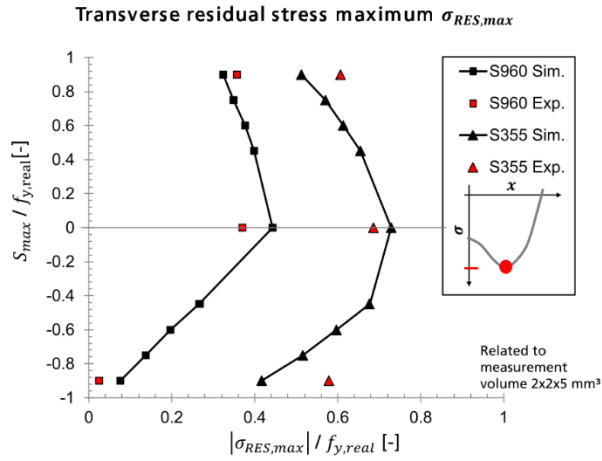
Numerical / Experimental residual stress analysis S960



12
 © Fraunhofer IWM



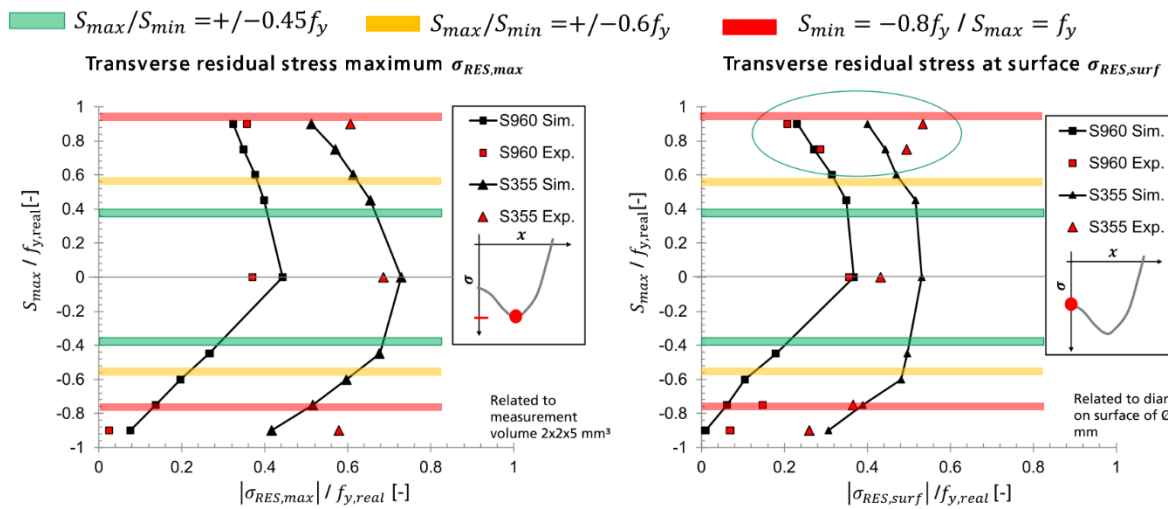
Residual stress analysis: $S_{max} \sim \Delta\sigma_{RES}$



S_{max} = Maximum nominal stress, f_y = yield strength of the base material

13
© Fraunhofer IWM

Residual stress analysis: $S_{max} \sim \Delta\sigma_{RES}$



S_{max} = Maximum nominal stress, $f_{y,real}$ = real yield strength of the base material

14
© Fraunhofer IWM

Conclusion

- Compressive overloads close to the base materials yield strength ($-0.9f_y$) lead to nearly full residual stress relaxation for S960 and around half residual stress relaxation for S355.
- For tensile overloads close to the base materials ($0.9f_y$) yield strength only minor residual stress (-10% to -35%) relaxation was observed for both steel grades.
- Significantly less residual stress relaxation was determined for S355 than for S960 at the same normalized nominal stress S_{max}/f_y .
- IIW-recommendation of S_{max}/f_y shows a clear over-conservatism.

15
© Fraunhofer IWM



Literature

- | | |
|---------------------------|--|
| Marquis et al. (2013) | G. B. Marquis, E. Mikkola, H. C. Yildirim, and Z. Barsoum, "Fatigue strength improvement of steel structures by high-frequency mechanical impact: proposed fatigue assessment guidelines," <i>Weld. World</i> , vol. 57, no. 6, pp. 803–822, Nov. 2013 |
| Haagensen & Maddox (2013) | P. J. Haagensen and S. J. Maddox, <i>IIW recommendations on post weld improvement of steel and aluminium structures</i> , no. 79. Cambridge: Woodhead Publishing Ltd, 2013. |
| Mikkola et al. (2013) | E. Mikkola and H. Remes, "Allowable stresses in high-frequency mechanical impact (HFMI)-treated joints subjected to variable amplitude loading," <i>Weld. World</i> , vol. 61, no. 1, 2017. |
| Kuhlmann et al. (2018) | U. Kuhlman, S. Breunig, T. Ummenhofer, and P. Weidner, "Entwicklung einer DASt-Richtlinie für höherfrequente Hämmerverfahren - Zusammenfassung der durchgeführten Untersuchungen und Vorschlag eines DASt-Richtlinien-Entwurfs (in German)," <i>Stahlbau</i> , vol. 10, no. 87, 2018 |

16
© Fraunhofer IWM



Interne Verfestigungsdomänen durch mechanische Oberflächenbehandlung während der additiven Fertigung

Dr.-Ing. Daniel Meyer

IWT Manufacturing Technologies

University of Bremen



Interne Verfestigungsdomänen durch mechanische Oberflächenbehandlung während der additiven Fertigung

Symposium Mechanische Oberflächenbehandlung
am
22. und 23. Oktober 2019

Dr.-Ing. D. Meyer
M.Sc. N. Wielki

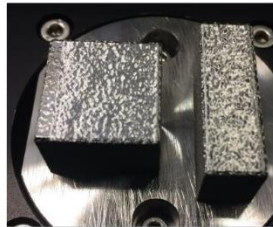
Scope of this presentation

Additive Manufacturing

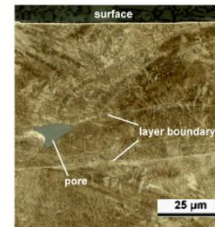


EOS.info

Parts with limited surface quality and complex microstructures



Leibniz-IWT



Brinksmeier et al., CIRP 2010

Post-Processing influencing the Surface Integrity

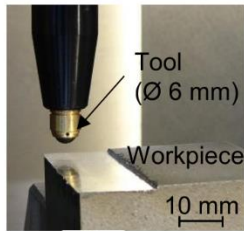


Dmgmori.com

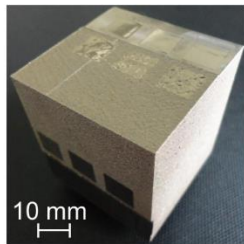
Leibniz-IWT

Potential of milling and deep rolling

in post-processing of AM parts



Experimental setup



Cube after processing

Printing parameters

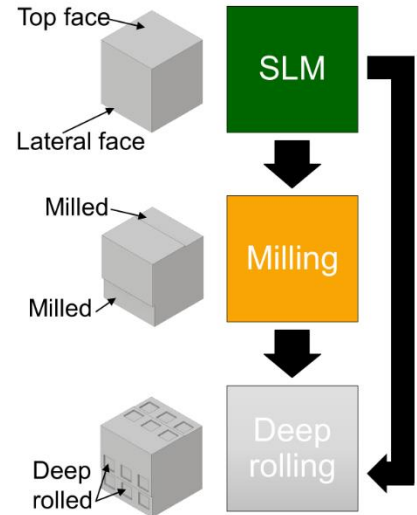
- Layer thickness l 50 μm
- Laser power P_L 235 W
- Scan velocity v_s 700 mm/s
- Hatch distance h_d 150 μm , 120 μm

Milling parameters

- Cutting speed v_c 80 mm/min
- Feed speed v_f 100 mm/min
- Depth of cut a_e 0.3 mm

Deep rolling parameters

- Ball diameter d_b 6 mm
- Deep rolling pressure p_r 100, 200, 400 bar
- Rolling speed v_r 100 mm/min
- Stepover s_r 0.1 mm

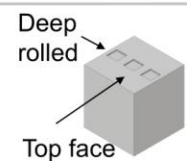
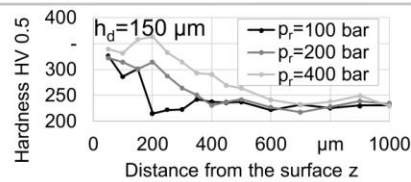
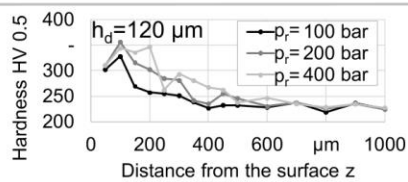


3

Hardness depth profiles

after milling and deep rolling of AM parts

Influence of hatch distance



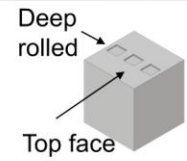
4

Hardness depth profiles

after milling and deep rolling of AM parts

Influence of hatch distance

- Increasing hardness with increasing deep rolling pressure for both hatch distances
- Hatch distance influences the density/prositiy and thus the hardness depth profiles

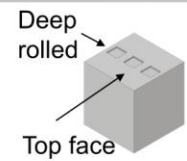


Hardness depth profiles

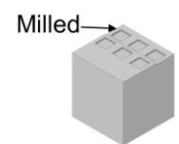
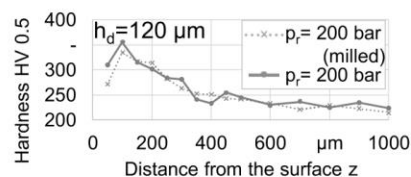
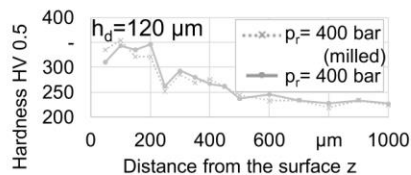
after milling and deep rolling of AM parts

Influence of hatch distance

- Increasing hardness with increasing deep rolling pressure for both hatch distances
- Hatch distance influences the density/prositiy and thus the hardness depth profiles



Influence of post-processing

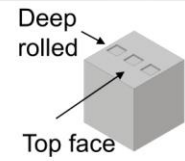


Hardness depth profiles

after milling and deep rolling of AM parts

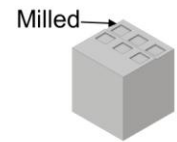
Influence of hatch distance

- Increasing hardness with increasing deep rolling pressure for both hatch distances
- Hatch distance influences the density/prositiy and thus the hardness depth profiles



Influence of post-processing

- Hardness values are comparable for both post-processing strategies



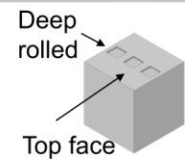
7

Hardness depth profiles

after milling and deep rolling of AM parts

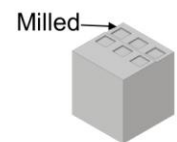
Influence of hatch distance

- Increasing hardness with increasing deep rolling pressure for both hatch distances
- Hatch distance influences the density/prositiy and thus the hardness depth profiles

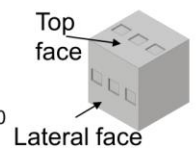
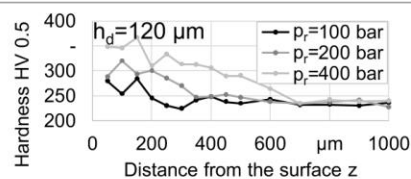
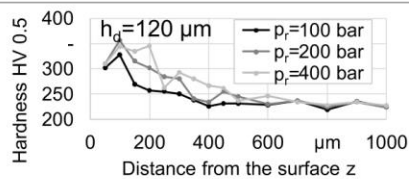


Influence of post-processing

- Hardness values are comparable for both post-processing strategies



Influence of layer orientation



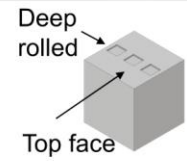
8

Hardness depth profiles

after milling and deep rolling of AM parts

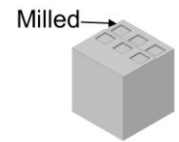
Influence of hatch distance

- Increasing hardness with increasing deep rolling pressure for both hatch distances
- Hatch distance influences the density/prosity and thus the hardness depth profiles



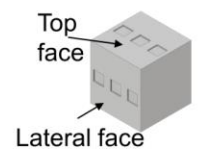
Influence of post-processing

- Hardness values are comparable for both post-processing strategies



Influence of layer orientation

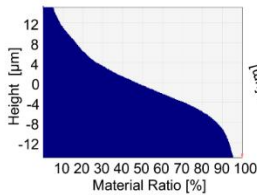
- Increasing hardness with increasing deep rolling pressure for both faces of the cube
- The courses differ more from each other at the lateral face



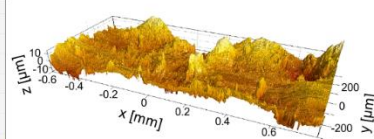
Surface topography

after deep rolling of AM parts

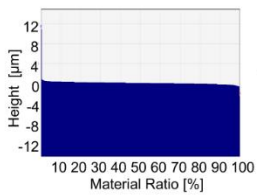
Top face



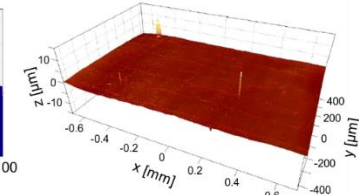
Sa = 6423.0 nm



As printed

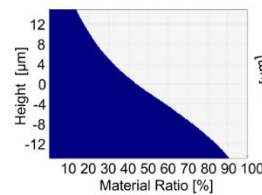


Sa = 162.7 nm

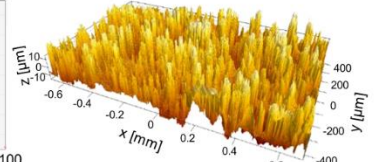


As printed + 400 bar

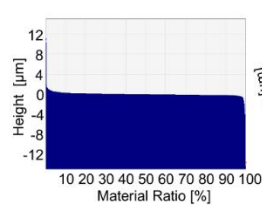
Lateral face



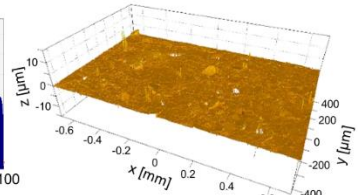
Sa = 10010.0 nm



As printed



Sa = 390.2 nm

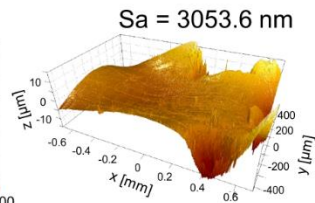
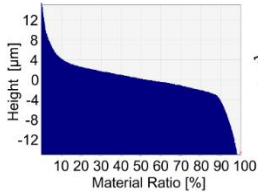


As printed + 400 bar

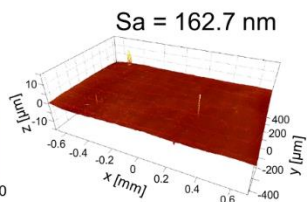
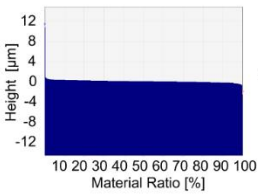
Surface topography

after deep rolling of AM parts

Deep rolled only



As printed + 100 bar

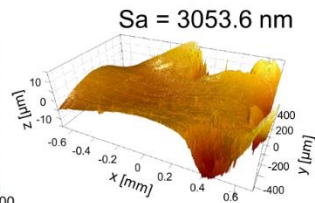
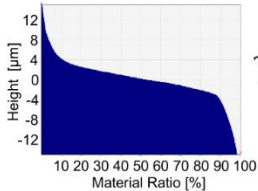


As printed + 400 bar

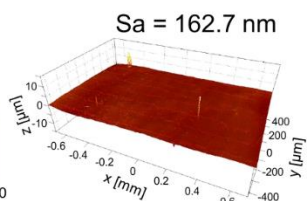
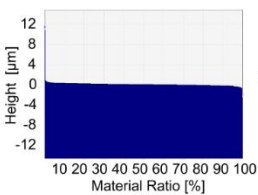
Surface topography

after deep rolling of AM parts

Deep rolled only

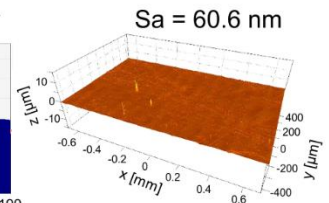
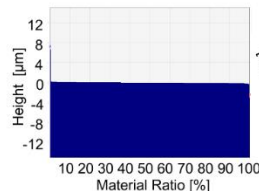


As printed + 100 bar

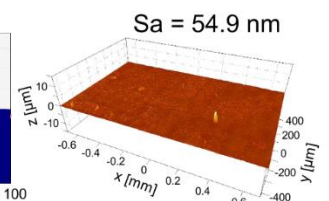
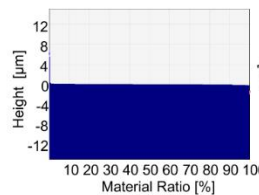


As printed + 400 bar

Milled + deep rolled



Milled + 100 bar



Milled + 400 bar

Scope of this presentation



Additive Manufacturing



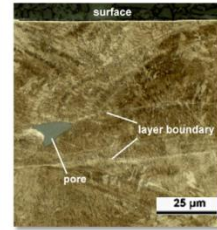
EOS.info



Parts with limited surface quality and complex microstructures



Leibniz-IWT



Brinksmeier et al., CIRP 2010

Post-Processing influencing the Surface Integrity



Dmgmori.com

Leibniz-IWT



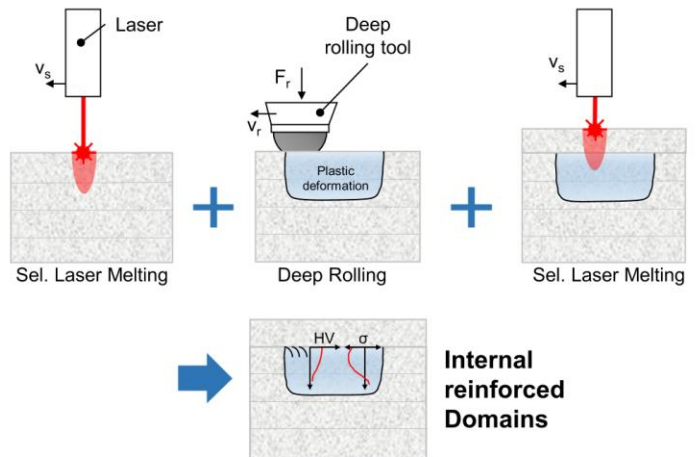
Influence the bulk material or inaccessible areas locally



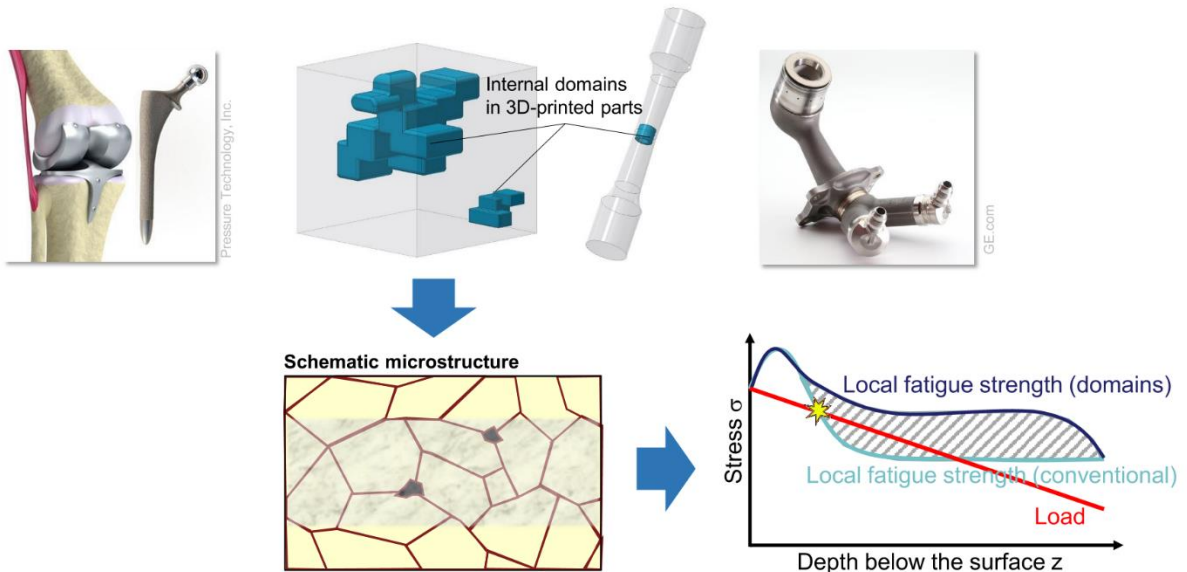
The concept of internal reinforced domains



- Make use of temporary accessibility of all areas during the build phase in AM
- Perform mechanical surface treatment with high depth effect locally
- Apply additional layers by Additive Manufacturing
- Generate three-dimensional internal reinforced domains with adapted Material Integrity

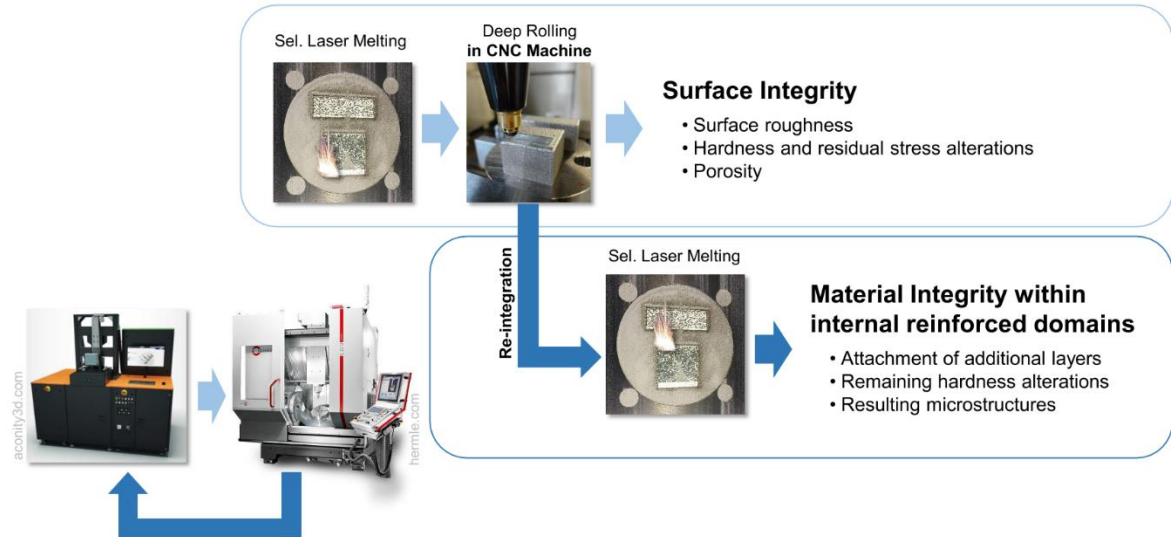


The vision behind the concept



15

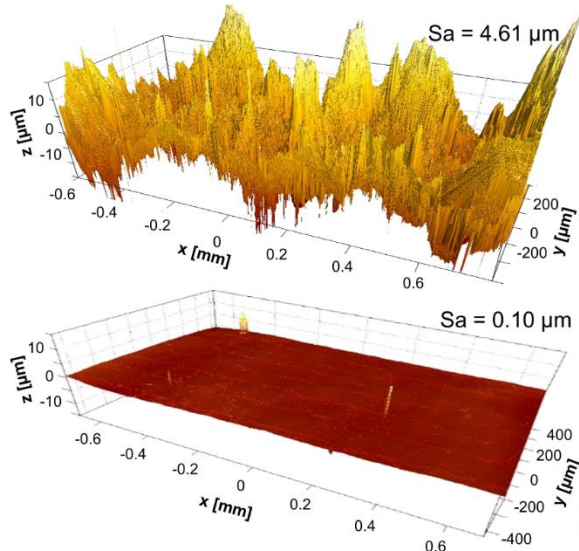
Approach



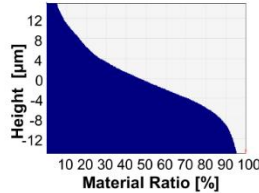
16

Surface Integrity after deep rolling of AM-parts

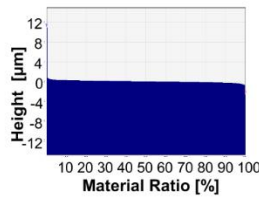
Surface Topography



As printed, top face



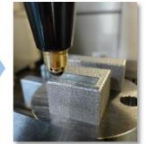
$F_r = 956 \text{ N}$, top face



Sel. Laser Melting



Deep Rolling in CNC Machine



Selective Laser Melting

Material: AISI 316L
 Part dimensions: 50 x 50 x 50 mm
 Laser power P_L : 235 W
 Layer thickness t_L : 50 μm
 Hatch distance h : 120 μm ; 150 μm
 Scanning velocity v_s : 700 m/s

Deep rolling

Ball diameter d_b : 6 mm
 Rolling pressure p_r : 100 bar; 200 bar; 400 bar
 Rolling force F_r : 205 N; 441 N; 956 N
 Feed f : 0.1 mm
 Rolling velocity v_r : 100 mm/min

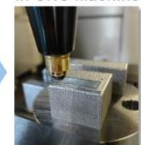
Sa-measurements: ISO 25178, applying a form operator and ISO 16610 Gaussian Filter, Talysurf CCI HD+ Software SPIP 6.7.4

Attachment of additional SLM-layers

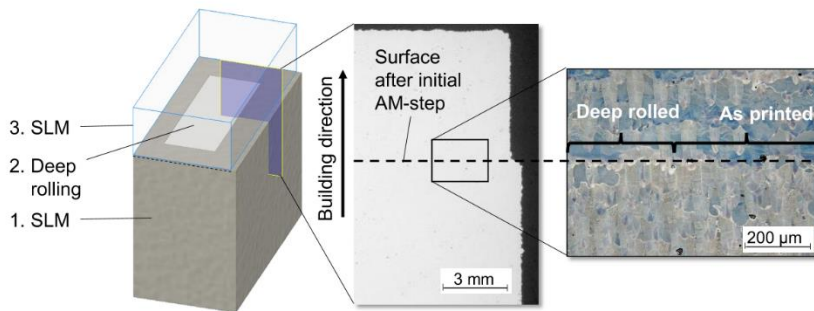
Sel. Laser Melting



Deep Rolling in CNC Machine



Sel. Laser Melting



Selective Laser Melting

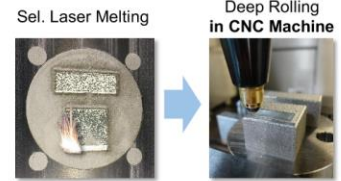
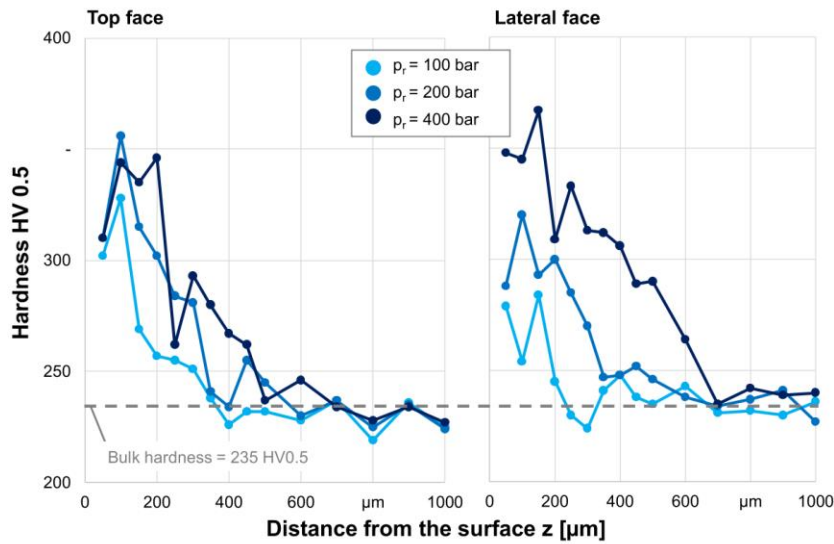
Material: AISI 316L
 Part dimensions: 50 x 50 x 50 mm
 Laser power P_L : 235 W
 Layer thickness t_L : 50 μm
 Hatch distance h : 120 μm
 Scanning velocity v_s : 700 m/s

Deep rolling

Ball diameter d_b : 6 mm
 Rolling pressure p_r : 400 bar
 Rolling force F_r : 956 N
 Feed f : 0.1 mm
 Rolling velocity v_r : 100 mm/min

Surface Integrity after deep rolling of AM-parts

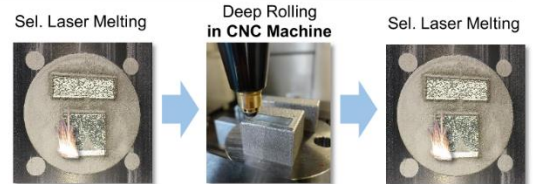
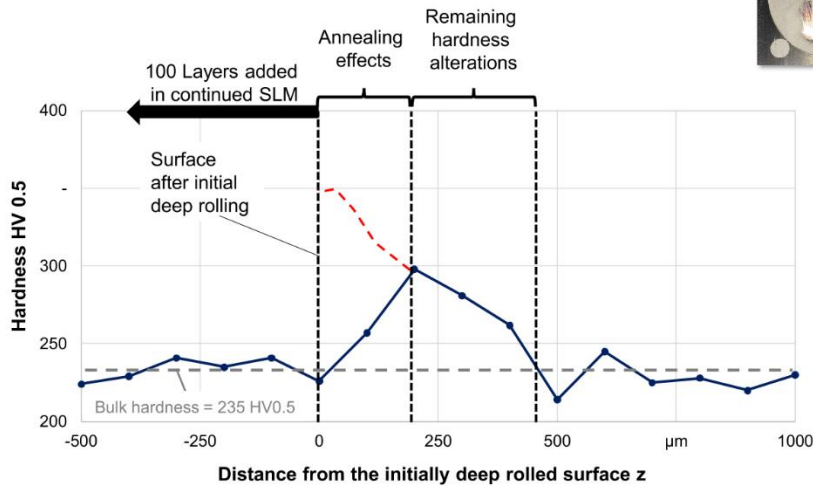
Hardness depth profiles



Selective Laser Melting	
Material	AISI 316L
Part dimensions	50 x 50 x 50 mm
Laser power P_L	235 W
Layer thickness t_L	50 μm
Hatch distance h	120 μm
Scanning velocity v_s	700 m/s
Deep rolling	
Ball diameter d_b	6 mm
Rolling pressure p_r	100 bar; 200 bar; 400 bar
Rolling force F_r	205 N; 441 N; 956 N
Feed f	0.1 mm
Rolling velocity v_r	100 mm/min

19

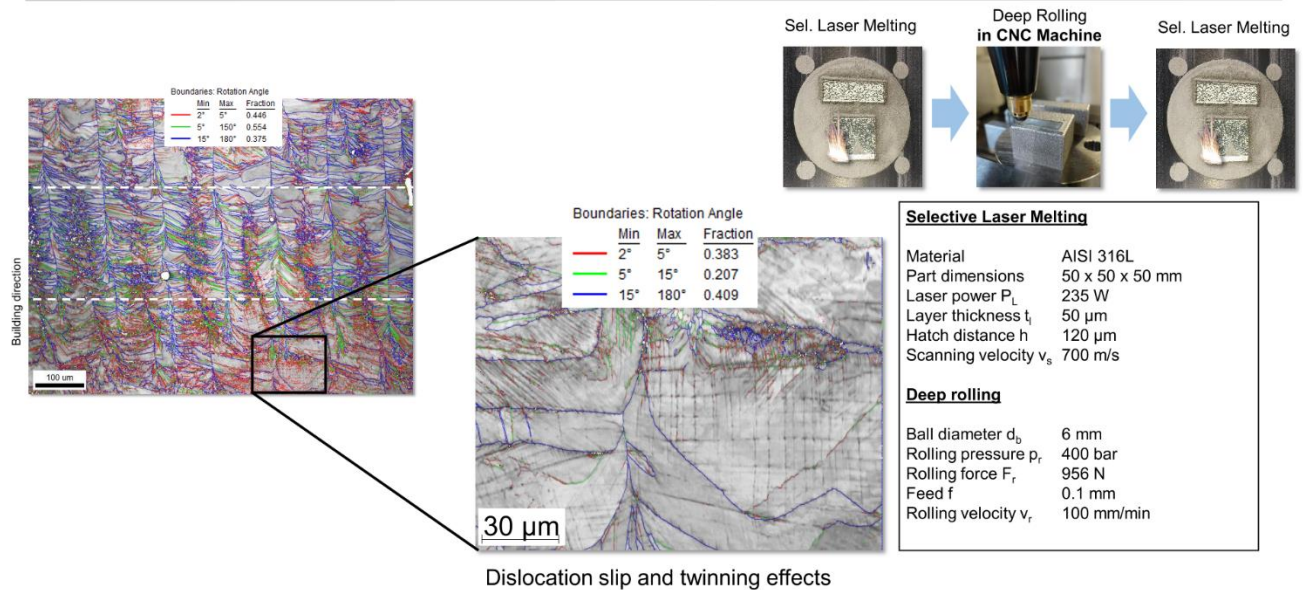
Remaining strain hardening after continued SLM



Selective Laser Melting	
Material	AISI 316L
Part dimensions	50 x 50 x 50 mm
Laser power P_L	235 W
Layer thickness t_L	50 μm
Hatch distance h	120 μm
Scanning velocity v_s	700 m/s
Deep rolling	
Ball diameter d_b	6 mm
Rolling pressure p_r	400 bar
Rolling force F_r	956 N
Feed f	0.1 mm
Rolling velocity v_r	100 mm/min

200

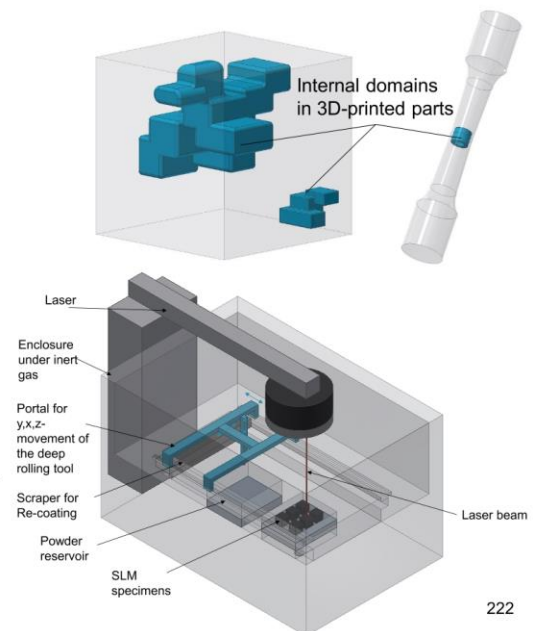
Remaining microstructural effects after continued SLM



Conclusions and Outlook

- Smooth surfaces do not cause issues regarding attachment of additional layers
- Parts of the strain hardening effects after deep rolling are preserved after continuation of SLM
- Recrystallization effects occur due to re-heating effects
- Internal reinforced domains with enhanced Material Integrity can be generated using conventional machines and printers

- Reduce the depth effect of re-heating by adaptation of SLM parameters
- Generate specific hardness profiles in an alternating operation mode
- Consider effects of varying temperature in the building chamber
- Integrate the deep rolling process into the 3D-printer





Thank you for your kind attention!

**Interne Verfestigungsdomänen durch mechanische
Oberflächenbehandlung während der additiven Fertigung**

Contact

Dr.-Ing. Dipl.-Biol. Daniel Meyer
Leibniz Institute for Materials Engineering (IWT)
Badgasteiner Str. 3
28359 Bremen, Germany
Tel.: +49(0) 421 218 51149
Fax: +49(0) 421 218 51101
E-Mail: dmeyer@iwt.uni-bremen.de

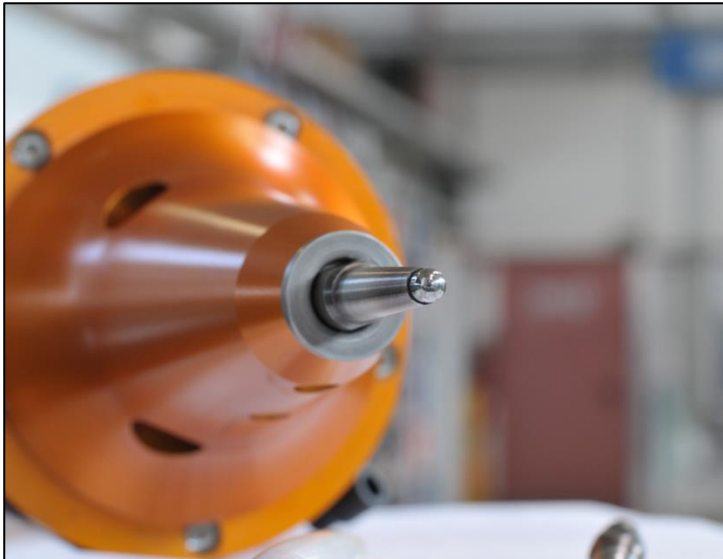
Influence of MHP on the material structure of CrNi steels

Markus Prießnitz

Institute of Production Engineering and Photonic Technologies

TU Wien






Influence of MHP on the material structure of CrNi steels

Workshop Machine Hammer Peening
October 23rd, 2019

Markus Prießnitz
Institute of Production Engineering and Photonic Technologies

MHP
TU WIEN **IFT** Institute of Production Engineering and Photonic Technologies
Univ.Prof. DI Dr.techn. habil. Friedrich Bleicher

Agenda



1	Background
1.1	Metastable austenitic stainless steels
1.2	Martensitic transformation in stainless steels
2	Experimental investigation
2.1	Material selection
2.2	Sensor
2.3	Setup
2.4	Outcomes
3	Application examples and outlook

TU Wien | IFT Institute of Production Engineering and Photonic Technologies Page 3

Background of the research



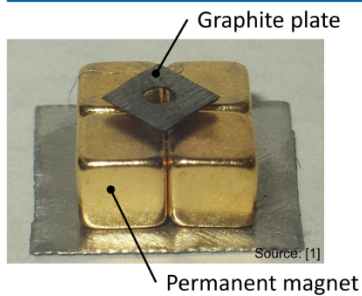
- Previous work
 - Krall S., Reiter M., Bleicher F.. "Influence of the machine hammer peening technology on the surface near material structure of stainless steel X5CrNi18-10." Materials Today: Proceedings 5.13 (2018): 26603-26608.
 - Magnetic properties of stainless steel can be affected by MHP
- Interest
 - Materials science behind the process
 - Systematization and application
 - Code material and detect code
- Dissemination
 - Bachelor thesis
 - Patent protection



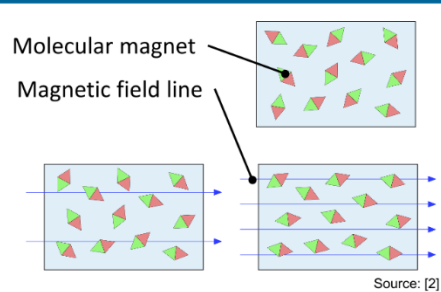
Types of magnetism



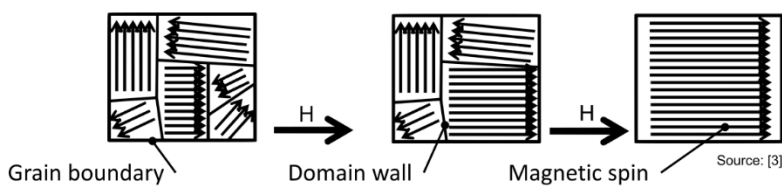
Diamagnetism



Paramagnetism



Ferromagnetism



Magnetic properties of stainless steels



Ferritic stainless steels

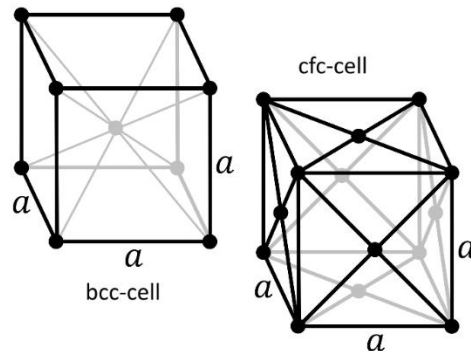
- Crystalline structure bcc
- Magnetically soft behaviour
 - Induction
 - Shielding of magnetic fields
- Regulation of magnetic properties through alloying and heat treatment

Austenitic stainless steels

- Crystalline structure fcc
- Diamagnetic behaviour
 - Neutral exposed to magnetic fields
- Paramagnetic properties due to plastic deformation and residual ferrite

Martensitic stainless steels

- Crystalline structure bcc
- Magnetically hard behaviour
- Regulation of magnetic properties through alloying and heat treatment



Source: [3]

Metastable austenitic stainless steels

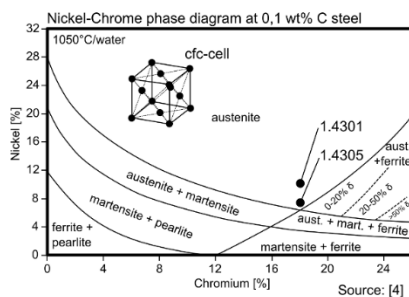


Stabilisation of austenite

- Mechanically
 - Increase in volume during austenite to martensite transformation
- Chemically
 - Nickel, carbon and cobalt widen austenitic phase field

Avoiding magnetisation

- Ferrite: Heat treatment
- Strain-induced martensite: special alloys with manganese

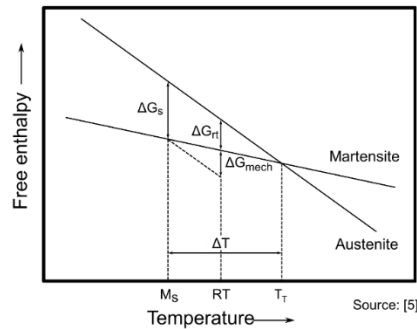


Relative permeability after cold working

Steel grade	μ_{rel} ($\phi=0$)	μ_{rel} ($\phi=0,1$)	μ_{rel} ($\phi=0,2$)	μ_{rel} ($\phi=0,3$)
X8CrNiS18-9 (1.4305)	1,003	1,050	1,620	3,420
X5CrNi18-10 (1.4301)	1,012	1,046	1,626	3,090
X2CrNiMo18-14-3 (1.4435)	1,007	1,008	1,024	1,130
X3CrNiCu18-9-4 (1.4567)	1,005	1,005	1,012	1,082

Martensite transformation - Initiation

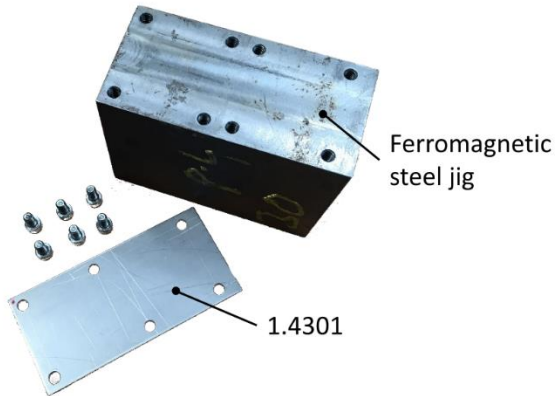
- Thermal initiation
 - Driving force due to supercooling
- Mechanical initiation
 - Deformation induced
 - Strain induced
- Initiating the transformation by introducing the necessary enthalpy difference
- If $M_S < RT$ no thermal initiation at RT
- Additional mechanical enthalpy enables transformation at RT
- Martensite quantity dependent on stacking error energy
- Effect in sheet metal working known and undesired
- Targeted control of the introduced enthalpy possible through MHP
- Targeted exploitation of the regionally changed magnetic properties



Agenda

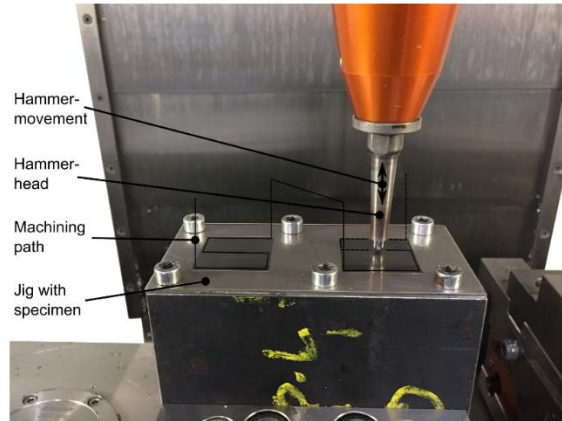
1	Background
1.1	Metastable austenitic stainless steels
1.2	Martensitic transformation in stainless steels
2	Experimental investigation
2.1	Material selection
2.2	Sensor
2.3	Setup
2.4	Outcomes
3	Application examples and outlook

Material selection



- X5CrNi18-10 (1.4301)
- 125x60x2mm
- E-MHP accurapuls
- Haas VF3

Parameter	Value and Unit
Diameter of hammerhead d	6mm
Hammering frequency f	200Hz
Stroke h	1mm
Feed rate v	1200mm/min
Stepover s	0,1mm
Distance between impressions a	0,1mm



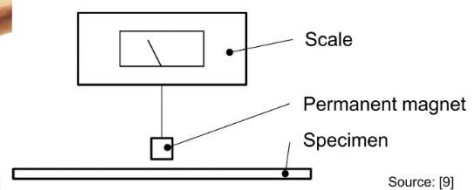
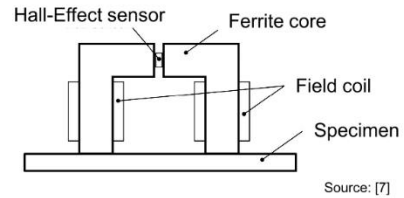
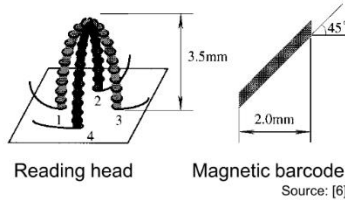
TU Wien | IFT Institute of Production Engineering and Photonic Technologies

Page 10

Detection of magnetic permeability



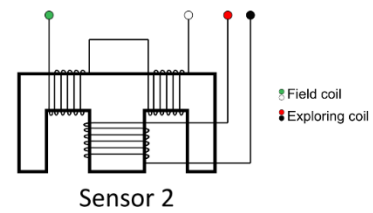
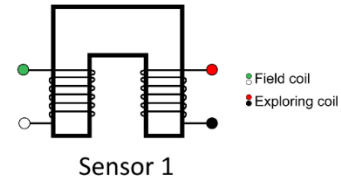
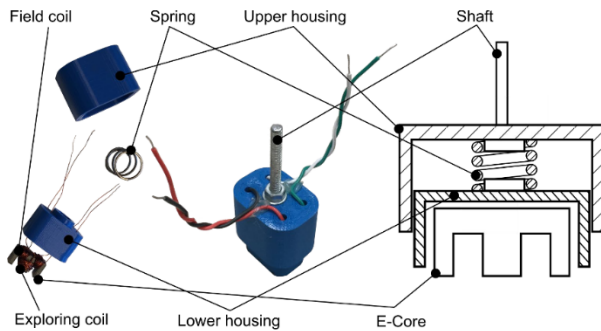
- Magnetic induction
 - Coil on core
- Magnetic flux density
 - Hall-Effect
 - Magnetoresistance
- Ferromagnetism
 - Magnetic scale



TU Wien | IFT Institute of Production Engineering and Photonic Technologies

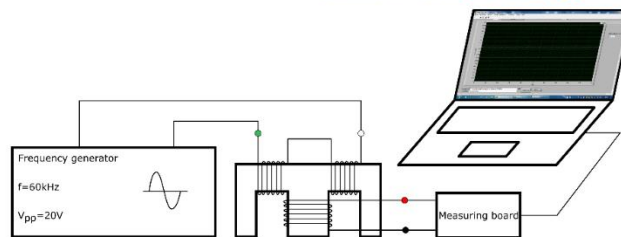
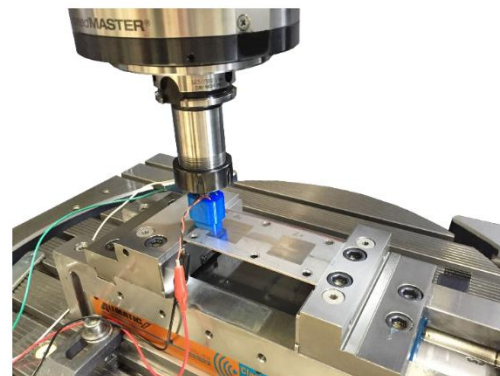
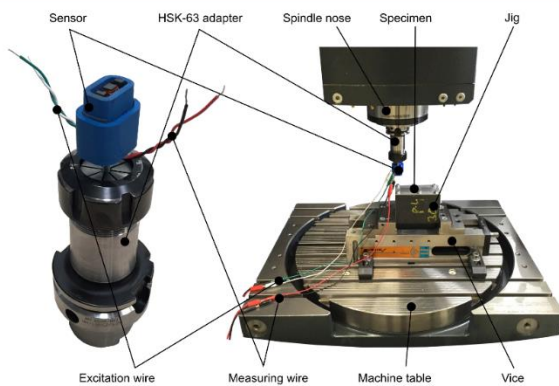
Page 11

Sensor design

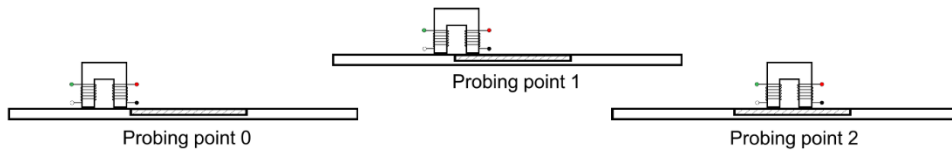


Parameter (Sensor 2)	Value and Unit
Windings of field coil	2x 30 windings
Wire diameter	0,25mm
Windings of exploring coil	30 windings
Wire diameter	0,25mm
Resistance of field coil	0,3028Ω
Inductance of field coil	27,3μH
Resistance of exploring coil	0,4376Ω
Inductance of exploring coil	106,92μH

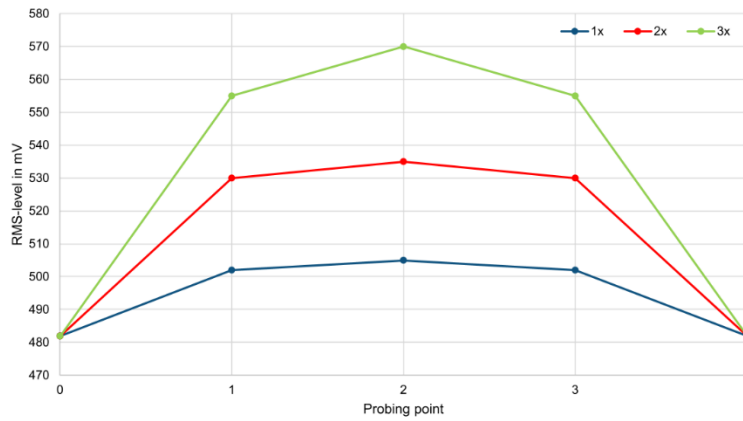
Experimental setup



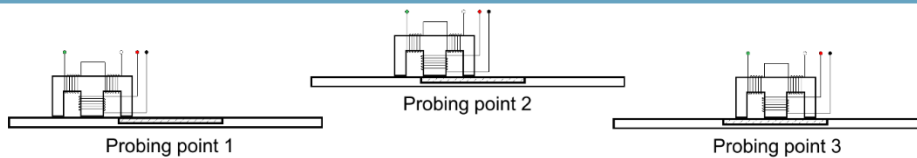
Outcomes – Sensor 1



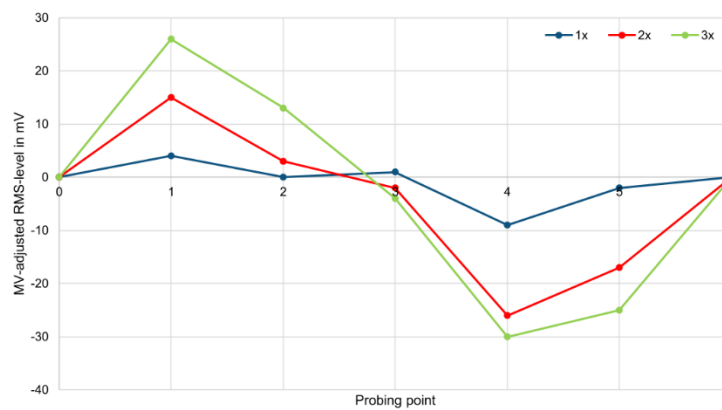
Static level C-Core



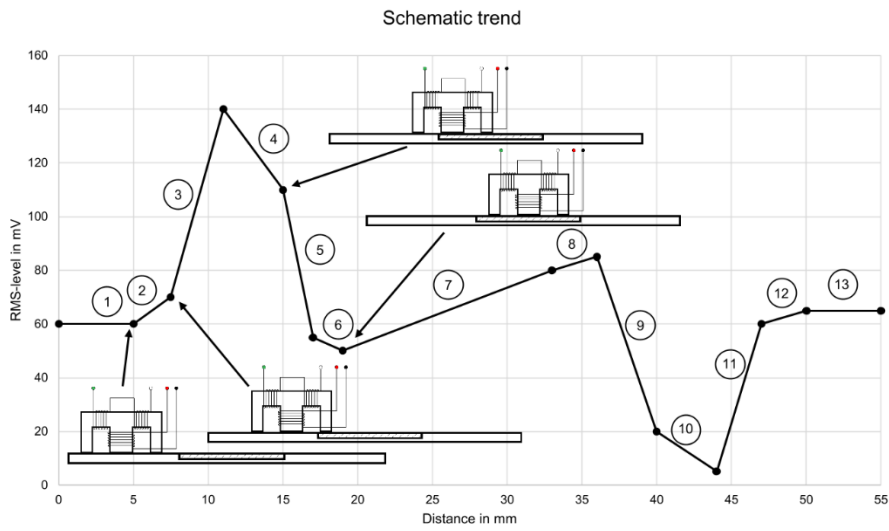
Outcomes – Sensor 2



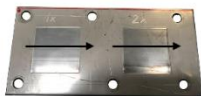
Edge detection E-Core



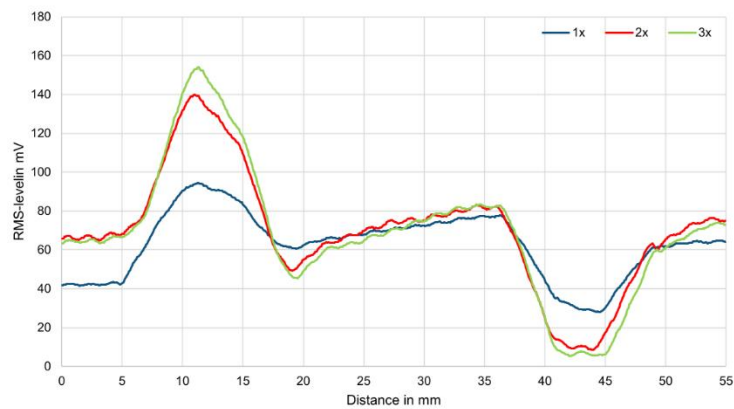
Outcomes – Sensor 2



Outcomes – Sensor 2



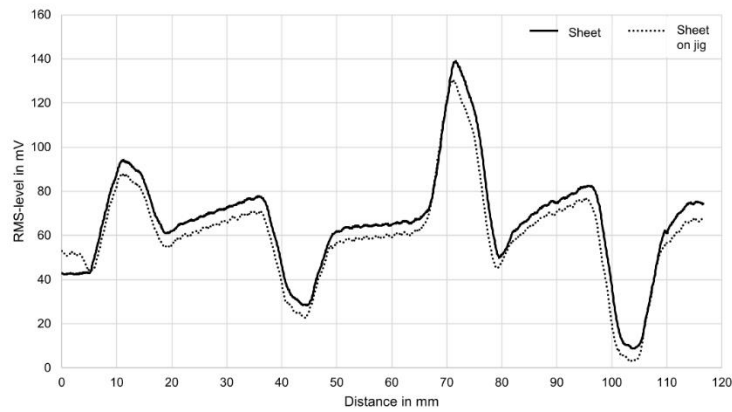
Single field probing without jig



Outcomes – Sensor 2



Double field probing (1x – 2x)



Agenda

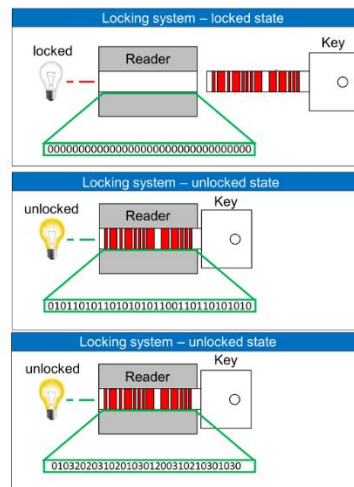


1	Background
1.1	Metastable austenitic stainless steels
1.2	Martensitic transformation in stainless steels
2	Experimental investigation
2.1	Material selection
2.2	Sensor
2.3	Setup
2.4	Outcomes
3	Application examples and outlook

Application examples



- Treatment with MHP system on conventional NC systems
- Removal of machining marks by surface removal or coating possible
- Codification, marking
- Position measuring systems
- Locking systems
- Protection against operating errors
- OEM parts monitoring



Intellectual property protection



- Patent application 2018111316194000DE
- “Verfahren zur Bearbeitung eines einen Informationsbereich aufweisenden Bauteils, Bauteil mit einem Informationsbereich und Messsystem”
- Area-wise applied information area on metallic surface with varied intensity
- Application using elastic/plastic forming
- Strain-induced microstructure transformation
- Use of information area
 - Codification, marking
 - Metrology
 - Locking systems
 - ...
- Reading head for decoding the workpiece

Outlook



- Miniaturisation and testing of spatial resolution
 - Sensor
 - MHP-Process
- Combined sensors
 - Static measurements
 - Edge detection
- Contactless detection
- Detection on smooth surfaces
- Alternative approaches for detection
 - Hall-Effect sensor



Discussion



Thank you for your attention!
Questions?

Influence of MHP process on the material structure of CrNi steels
Markus Prießnitz
priessnitz@ift.at

We thank the *Machine Tool Technologies Research Foundation (MTTRF)* for the loaned equipment, on which part of the presented work has been carried out.



Contact



Contact Person

Markus Prießnitz
E priessnitz@ift.at
T +43 1 58801 31182

Vienna University of Technology
Institute of Production Engineering and Photonic Technologies

Laboratory for Production Engineering

Franz-Grill-Strasse 4 Building OA
1030 Vienna
AUSTRIA

T +43 1 58801 31101
E office@ift.at

Image sources



- [1]: Diamagnetic graphite levitation, Author: Splarka, CC0 1.0.
 - [2]: Paramagnetic probe with varying magnetic fields, Author: Jens Böning, CC0 1.0.
 - [3]: P. H. Mayrhofer, "Skriptum zur VO Ingenieurwerkstoffe", TU Wien, 2015.
 - [4]: M. Zimmermann, Grigorescu, Müller-Bollenhagen, and Christ, "Metastable Austenitic Stainless Steels and the Effect of Deformation-Induced Phase Transformation on the Fatigue Properties", 2014.
 - [5]: J. Scheil, "Entwicklung von Austenitisch- Ferritischem Gusseisen (ADI) aus EN-JS2070: Mikrostruktur, mechanische Eigenschaften und deren Auswirkung auf die Oberflächenbearbeitung durch das Maschinelle Oberflächenhämmern", TU Darmstadt, Darmstadt, 2016.
 - [6]: N. Watanabe, I. Sasada, and N. Asuke, "A new high density magnetic bar code system", J. Appl. Phys., Vol. 85, No. 8, P. 5462–5464, Apr. 1999.
 - [7]: F. Oberhauser, "Measurement Device for Magnetic Permeability of Steel in Production Processes", TU Graz, Graz, 2014.
 - [8]: Helmut Fischer GmbH, "Broschüre Feritscope FMP30"
 - [9]: J. Talonen, P. Aspegren, and H. Hänninen, "Comparison of different methods for measuring strain induced α -martensite content in austenitic steels", *Mater. Sci. Technol.*, Vol. 20, No. 12, P. 1506–1512, Dec. 2004.
- Images without source number: M. Prießnitz, "Einfluss der MHP Bearbeitung auf das Werkstoffgefüge von CrNi Stählen", TU Wien, Wien, 2018.

Influence of the hammer head geometry when machining higher strength materials by MHP

Peter Sticht

Institute for Production Engineering and Forming Machines

Technische Universität Darmstadt



Machine hammer peening (MHP) is a dynamic process to smoothen tool surfaces, increase hardness and introduce residual compressive stresses into the surface layer. Additionally, MHP can be used to apply surface textures that act as lubricant pockets onto tools with specifically shaped hammer heads. MHP-treated surfaces have proven to minimize friction and decrease wear and tear of sheet metal forming tools. As of now, the applicability on higher strength materials in the context of bulk metal forming processes has not yet been investigated sufficiently.

The presentation focuses on the application of MHP in the field of cold forging tools. High strength materials as hardened tool steel, powder metallurgical steel and cemented carbide are treated by MHP and the surface characteristics by means of roughness are investigated.

It is shown that MHP allows for a mechanical treatment of higher strength material and that adapted hammerhead geometries can lead to enhanced surface characteristics.

Forming processes and their reliability are heavily affected by the surface integrity of the tools used. Therefore, high effort is put into the finishing of tool surfaces. [1] MHP is commonly used for smoothing technical surfaces [2] and introducing residual compressive stresses [3] as well as causing strain hardening in the surface layer of the components treated [4]. By using specially shaped hammer heads, surface textures, which serve as lubricant pockets, can be applied onto the surface in the same process step [5]. The aforementioned effects are caused by an oscillating hammerhead that is deterministically guided over the surface by an industrial robot or a machining center [6].

Within the modern industrial environment, mainly electro-magnetic [7] or pneumatic [8] systems are used, whereas piezo-electric [9] actuators are used in current research applications. Primarily, MHP is used in the tool and mold making industry to ensure the surface integrity of the tools that will be involved in production processes such as deep drawing. It has been shown that micro textures can lower the friction coefficients by about 30 % compared to manually polished surfaces [5]. Also, wear phenomena and locations change, as particles that would be able to move in process direction are being caught by the micro textures and prevented from causing further abrasive wear on the tool [10]. Not only sheet metal forming processes, but also cold forging processes can benefit from hammer peened surfaces. The tribological loads in these processes are considerably higher and therefore, higher strength materials are selected to meet the criteria regarding durability.

So far, the effect of different hammerhead diameters on the smoothening behavior on tool steel and nodular cast iron has been investigated extensively whereas always spherical hammerheads have been used.

Different tool materials are measured in a variety of conditions. These values define the benchmark for the ongoing surface treatment by machine hammer peening.

In the next step, higher strength materials commonly used in the cold forging industry are treated by machine hammer peening with different parameter settings and an increasing number of repetitions, where necessary. It is shown that, for the most materials, it is possible to reach the desired characteristic surface values.

Following the study an approach to improve the MHP-treatment of higher strength material is presented, taking different hammer head geometries into consideration. The latest

developments regarding the MHP treatment of higher strength materials as well as an outlook on further investigations conclude the presentation.

The authors would like to thank all participating industrial partners as well as the funding organizations for their contribution to the MHP technology.

References

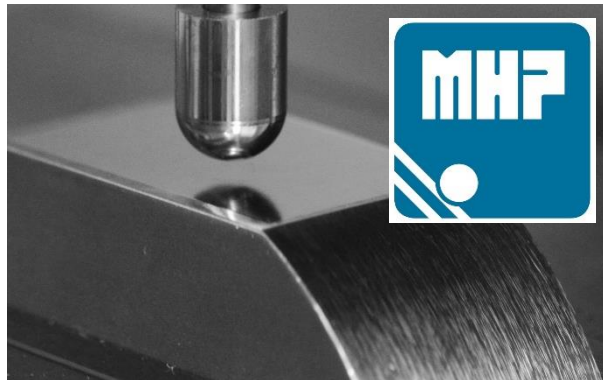
1. Schulze, V., Bleicher, F., Groche, P., Guo, Y.B., Pyun, Y.S.: Surface modification by machine hammer peening and burnishing: CIRP Annals – Manufacturing Technology 65 (2016), pp. 809-832
2. Wied, J.: Oberflächenbehandlung von Umformwerkzeugen durch Festklopfen: PhD-Thesis, Darmstadt (2011)
3. Hacini, L., van Le, N.: Effect of impact energy on residual stresses induced by hammer peening of 304L plates: in Journal of Materials Processing Technology 208 (2008), pp. 542-548
4. Groche, P., Engels, M., Müller, C.: Wear behavior of sheet metal forming tools made from nodular cast iron after mechanical surface treatments: in Transactions of NAMRI of SME (2010), pp. 531 – 538
5. Steitz, M. Stein, P., Groche, P.: Influence of Hammer-Peened Surface Textures on Friction Behavior: Tribology Letters (2015) 58:24
6. Steitz, M. Scheil, J., Müller, C. Groche, P.: Effect of Process Parameters on Surface Roughness in Hammer Peening and Deep Rolling: in Key Eng. Mat., Trans Tech Publications, Switzerland, 554-557 (2013), pp. 1887 – 1901
7. Patent DE 10 2006 033 004 A1: Klopfvorrichtung- und Verfahren, Deutsches Patent- und Markenamt, Germany (2006)
8. Patent 10 2010 019 547 A1: Kaltschmiedevorrichtung und Kaltschmiede-verfahren, Deutsches Patent- und Markenamt, Germany (2010)
9. Lienert, F., Hoffmeister, J., Schulze, V.: Residual Stress Depth Distribution after Piezo Peening of Quenched and Tempered AISI 4140: in Materials Science Forum, Vol. 768 – 769 (2014), pp. 526-533
10. Steitz, M, Klasen, P., Groche, P.: Wear behavior of hammer peened surface textures during strip drawing test: IDDRG 2015 Conference, Shanghai, China (2015)

Optimization of the stream finishing process for mechanical surface treatment by numerical and experimental process analysis

Patrick Neuenfeldt

wbk Institute of Production Science

Karlsruhe Institute of Technology





**OPTIMIZATION OF THE STREAM FINISHING
PROCESS FOR MECHANICAL SURFACE
TREATMENT BY NUMERICAL AND EXPERIMENTAL
PROCESS ANALYSIS**

P. Neuenfeldt, A. Kacaras, F. Zanger, V. Schulze

KIT – The Research University in the Helmholtz Association

www.wbk.kit.edu

AGENDA



- 1 **Explanation of the Stream Finishing process**
- 2 Discrete element modeling
- 3 Scientific gaps
- 4 Experimental setup and discrete element modeling
- 5 Results
- 6 Conclusion and outlook

EXPLANATION OF THE STREAM FINISHING PROCESS

Process properties

- Rotating bowl filled with granular material (media)
- Types of media
 - Bonded media: abrasive particles fixed in a matrix
 - Unbonded media
- Defined positioning of workpiece
→ relative velocity between media and workpiece's surface



Different types of bonded media



Stream Finishing of a turbine blade

3

16.10.2019

Prof. Dr.-Ing. J. Fleischer, Prof. Dr.-Ing. G. Lanza, Prof. Dr.-Ing. habil. V. Schulze

AGENDA

- 1 Explanation of the Stream Finishing process
- 2 **Discrete element modeling**
- 3 Scientific gaps
- 4 Experimental setup and discrete element modeling
- 5 Results
- 6 Conclusion and outlook

4

16.10.2019

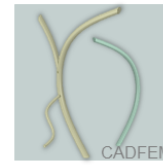
Prof. Dr.-Ing. J. Fleischer, Prof. Dr.-Ing. G. Lanza, Prof. Dr.-Ing. habil. V. Schulze

DISCRETE ELEMENT MODELING

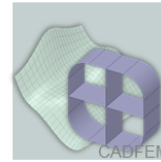


Simulation method

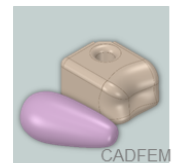
- Numerical method to determine the movement of solids
- No meshing of the computation area needed like e.g. in CFD
- Meshing of solids only
- Different kinds of geometries and properties of solids possible
- DEM-Software Rocky DEM



Fiber



Sheet



Volume

Simulation procedure in general

- Definition of boundary conditions
- Definition of machine and workpiece kinematics
- Filling of the calculation area by stochastic distribution of solids
- Time-discrete calculation while executing machine and workpiece kinematics
 → transient simulation

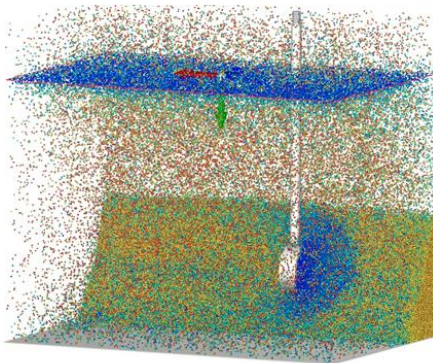
5

16.10.2019

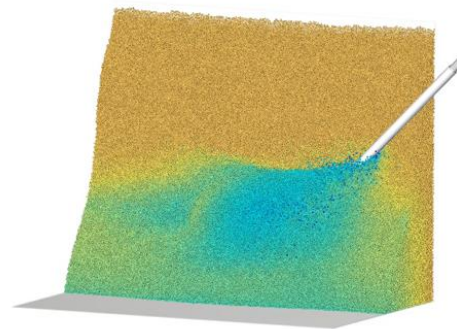
Prof. Dr.-Ing. J. Fleischer, Prof. Dr.-Ing. G. Lanza, Prof. Dr.-Ing. habil. V. Schulze



DISCRETE ELEMENT MODELING



Filling of the calculation area



Executing machine and workpiece kinematics

6

16.10.2019

Prof. Dr.-Ing. J. Fleischer, Prof. Dr.-Ing. G. Lanza, Prof. Dr.-Ing. habil. V. Schulze



AGENDA



- 1 Explanation of the Stream Finishing process
- 2 Discrete element modeling
- 3 **Scientific gaps**
- 4 Experimental setup and discrete element modeling
- 5 Results
- 6 Conclusion and outlook

7

16.10.2019

Prof. Dr.-Ing. J. Fleischer, Prof. Dr.-Ing. G. Lanza, Prof. Dr.-Ing. habil. V. Schulze

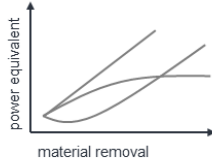


INTRODUCTION

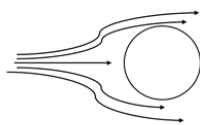
Present scientific gaps for mass finishing



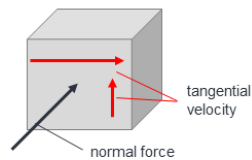
Proportional relationship between material removal and the power equivalent is still unproven for mass finishing (Brocker)



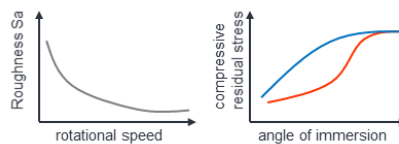
No approach for a realistic description of spatial flow formation is available



Knowledge of local contact forces and velocities is not available



No consideration of surface states besides surface topography and correlation with process parameters



Scientific goal

- Cause-effect relationships between process parameters, contact conditions and surface integrity
- Experiment:
 - Normal force F_N
 - Material removal Δm
 - Roughness S_a
 - Residual stress σ^{RS}
- Simulation:
 - Normal force F_N
 - Tangential velocity v_t
 - $\rightarrow P = F_N \cdot v_t$

8

16.10.2019

Prof. Dr.-Ing. J. Fleischer, Prof. Dr.-Ing. G. Lanza, Prof. Dr.-Ing. habil. V. Schulze



AGENDA



- 1 Explanation of the Stream Finishing process
- 2 Discrete element modeling
- 3 Scientific gaps
- 4 **Experimental setup and discrete element modeling**
- 5 Results
- 6 Conclusion and outlook

9

16.10.2019

Prof. Dr.-Ing. J. Fleischer, Prof. Dr.-Ing. G. Lanza, Prof. Dr.-Ing. habil. V. Schulze

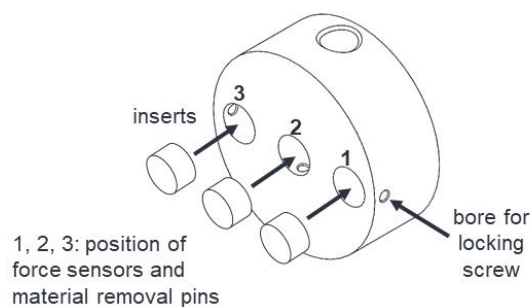


EXPERIMENTAL SETUP AND DISCRETE ELEMENT MODELING

Equipment and target values

Experimental equipment

- Stream finishing machine SF1 68
- Alumina media KXMA 16 wetted with water and compound SC15 (grain size 1.7 to 2.4 mm)
- Disc shaped quenched and tempered AISI 4140 specimen
- Piezo resistive normal force sensors



Stream Finishing of a specimen using KXMA 16

10

16.10.2019

Prof. Dr.-Ing. J. Fleischer, Prof. Dr.-Ing. G. Lanza, Prof. Dr.-Ing. habil. V. Schulze



EXPERIMENTAL SETUP AND DISCRETE ELEMENT MODELING

Processing parameters


Constant parameters

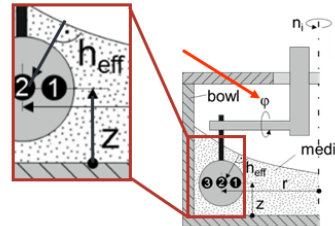
- Radius of immersion $r = 270$ mm
- Media height of 220 mm

Varied parameters

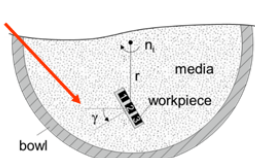
- To evaluate the influence of process parameters a broad parameter range was used

Height above the bowl bottom	z	75 to 150	mm
Rotational speed	n	30 to 90	U/min
Angle of immersion	φ	0° to 45°	
Workpiece orientation	γ	-50° to 50°	

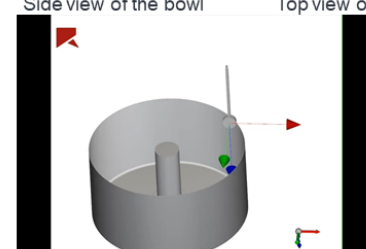




Side view of the bowl




Top view of the bowl



Visualisation of varied parameters

11


16.10.2019 Prof. Dr.-Ing. J. Fleischer, Prof. Dr.-Ing. G. Lanza, Prof. Dr.-Ing. habil. V. Schulze



EXPERIMENTAL SETUP AND DISCRETE ELEMENT MODELING

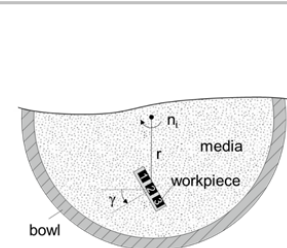
Simulative approach

- Abstracting trough a linear analogy channel
- Velocity distribution trough discrete path velocities on the ground
- particle distribution trough gravitational acceleration equivalent normal to the outer wall
- Media modelled by spheres ($\varnothing 2$ mm)

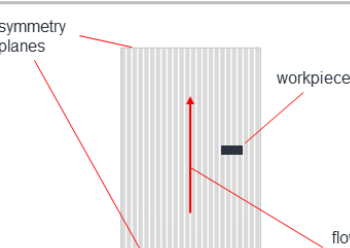


- Physical media properties according to dry Al_2O_3 [7, 8, 9]
- 1.25 Mio. particles
- Particles Young's modulus reduced by factor $1 E3$ [10], [11]

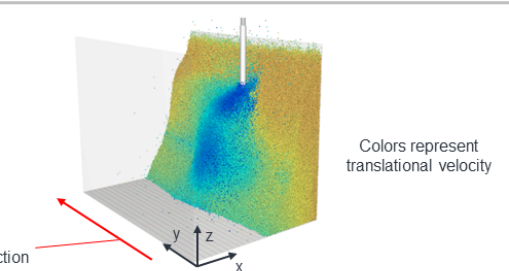
→ Downscaling provides comparable particle velocity vectors and flow formation [11]



Top view of the bowl



Abstracted analogy channel




Exemplary representation of the simulation model

Colors represent translational velocity

12

16.10.2019 Prof. Dr.-Ing. J. Fleischer, Prof. Dr.-Ing. G. Lanza, Prof. Dr.-Ing. habil. V. Schulze



AGENDA



- 1 Explanation of the Stream Finishing process
- 2 Discrete element modeling
- 3 Scientific gaps
- 4 Experimental setup and discrete element modeling
- 5 **Results**
- 6 Conclusion and outlook

13

16.10.2019

Prof. Dr.-Ing. J. Fleischer, Prof. Dr.-Ing. G. Lanza, Prof. Dr.-Ing. habil. V. Schulze

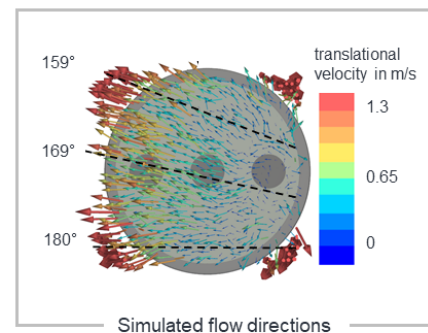
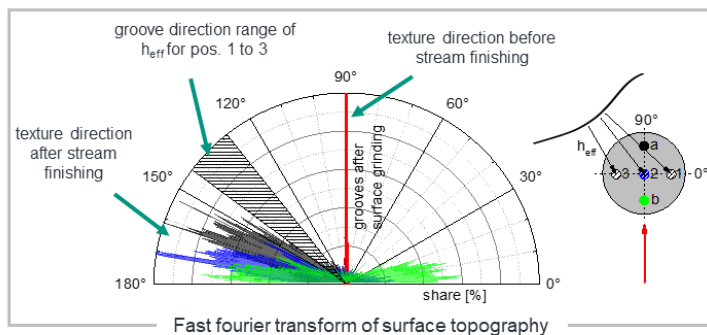


RESULTS

Correlation of simulation and experiments



- Vertically oriented groove direction before stream finishing (after surface grinding)
- Range of h_{eff} is largely in accordance to the experimental determined texture directions
- Good correlation of local texture directions (pos. a, 2, b) between experiment and simulation



14

16.10.2019

Prof. Dr.-Ing. J. Fleischer, Prof. Dr.-Ing. G. Lanza, Prof. Dr.-Ing. habil. V. Schulze



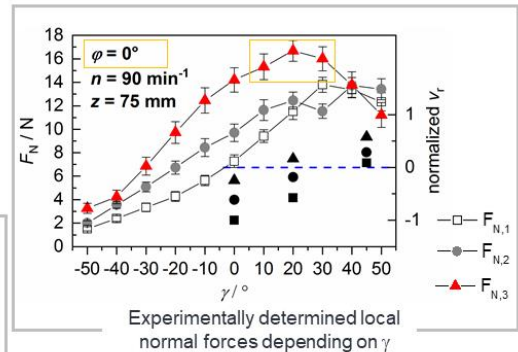
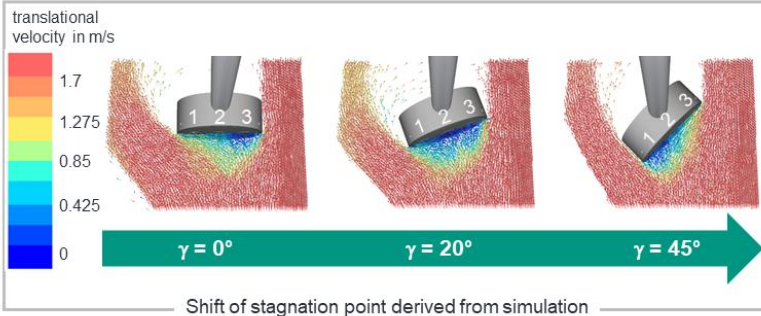
RESULTS

Normal Force



Variation of process angles

- Variation of γ or φ to higher/lower values than 0 should always lead to reduced normal force F_N due to
 - Vector distribution of forces
 - Reduced impoundment effects due to a reduced projected area



Inverse relation between normal force and tangential velocity is expected

15

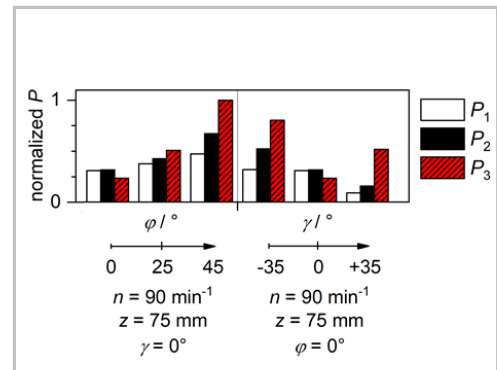
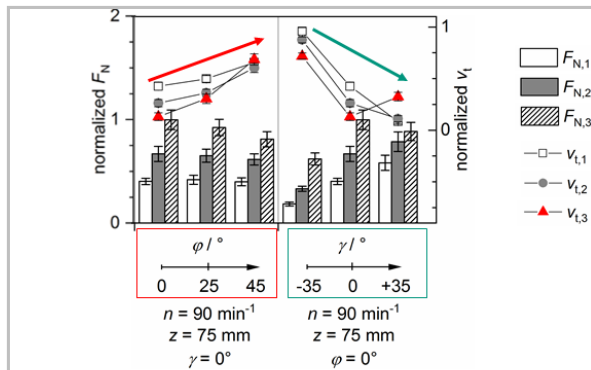
16.10.2019

Prof. Dr.-Ing. J. Fleischer, Prof. Dr.-Ing. G. Lanza, Prof. Dr.-Ing. habil. V. Schulze



RESULTS

Simulation results



- Normal force F_N and tangential velocity v_t are inversely influenced by process parameters
 - Increase of v_t leads to a decrease of F_N
 - Decrease of v_t leads to an increase of F_N

Introduction of the power equivalent P is necessary for a holistic process description

16

16.10.2019

Prof. Dr.-Ing. J. Fleischer, Prof. Dr.-Ing. G. Lanza, Prof. Dr.-Ing. habil. V. Schulze



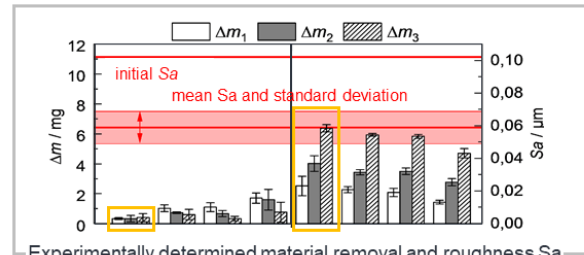
RESULTS

Material removal

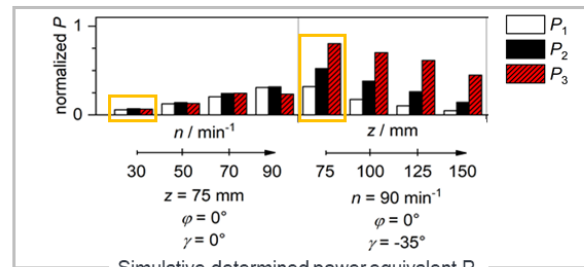
- 20 min of stream finishing for each parameter
- Stationary roughness state despite of highly varying material removal
- P/ Δm ratio shows standard deviation of 68 %
- Prestons law is therefore not applicable
- Results by Brocker can be confirmed

→ No proportional correlation!

➔ Increase of power equivalent P leads to an increase of material removal Δm (qualitatively)



Experimentally determined material removal and roughness Sa



Simulative determined power equivalent P

17

16.10.2019

Prof. Dr.-Ing. J. Fleischer, Prof. Dr.-Ing. G. Lanza, Prof. Dr.-Ing. habil. V. Schulze

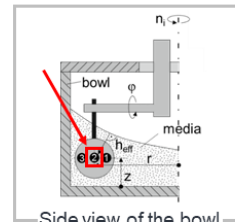


RESULTS

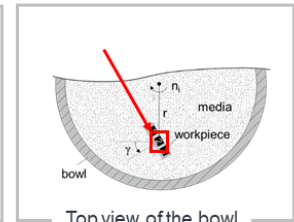
Surface integrity

- Comparison of residual stress σ^{RS} and P
- Residual stress measured at position 2
- Evaluation of depth profiles up to 5 μm is reasonable
- Qualitative correlation of P and σ^{RS}
- Assumption of Kacaras et al. can clearly be confirmed

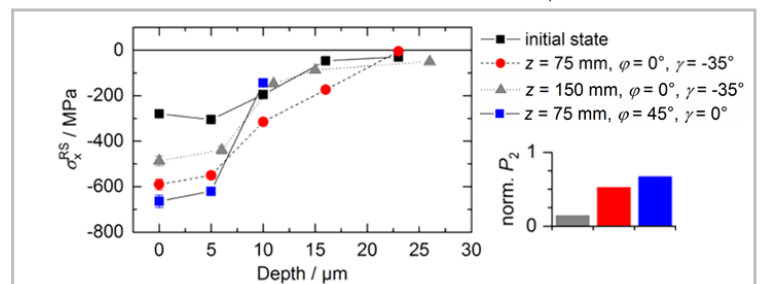
➔ Increase of power equivalent P leads to an increase of compressive residual stress



Side view of the bowl



Top view of the bowl



Residual stress states for defined process parameters and corresponding values of P

18

16.10.2019

Prof. Dr.-Ing. J. Fleischer, Prof. Dr.-Ing. G. Lanza, Prof. Dr.-Ing. habil. V. Schulze



AGENDA



- 1 Explanation of the Stream Finishing process
- 2 Discrete element modeling
- 3 Scientific gaps
- 4 Experimental setup and discrete element modeling
- 5 Results
- 6 **Conclusion and outlook**

19

16.10.2019

Prof. Dr.-Ing. J. Fleischer, Prof. Dr.-Ing. G. Lanza, Prof. Dr.-Ing. habil. V. Schulze



CONCLUSION AND OUTLOOK

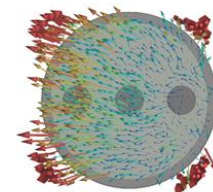


Key findings

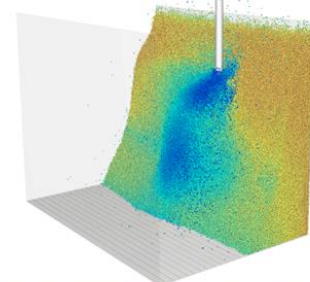
- Local consideration of normal force and tangential velocity is mandatory
- Process efficiency can effectively be influenced by the
 - Angle of immersion φ
 - Workpiece orientation γ
- Power equivalent P is a valid qualitative measure for Δm and σ^{RS}

Outlook

- Improve simulative approach to gain quantitative normal force values
- Validate findings using a complex geometry



Simulated flow directions






Exemplary representation of the simulation model

20

16.10.2019

Prof. Dr.-Ing. J. Fleischer, Prof. Dr.-Ing. G. Lanza, Prof. Dr.-Ing. habil. V. Schulze






Thank you for your kind attention!


Patrick Neuenfeldt, M.Sc.
Research Associate
Tel.: +49 1523 9502602
E-Mail: patrick.neuenfeldt@kit.edu

wbk Institut of Production Science
Kaiserstraße 12
76131 Karlsruhe
<https://www.wbk.kit.edu/>

21 16.10.2019 Prof. Dr.-Ing. J. Fleischer, Prof. Dr.-Ing. G. Lanza, Prof. Dr.-Ing. habil. V. Schulze



REFERENCES



- [1] Hashimoto F, Yamaguchi H, Krajnik P, Wegener K, Chaudhari R, Hoffmeister HW, Kuster F (2016) Abrasive Fine-Finishing Technology. CIRP Annals – Manufacturing Technology 65:597–620.
- [2] Kacaras A, Gibmeier J, Zanger F, Schulze V (2018) Influence of Rotational Speed on Surface States After Stream Finishing. Procedia CIRP 71:332–226.
- [3] Preston FW (1927) The Theory and Design of Plate Glass Polishing Machines. Journal of the Society of Glass Technology 11:214–256.
- [4] Brocker R (2015) Relativgeschwindigkeiten und Kontaktkräfte beim ungeführten Vibrationsgleitschleifen, Dissertation RWTH Aachen University.
- [5] Makiuchi Y, Hashimoto F, Beaucamp A (2019) Model of material removal in vibratory finishing, based on Preston's law and discrete element method. CIRP Annals – Manufacturing Technology 68:365–368.
- [6] Shahinian H, Mullany B (2016) Optical Polishing Using Fiber Based Tools. Procedia CIRP 45:183–186.
- [7] Poser K, Zum Gahr KH, Schneider J (2005) Development of Al₂O₃ based ceramics for dry friction systems. Wear 259:529–538.
- [8] DellaCorte C, Pepper SV, Honey FS (1991) Tribological properties of Ag/Ti films on Al₂O₃ ceramic substrates. NASA Technical Memorandum 103784.
- [9] Blau PJ (2008) Friction Science and Technology – From concepts to applications. CRC Press Taylor & Francis Group, ISBN:978-14200-5404-0.
- [10] Washino K, Chan EL, Tanaka T (2018) DEM with Attraction Forces Using Reduced Particle Stiffness. Powder Technology 325:202–208.
- [11] Stewart RL, Bridgwater J, Zhou YC, Yu AB (2001) Simulated and Measured Flow of Granules in a Bladed Mixer – A Detailed Comparison. Chemical Engineering Science 56:5457–5471.

22 16.10.2019 Prof. Dr.-Ing. J. Fleischer, Prof. Dr.-Ing. G. Lanza, Prof. Dr.-Ing. habil. V. Schulze

